ELISABETE CRUZ DA SILVA

Integrin alpha5beta1 and resistance to cancer therapies

Role of endocytosis in resistance to gefitinib

Departamento de Ciências
Biomédicas e Medicina

2016/2017

ELISABETE CRUZ DA SILVA

Integrin alpha5beta1 and resistance to cancer therapies

Role of endocytosis in resistance to gefitinib

Mestrado em:

Oncobiologia - Mecanismos Moleculares do Cancro

Trabalho efetuado sob a orientação de:

Professor Maxime Lehmann

Doutora Bibiana Ferreira

Departamento de Ciências Biomédicas e Medicina

2016/2017

Titulo do trabalho:

"Integrin alpha5beta1 and resistance to cancer therapies: Role of endocytosis in resistance to gefitinib "

Declaro ser a autora deste trabalho, que é original e inédito. Autores e trabalhos consultados estão devidamente citados no texto e constam da listagem de referências incluída.

Acknowledgements

"Education is not the filling of a pail but the lighting of a fire"

by William Butler Yeats

First, I would like to thank the greatest opportunity given by Professor Monique Dontenwill by accepting me into her team and allowing me to live this experience.

To Professor Maxime Lehmann for all the time spent teaching me, for giving me the joy of sharing his knowledge, for giving me support in all moments and for being inspiring full.

To the whole team for their help and support mainly to Fanny Noulet. Also to the collaborators Romain Vauchelles and Oleksandr Glushonkov for their help in the experiments.

To all the Professors at the Master in Oncobiology - Molecular Mechanisms of Cancer for their support and knowledge given, specially to Doutora Bibiana Ferreira and Professor Doutor Alvaro Tavares that were my support in the university.

"The greatest gift of life is friendship, and I have received it"

by Hubert H. Humphrey

From the oldest to the newest, thank you to all my friends, especially to Vanessa Henriques, Bastien Lambert, Marie-Cecile Mercier and Mickaële Hémono.

"Family is not an important thing, it is everything"

by Michael J. Fox

For all the love, support and affection I would like to thank to my family. Because even with the distance, without them nothing would be possible!

Abstract

Glioblastoma is an aggressive, invasive and resistant brain cancer. Despite the promisor role of EGFR, targeted therapies failed without giving insights about predictive factors. EGFR endocytosis and trafficking have been reported to influenciate therapy resistance. Integrin is known as a regulator of EGFR oncogenic activity during tumor progression by affecting its trafficking. Previous results from the team in cell evasion showed that α5 integrin depletion sensitizes cells to gefitinib treatment. For that, my main objective was to determine if the endocytic pathway is involved in the integrin-mediated resistance to gefitinib.

Endocytosis involvement on gefitinib treatment was evaluated by dynamin inhibition. Dynamin is GTPase involved in the fission of endocytic vesicles. There were performed cellular evasion and EGFR internalization assays under gefitinib treatment with or without dynamin chemical inhibitiors (dynasore and dyngo4a). We showed that endocytosis is involved in the gefitinib-mediated inhibition of U87 cell evasion regardless the α5 integrin expression level. Gefitinib induces ligand-bound EGFR internalization, being this impaired with the addiction of dynasore. EGFR and α5β1 integrin distribution were evaluated using immunofluorescence confocal microscopy. Gefitinib was shown to induce internalization of both receptors, being them founded co-localized inside of early endosomal vesicles. Gefitinib induced EGFR internalization occurs in U87 and others glioma cell lines independently of α5 level.

We postulate that α5β1 integrin may impact on EGFR trafficking and function during membrane trafficking after endocytosis confering resistance towards gefitinib treatment. There was already described a regulatory role of integrin in EGFR trafficking to promote carcinoma cell invasion, for that this role of integrin should be further evaluated.

In conclusion, endocytosis plays a relevant role in gefitinib treatment. EGFR trafficking gains here a strong evidence for its role in therapy resistance. Modulators of this endosomal trafficking, such as α5β1 integrin can predict responsiviness towards EGFR targeted therapies.

Keywords: Glioblastoma, EGFR, Gefitinib, α5β1 Integrin, Endocytosis

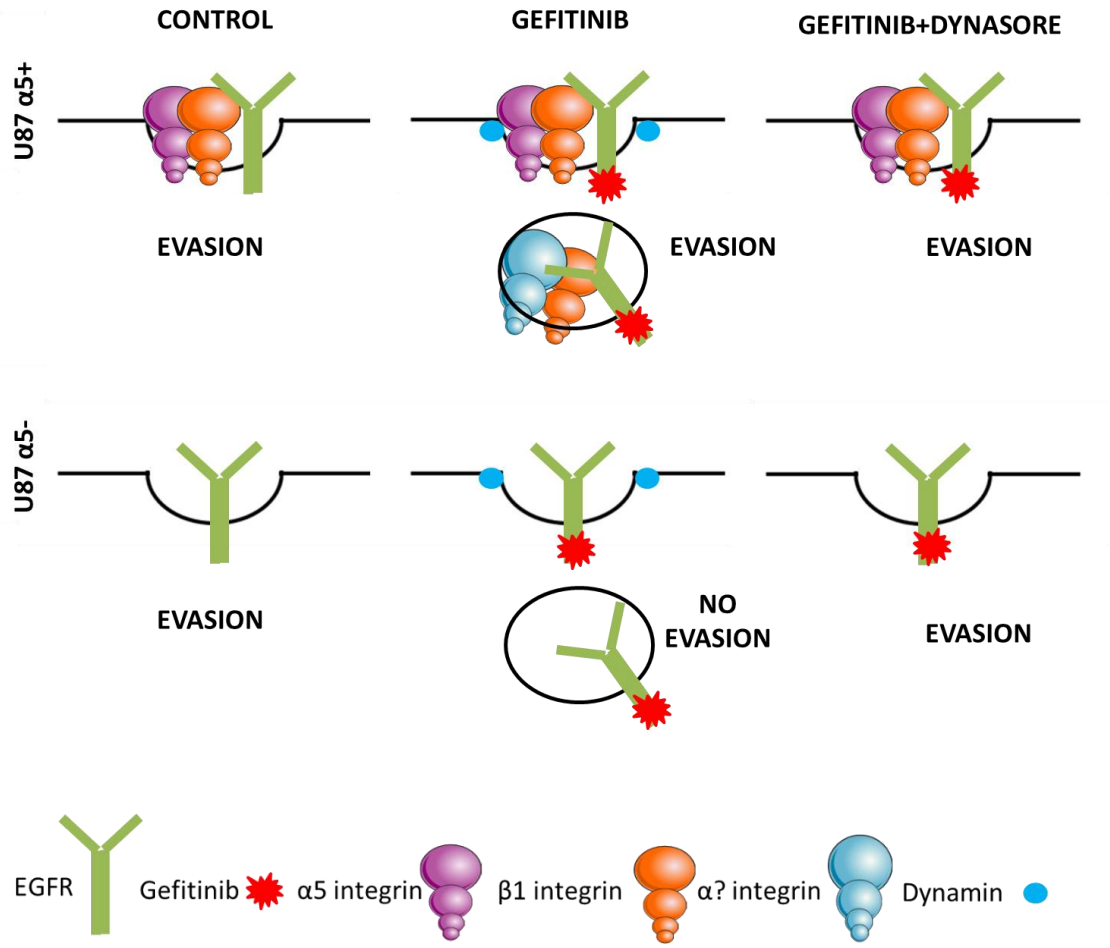

Graphical abstract: Dynamin inhibition enhances gefitinib resistance. Gefitinib treatment induces EGFR internalization independently of integrin expression level. α5 integrin depletion sensitizes cells to gefitinib treatment, since there is no evasion under these conditions. When endocytosis is impaired, cells become resistant (with a more evading behaviour) to gefitinib independently of α5 level. α5β1 integrin may impact on EGFR trafficking and function during membrane trafficking after endocytosis confering resistance towards gefitinib treatment.

Resumo

Glioblastoma é um dos tumores cerebrais mais agressivos, sendo extremamente invasivo e resistente à terapia. Na sua progressão ocorrem diversas alterações génicas, sendo uma delas a amplificação e/ou mutação do gene *erbB* 1.

O gene *erbB* 1 codifica o receptor tirosina cinase EGFR, um receptor de sinalização que está envolvido em muitos processos celulares Incluindo a migração, constituindo um importante alvo terapêutico no tratamento do glioblastoma. No entanto, as terapias dirigidas não têm sido bem sucedidas em ensaios clínicos. De momento, não existem quaisquer marcadores predictivos que determinem o carácter responsivo de um paciente a este tipo de terapia. Em outros tipos de cancro, já se encontram descritos diversos mecanismos de resistência, sendo um deles a cooperação entre EGFR e outros receptores, como por exemplo com as integrinas.

As integrinas são receptores de adesão celular. Em particular, a integrina α5β1 desempenha um papel importante na progressão do glioma, sendo um descrito alvo terapêutico. Esta integrina encontra-se sobreexpressa em estadios mais avançados da progressão do glioma, estando associada a um pior prognóstico e a um carácter mais invasivo e resistente do tumor. As integrinas e receptores de factores de crescimento como o EGFR cooperam em diversos níveis. A regulação do trafego intracelular já se encontra descrita como um mecanismo de resistência a terapias.

Devido ao interesse do grupo no papel da integrina α5β1 na progressão tumoral do glioblastoma, foi previamente geneticamente manipulada uma das mais comuns linhas celulares de glioblastoma (U87). Esta manipulação teve como objectivo a sobre-expressão e a sub-expressão da integrina α5. Estas linhas celulares foram tratadas com gefitinib, um inibidor tirosina cinase especifico para o receptor EGFR, e foi avaliada a evasão celular. A evasão celular foi avaliada através da migração de células de um pequeno agregado celular (esferoide). As células com níveis acrescidos de integrina α5 demonstraram um comportamento resistente após o tratamento com gefitinib. Foi também verificada uma internalização do receptor EGFR após tratamento através da técnica de imunofluorescência.

Perante estes resultados os objectivos do meu trabalho foram a verificação do papel da endocitose no tratamento com gefitinib e a importância da integrina α5β1 neste fenótipo.

A endocitose foi perturbada pela inibição da dinamina. A dinamina é uma GTPase envolvida na remodelação da membrana celular. Em mamiferos, a família das dinaminas é composta por três isoformas homólogas mas com diferentes padrões de expressão. A dinamina 1 encontra-se apenas expressa em neurónios, a dinamina 2 tem uma expressão ubíqua e a dinamina 3 encontra-se expressa no cérebro e nos testículos. A dinamina está envolvida na fissão de vesículas endociticas, sendo esta função dependente da sua actividade como GTPase. Após a ligação de GTP, a dinamina polimeraliza em torno do pescoço da vesícula. A hidrólise do GTP altera a conformação da dinamina, levando a fissão da vesícula pela geração de forças. A inibição da dinamina foi provocada por dois inibidores químicos diferentes. Dynasore é um inibidor não competitivo da actividade GTPase de ambas dinamina 1 e 2. Dynasore interfere com a actividade catalítica da proteína. Dyngo-4a é um inibidor mais potente, embora seja mais selectivo para dinamina 1 do que para dinamina 2. Dyngo-4a inibe a atividade GTPase ao ligar-se ao domínio G responsável pela ligação e hidrólise ao GTP.

A evasão celular foi avaliada com o tratamento com gefitinib e com ou sem inibição das dinaminas. Observou-se uma diminuição da evasão celular após tratamento com gefitinib, verificando-se novamente um carácter mais resistente por parte das células que sobre-expressam integrina α5. A inibição da dinamina reverte completamente o efeito negativo do gefitinib em relação à evasão celular, independentemente do nivel da integrina α5. Observou-se ainda um aumento da evasão celular com os inibidores da dinamina mas apenas na presença de gefitinib.

O efeito do gefitinib e dos inibidores da dinamina na internalização do ligando EGF foi avaliado recorrendo ao uso de EGF acopolado com fluorforo. Pode verificar-se que o tratamento com gefitinib aumenta a internalização do ligando, sendo este aumento inibido com a inibição da dinamina. Este fenótipo é integrina α5 independente semelhante ao estudo da evasão celular.

Para se averiguar a importância da endocitose no tratamento com gefitinib, imunofluorescência foi efetuada com anticorpos anti-EGFR e anti-EEA1. EEA1 é um marcador de endosomo inicial, sendo este a primeira estrutura vesicular após endocitose/internalização. Foi demonstrado que, após tratamento com gefitinib, EGFR é internalizado e encontra-se em proximidade de EEA1. Esta co-localização aumenta com o tempo de incubação com gefitinib e é integrina α5 independente. Isto demonstra a importância da endocitose neste tratamento.

Para determinar se as integrinas também são internalizadas após tratamento com gefitinib, foi realizada imunofluorescência usando anticorpos anti-EGFR e anti-integrina α5 ou integrina β1. Foi demonstrado que após tratamento, EGFR é internalizado juntamente com as integrinas. Devido à limitada resolução da microscopia confocal, esta co-localização foi confirmada por microscopia de super resolução, mais propriamente microscopia estocástica de reconstrução optica. Deste modo, confirmou-se a proximidade destas duas proteínas dentro de estruturas endomembranares.

Para verificar se este fenómeno de endocitose ocorre transversalmente em diferentes linhas celulares de glioma foi realizada imunofluorescência usando anticorpos anti-EGFR e anti-integrina β1. Verificou-se que o EGFR foi internalizado em todas as linhas celulares, e que este fenótipo é independente do nível de expressão de integrina α5, visto que as linhas celulares que apresentam um fenótipo mais marcante são as que quase não expressam esta proteína. É de reforçar que nestas linhas celulares apenas foi averiguado a occorrência da internalização de EGFR e integrina β1. Para averiguar o carácter resistente ou sensitivo destas células ao tratamento com gefitinib é necessário futuramente realizar estudos de evasão celular. Além do mais, foram utilizadas as condições de tratamento de gefitinib usadas na linha celular U87. Não foram efetuados nenhuns estudos de toxicidade ou efetividades do gefitinib, de modo a determinar as condições ótimas de concentração e duração de tratamento.

Os resultados obtidos sugerem que a migração é independente da endocitose do receptor EGFR, visto que quando a endocitose do receptor é impedida a migração celular é aumentada. A internalização do receptor EGFR após tratamento com gefitinib aparenta ser uma forma de diminuir a sinalização do receptor. A influência da integrina α5 na resistência ao tratamento com gefitinib deverá ser independente da endocitose, provavelmente tendo um papel **após** a internalização do receptor Alguns estudos mostraram que as alterações no tráfego dos receptores bem como a promoção da sua reciclagem por parte das integrinas funcionam como promotores de tumorigénese e potenciam a progressão tumoral. No caso do glioblastoma ainda não se encontram descritas alterações no tráfego de receptores como promotores de progressão tumoral.

Deste modo, este trabalho é um inovador ao demonstrar a importância da endocitose e do trafégo intracelular na resistência à terapia em glioblastoma.

Palavras-chave: Glioblastoma, EGFR, Gefitinib, Integrina α5β1, Endocitose

Contents

Figures Index

Abbreviations

A

ANOVA – Analysis of Variance
AP-2 – Adaptor protein 2
APPL1 - Adaptor protein, phosphotyrosine interacting with PH domain and leucine zipper 1
ARF - ADP Ribosylation Factors
ASCL1 - Achaete-scute homolog 1
ATCC – American Type Culture Collection
ATP – Adenosine triphosphate

B

BBB – Blood-brain barrier
bFGF - Basic fibroblast growth factor
BSA – Bovine serum albumin
BTC- Betacellulin

C

CD - Cluster of differentiation
CDK4 - Cyclin-dependent kinase 4
CDKN2A - Cyclin Dependent Kinase Inhibitor 2A
CHI3L1 - Chitinase 3 Like 1
CNS – Central Nervous System
CR - Cysteine residue
CYP – Cytochromo P450

D

DAPI - 4',6-diamidino-2-phenylindole
DCX – Doublecortin
DLL3- Delta Like Canonical Notch Ligand 3
DMSO - Dimethyl-sulfoxide
DNA - Deoxyribonucleic acid
DPBS - Dulbecco's phosphate buffered saline
DRP1 - Dynamin-related protein 1

E

ECM - Extracellular matrix
EDTA - Ethylenediamine tetraacetic acid
EEA1 - Early Endosome Antigen 1
EGFR – Epidermal growth factor receptor
EMEM - Eagle's Minimum Essential Medium
EPGN - Epithelial Mitogen
EPS - Epidermal Growth Factor Receptor Pathway Substrate
EREG – Epiregulin Gene
ERK - Extracellular signal-regulated kinases
ESCRT - Endosomal sorting complexes required for transport

F

FAK- Focal adhesion kinase
FDA – Food and drug administration
FRET - Förster resonance energy transfer

G

GABRA1 - Gamma-Aminobutyric Acid Type A Receptor Alpha1 Subunit
GBM - Glioblastoma
G-CIMP – Glioma CpG island methylator phenotype
GDP – Guanosine diphosphate
GED - GTPase effector domain
GFAP - Glial fibrillary acidic protein
GFP – Green fluorescent protein
GFR –Growth factor receptor
GPCR - G protein–coupled receptors
GPI - Glycosylphosphatidylinisotol
GTP - Guanosine-5'-triphosphate

H

HB-EGF - Heparin-binding EGF-like growth factor
HCl - Hydrochloric acid
HER - Human epidermal growth factor receptor
HRP - Horseradish peroxidase
hTERT - Human telomerase reverse transcriptase

I

IC_{50} - Half maximal inhibitory concentration
IDH - Isocitrate dehydrogenase
IGFR - Insulin-like growth factor receptor
ILK – Integrin linked kinase

J

JACOP – Just another co localization plugin

K

kDa – Kilo daltons
KRAS - Kirsten rat sarcoma viral oncogene homolog

M

mAb – Monoclonal antibody
MAP2 – Microtubule associated protein 2
MAPK - Mitogen Activated Protein Kinases
MDM2 - Mouse double minute 2 homolog
MEK – Mitogen-activated protein kinase kinase
MGMT - O^6-methylguanine DNA methyltransferase
MIG6 - Mitogen-inducible gene-6
MMP - Matrix metalloproteinases
mRNA – Messenger ribonucleic acid
MTIC-3-methyl-(triazen-1-yl)imidazole-4-carboxamide
mTOR - Mammalian target of rapamycin
MTT-3-(4,5-dimethylthiazol-2-yl)-2,5-diphenyltetrazolium bromide
MVE – Multi-vesicular endosome

N

NEFL – Neurofilament light
NF1 - Neurofibromin 1
NF-ƙb - Nuclear *factor* kappa B
NOS – Nitric oxide synthase
NSCLC – Non-small cell lung carcinoma

O

OCT4 - Octamer-binding transcription factor 4
OLIG2 - Oligodendrocyte transcription factor

P

PI3K - Phosphatidylinositol-4,5-bisphosphate 3-kinase
PBS - Phosphate buffered saline
PDGFR - Platelet-derived growth factor receptor
PDX – Patient- derived xenograft
pH – Potential of hydrogen
PH - Pleckstrin homology domain
PIQ - Plateforme d'Imagerie Quantitative (http://imageriepiq.u-strasbg.fr)
PLC- Phospholipase C
PRD - PTS Regulation Domain
PTEN - Phosphatase and tensin homolog
PTP1B - Protein-tyrosine phosphatase 1B
PVDF - Polyvinylidene fluoride

R

RALT - Receptor-associated late transducer
Rb1 – Retinoblastoma 1
RGD - Arginylglycylaspartic acid
ROS – Reactive oxygen species
rpm - Revolutions per minute
RTK – Receptor tyrosine kinase

S

SDS - Sodium dodecyl sulfate
SEM - Standard error of the mean
SLC12A5 - Solute Carrier Family 12 Member 5
SNP - Single nucleotide polymorphism
SPRY2 - Sprouty RTK Signaling Antagonist 2
STAT – Signal transducer and activator of transcription
STORM-Stochastic Optical Reconstruction Microscopy
SYT1 - Synaptotagmin 1

T

TBS - Tris-buffered saline
TCF4 - Transcription Factor 4
TCPTP - T cell protein tyrosine phosphatase
TG - Tris-Glycine
TGF - *Transforming growth factor*
TIC – Tumor initiating cell
TIMP - Tissue inhibitor of metalloproteinase
TJ – Tight Junction
TK – Tyrosine kinase
TKI - Tyrosine kinase inhibitor
TMZ - Temozolomide
TNF – Tumor necrosis factor
TP53 – Tumor protein p53
TRADD - Tumor necrosis factor receptor type 1-associated death domain

U

UK – United Kingdom
uPA – Urokinase- type plasminogen activator
USA – United States of America
UV - Ultraviolet

V

VEGF – Vascular endothelial growth factor

W

WHO – World Health Organization

1. Introduction

1.1 Glioblastoma

Epidemiology

In Europe, central nervous system (CNS) tumors are the 17th most common cancer type, with 57 100 new cases diagnosed in 2102. They are the 11th cause of cancer death, with around 45 000 deaths in 2012 (1). Glioblastoma (GBM) is the most common and most aggressive malignant tumor in CNS representing 20% of all the primary brain neoplasm. GBM are the highest-grade astrocytoma and remained essentially incurable. Despite numerous efforts, the overall 5 years survival rate does not exceed 5 years and median survival is around 15 month (2). GBM can appear anywhere in the brain, but their preferred localization is the supratentorial region, having edema surrounding the tumor (3). GBM is more prominent in men than women, having a peak of incidence between 45 and 70 years old (2).

Risk factors for CNS tumors

The risks factor associated with GBM development are ionizing radiation, decreased susceptibility to allergy and immune factors and genetic alterations. There are single nucleotide polymorphisms (SNP) that increase risk of GBM with inherited variation, in the chromosome 9p21 that contain cyclin-dependent kinase inhibitor 2B gene, and two SNPs in the regulator of telomere elongation helicase 1 (3,4).

Symptoms of GBM

The usual symptoms englobe headache, seizures, nausea, vomiting and hemiparesis. The diagnosis is made by cranial magnetic resonance imaging (fig.1.1) (3,4).

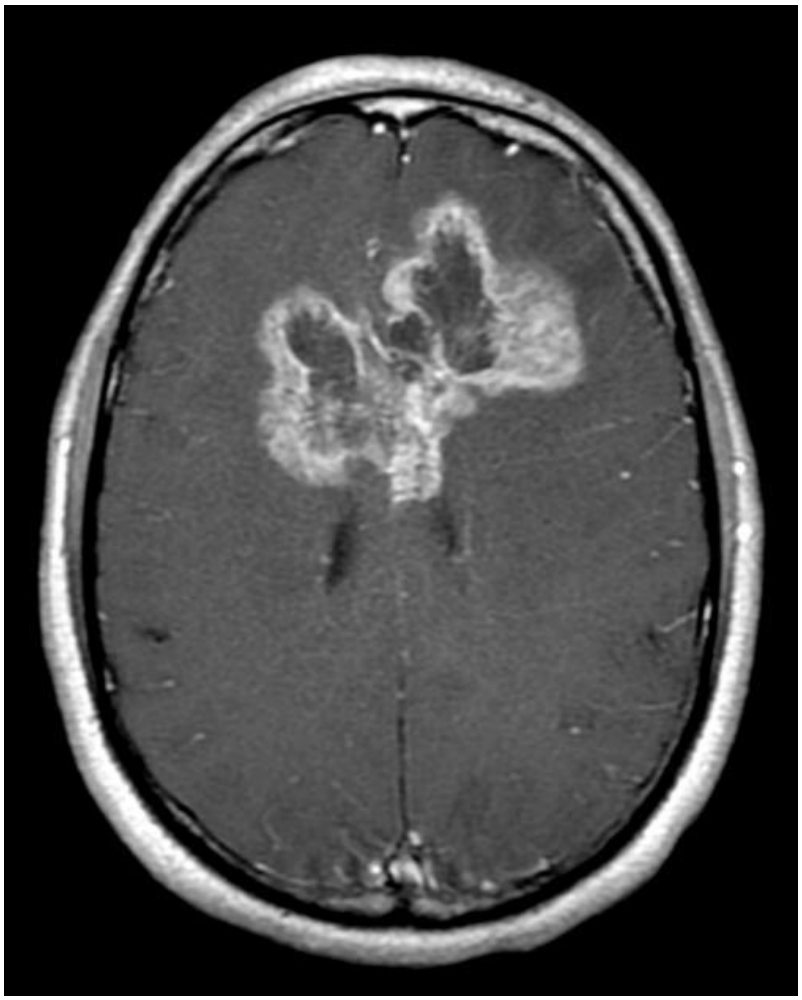

Figure 1.1: Magnetic resonance image from a glioblastoma tumor.
Adapted from (5)

Glioblastoma classifications and characterization

For decades, brain tumor classification was based on their histology and the microscopic similarities observed on light microscope after various coloration. This bring to the creation of groups of tumors that can be highly heterogeneous such as the astrocytoma or the oligodendrocytoma. In 2016, the World Health Organization (WHO) presented a new classification of CNS tumors based in integrated phenotypic and genotypic parameters (Fig.1.2) (6). Glioblastomas are now classified as grade IV diffuse astrocytic and oligodendroglial tumors. Glioblastomas are further segregated depending of their analysis of IDH status. *IDH*-wildtype GBM represent 90% of the GBM and the other 10% shared a genetic driver mutation on *IDH1* and *IDH2* genes. The evaluation of IDH status is made by R132H IDH1 immunohistochemistry and *IDH* sequencing. When IDH

evaluation cannot be performed, the GBM are denominated GBM NOS (not otherwise specified) (6).

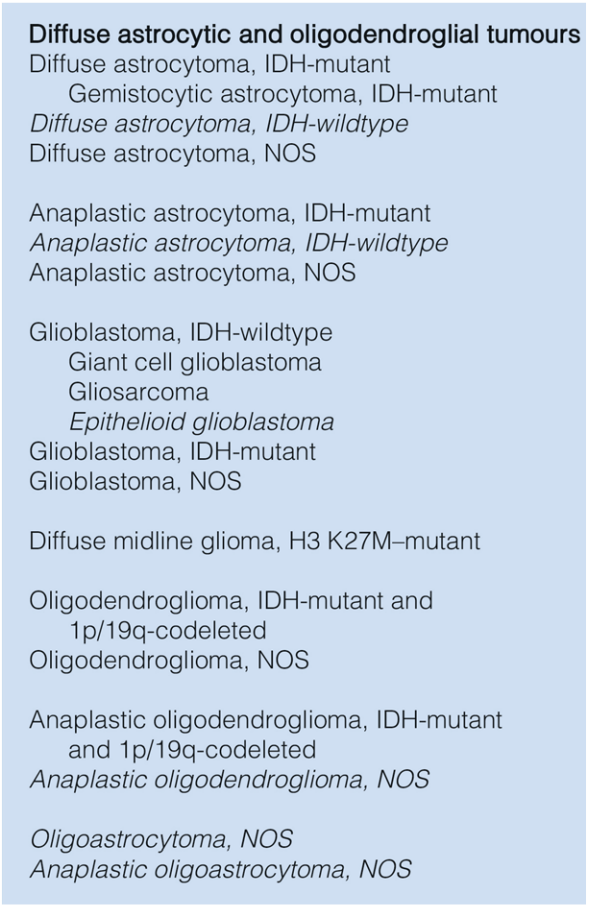

Figure 1.2:Diffuse astrocytic and oligodendroglial tumours subcategorization in 2016 WHO Classification for CNS tumors. Adapted from (6)

But in this classification the subcategorization of GBM is only based in one molecular marker, the IDH status.

GBM can also be divided into de novo and secondary GBM, each characterized by different pathways (Fig.1.3). De novo GBM doesn't have evidences of previous lesions, being 80% of all GBM and usually affects older patients (over 55 years old).

Genetically, de novo GBMs are characterized by *HER1* amplification, *PTEN* mutations and *p16* deletions. They are also *IDH1* wild type and mutated in *hTERT* promoter. The chromosomal events underneath de novo GBM formation could be the amplification of 12q14 region, where are encoded the *CDK4* and *MDM2* genes, occurring then a disruption of p53 and Rb1 pathways; the homozygous deletion of 9p, where are encoded the genes

p16, *p15* and *p14* ARF; the loss of heterozygosity of 10q, where are encoded the gene *PTEN*. *HER1* amplification is found in 40% of de novo GBM, followed by mutations that result in the constitutive activation of EGFR. *PTEN* mutation is found into 45% of de novo GBM, leading to a constitutive activation of PI3K/AKT pathway.

Secondary GBM affects young patients and develops from previously described low grade astrocytoma or anaplastic astrocytoma. In secondary GBM there are low grade genetic alterations, such as *TP53*, *PDGF-A*, *Rb1*, *ATRX*, and *IDH1*. (2,4,7,8).

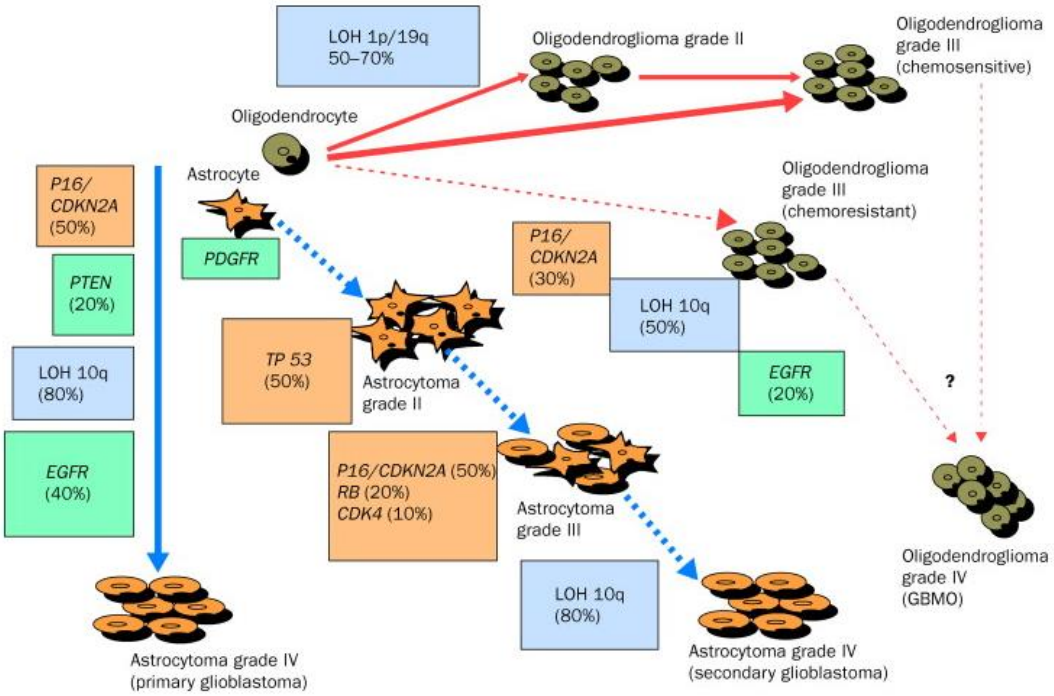

Figure 1.3:Molecular changes in primary brain tumor progression. In orange there is represented the cell cycle alterations, in green the signaling pathways alterations and in blue the heterozygous alterations. Adapted from (7)

In a preclinical study, *Verhaak et al* described four subtypes of GBM (Proneural, Neural, Classical and Mesenchimal) based on gene expression, demonstrating a greater inter heterogeneity between patients. In figure 1.4, are represented the main genetic alterations that distinguish these subtypes. The proneural subtype is characterized by alterations of *PDGFRA*, points mutations in *IDH1* and *TP53* mutations. Focal amplification of *PDGFRA* is associated also with high levels of *PDGFRA* gene expression. *Tp53* mutations were associated with loss of heterozygosity. Its signature also has proneural developmental genes (*SOX*, *DCX*, *DLL3*, *ASCL1* and *TCF4*) and oligodendrocytic ones (*PDGFRA*, *NKX2-2*, *OLIG2*) (9). The neural subtype has expression of neuron markers

such as NEFL, GABRA1, SYT1 and SLC12A5 (9). Classical subtype has the typical GBM amplification of chromosome 7 and loss of the 10. Classical GBM are characterized by high expression levels of *erbB1*, without the presence of mutations on *TP53*. However, alterations in RB pathway with homozygous deletion of *CDKN2A* are found. In this subtype there are also expression of neural precursor markers NES, as markers from Notch and Sonic Hedgehog pathways (9). The classical subtype is more responsive to therapy (temozolomide/radiotherapy). Finally, the mesenchymal GBM are characterized by the focal hemizygous deletion at 17q11.2 leading to loss of *NF1*. The expression of mesenchymal markers (CHI3L1 and MET) is associated with epithelial-to-mesenchymal transition. The significant existence of necrosis and inflammation can be explained by the expression of genes from TNF and NF-Kb pathways (*TRADD, RELB*) (9).

Intra-tumoral heterogeneity is a hallmark of GBM. To explain this heterogeneity there are three theories: the clonal evolution, the cancer stem cell theory and interclonal cooperativity. In the clonal evolution, the initial cell suffers somatic alterations giving arise to different clones that are genetically unstable. From these clones, only the ones with the most aggressive behavior and less sensitive to therapy are favored and survive. In the cancer stem cell theory, only a group of cells have the ability to self-renew, continuous proliferation and ability to give arise to different clones. Numerous works describe that these cells are also resistant to therapy. In the interclonal cooperativity theory, the heterogeneity is due to the interactions between tumor cells and a changing microenvironment (immune cells, stromal cells and the extracellular matrix). For example, tumor evolution and self-renewing of glioblastoma cancer stem are affected by the hypoxic perivascular niche (9–11).

Intra-heterogeneity has a relevant clinical implication because it usually leads to therapy failure. So it should be important to perform the molecular analysis in distinct tumor biopsies from different parts of the tumor (10).

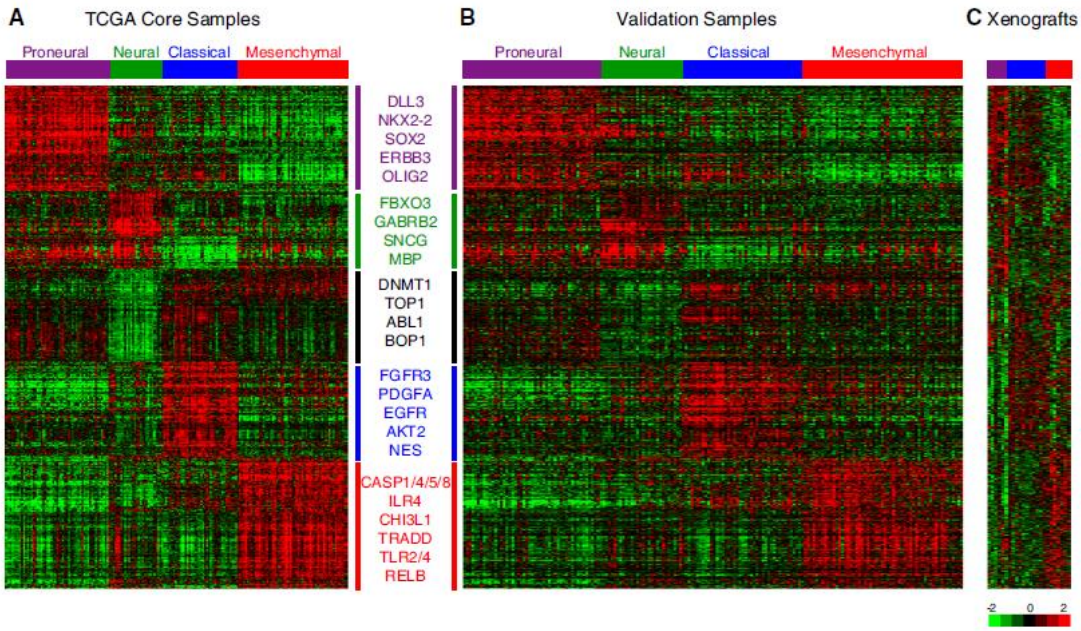

Figure 1.4: Gene expression of the four subtypes of glioblastoma. The heatmap represents three different sources of DNA, where DNA microarrays for the main genes that characterized each GBM subtype were analyzed. The results are represents in a gradient colorated scale when green means a loss of expression and red a gain of expression. Adapted from (9).

Glioblastoma Invasive behavior

GBM is a very locally invasive tumor. This migration capacity allows cells to develop tumor in the opposite hemisphere from the primary site or even multifocal GBM tumors (3).

Primary brain tumors have a unique pattern of invasion and rarely metastasize outside of the brain. Usually GBM cells, invade as single cells to almost anywhere in the brain. They infiltrate along blood vessel walls periphery, corpus callosum of neural fibers and astrocytes glia limitans externa. This invasion phenotype is not the same in tumors that metastasize to the brain, since these are more static, and when they invade it happens in group and only in short distances (13).

During evasion, cellular morphology changes (fig.1.5). When GBM cells migrate along blood vessels, they present a spindled shape with a single pseudopodium that extends toward the movement direction by polarization of actin polymerization. When they migrate through the brain parenchyma, they present multiple pseudopodia pointed in different directions. One of these directions will be chosen and be an invasion guide. GBM cells migrate using mesenchymal motility form that is dependent on the adhesion to the extra cellular matrix (ECM) and their remodulation. The invasion results then on

the combination of cell shape, position and tissue architecture, being needed PI3K signaling activation and also small GTPases. The pseudopodium interacts with ECM mainly through integrins and their focal adhesion complexes, acid hyaluronan receptor CD44. These two receptors have as main ligands proteins that are abundant in brain parenchyma as hyaluronan, collagen, fibronectin and laminin. ECM is remodeled by serine proteases, cysteine proteases and metalloproteases (MMP). In the serine proteases, the most studied is the complex urokinase-type plasminogen activator (uPA)/ uPA receptor that activates plasmin and degrades fibronectin and laminin. In the cysteine proteases, Cathepsin B is involved in laminin and collagen degradation and in GBM invasion. In GBM, the most important MMPs involved in cell invasion are MMP-2 and -9. The inhibition of these MMPs leads to less migration and invasion in glioma cell lines and also in glioma cells xenografts. Tissue inhibitors of MMP (TIMP) modulates the proteases activity by forming complexes with them. Their addiction is reported to decrease cell invasion (14–18).

Invasion is a process with multiple involving factors that can be targeted in a way to treat GBM.

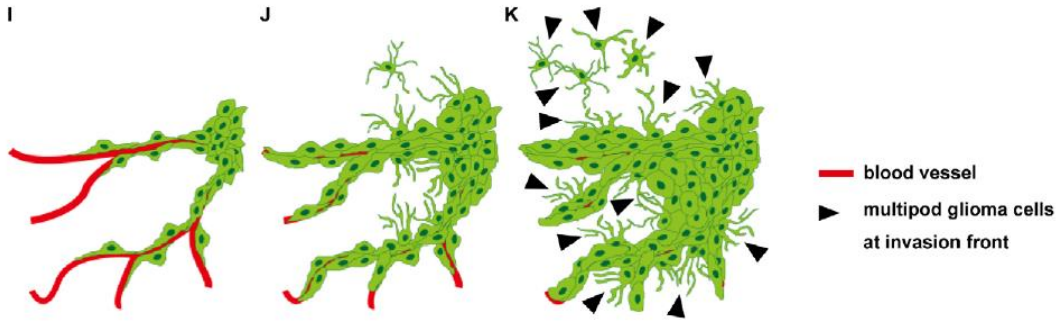

Figure 1.5: Hypothetic model of GBM progression. Two distinct cellular morphologies whether cells invade along the periphery of blood vessels (I) or through the brain parenchyma (K). Adapted from (19).

Glioblastoma Treatment

GBM treatment starts with surgical resection, followed by radiotherapy and chemotherapy. Until 2005, after surgical resection were performed a radiotherapy with adjuvant carmustine, a nitrosourea drug with alkylating function (4). A clinical trial (trial 22981/26981) showed that concomitant administration of temozolomide (TMZ) with radiotherapy, with adjuvant TMZ resulted in a better survival for the patient with minimal

levels of toxicity (20). Surgical resection is decompressive and cytoreductor, being associated with the increase of survival if there is complete resection of the tumor. To facilitate the tumor removal, a tumor fluorescence derived from 5-aminolevulinic acid is used to enhance the contrast of normal-tumor tissue (21).

The radiotherapy used in the study was a fractionated focal type, where occured a irradiation of 2 Gy/ fraction, once a day for five days/week, for a period of six weeks (total of radiation given to the patient was 60Gy) (22).

The drugs used to treat GBM must be able to cross the blood-bran barrier (BBB), so they must have a low molecular weight, high lipidic solubility and low ionization, and they also must have minimal protein binding capability (23). TMZ is an oral alkylating agent. It is a pro-drug that is spontaneous converted to the active metabolite, imidazole-4-carboxamide. It is able to methylate DNA, in N-7 or O-6 positions of guanine residues. TMZ is a small, lipophilic compound and so it is able to cross the BBB (24,25). TMZ is given concomitantly with radiotherapy for the following reasons:

- A daily administration of low doses has a greater intensity of activity without additional toxicity,

- After radiotherapy, the enzyme MGMT is activated and repairs the DNA damage. A continued administration of an alkylating agent such as TMZ depletes this enzyme.

- It was observed an *in vitro* synergetic effect by the concomitant use of TMZ and radiotherapy.

- TMZ was also chosen by its capability of crossing the BBB and the spontaneous conversion into the active metabolite (MTIC).

TMZ was administrated daily, all days of the week during radiotherapy, and for 5 days in the adjuvant six cycles that occurred during 4 weeks (22).

Even with treatment, the median survival rate is less than a year, between 9 to 15 months (26). After recurrence, the tumor is often different from the primary. The recurrent tumor doesn't respond well to TMZ, and it also presents high expression levels of VEGF. In a clinical trial for recurrent GBM, combined treatment with bevacizumab (humanized IG1 monoclonal antibody for VEGF) and irinotecan (topoisomerase1 inhibitor) gives a survival rate of 7-9 months after treatment, similar to the conventional treatment (27).

Predictive and prognostic factors of GBM

Predictive factors/markers are used to evaluate the responsiveness to a treatment, with the objective of stratifying the patients according to the benefit or not from a specific treatment. Prognostic factors/markers are used to evaluate the overall outcome of the patients (28,29).

In GBM, there are good prognostic factors such as young age at diagnosis, cerebral location and maximal tumor resection. The Methylation status of the O6-methylguanine-DNA methyltransferase (*MGMT*) promotor, *IDH1/2* mutation, *erbB1* amplification, glioma-CpG island methylator phenotype (G-CIMP), *TP53* mutation and losses of chromosomes are genetic prognostic factors. The MGMT is an enzyme that removes alkyl groups from the O6-guanine, producing a resistance to alkylating agents. After methylation of the *MGMT* promotor, this one is silenced and cells are incapable to repair the DNA damage and become more sensitive to TMZ. *MGMT* promoter methylation has then a prognostic significance. Besides this, *MGMT* promoter methylation also has a predictive one since it predicts tumor responsiveness to alkylating agents such as TMZ. The MGMT promoter is methylated in approximately 50% of GBM, being associated with *IDH1/2* mutations (common in secondary GBM). In *IDH1/2* mutations the more frequent ones are in *IDH1* appearing mainly in secondary GBM. This mutation is associated with lesions with less necrosis and small areas of tumor, having then a more favorable prognosis. G-CIMP occurs in 10% of GBM, more common in secondary ones, being associated with *IDH1/2* mutations (3,30). Mutations in *ATRX* cause alternative lengthening of telomeres, being present associated with *IDH1/2* and *TP53* mutations, mainly in secondary GBM. *TERT* mutation is most frequent in de novo GBM, being correlated with *erbB1* amplification and a shorter patient survival (3,30). EGFR overexpression was associated with worse prognosis in younger patients bearing *Tp53*-wildtype tumors, while in older ones appears to have a better prognosis. So, *TP53* mutations are not a definitive prognostic marker (3,30).

Cancer initiating tumor cells

Tumor initiating cells (TIC) are a subpopulation of cells in a tumor. These cells have some stem cell properties such as: renewing capability, unspecialized characteristics and capability to become into differentiated cells. To evaluate these stem cells properties, must be study the self-renewal properties and their capability to initiate a tumor (31,32).

Neural stem and progenitor cell are cell types present in the brain, expressing both CD133+. In Singhs *et al* study, CD133+ cells with stem cell properties *in vitro* were isolated from human brain tumors. CD133+ GBM cells represent a proportion between 3-30% of the tumor. These cells were capable to produce tumors in NOCID mice. These tumors resemble the human tumor in the expression of markers such as nestin, MIB-1, GFAP, MAP2. In the tumor obtained, were found CD133 positive and negative cells, and the CD133+ cells were different to MAP2+ cells. These data evidence that the CD133+ initiating cells could give arise to differentiated cells. These study showed that the hypothesis of TIC in GBM should be taken seriously, due to the fact that conventional therapies don't kill them, having them the possibility to allow tumor progression or relapse (33). Sub-populations of TIC have high levels of SOX2, OCT4, and NANOG, all known to maintain self-renewal and cellular proliferation (30).

Effect of brain tumor in BBB permeability

Brain tumors increase BBB permeability by disruption of tight junctions (TJ) and due to increased angiogenesis. It is well known that GBM is characterized by a high level of angiogenesis. In GBM, vessels are tortuous and leaky. One growth factor responsible for angiogenesis, VEGF, is present in high levels in GBM. VEGF enhances endocytosis of VE-cadherin, and consequently there is a disruption of the endothelial barrier, increasing in this way also its permeability. Other factors produced in GBM, such as TGF-β2, caveolin-1, ROS and aquaporins, induce secretion and activation of MMPs that degrade TJ. It has been reported the loss of claudin3 and occludin in primary brain tumors that enhances disruption of BBB permeability. In GBM there are also increased levels of membrane transporters such as folate and insulin receptors that can facilitate the entry of molecules through the BBB. By another way, even with BBB permeability changed, others mechanism involved into the protection of chemical entry into the brain are intact. It has been shown that the expression of P-gp was not altered in GBM, remaining functional and limiting the brain diffusion of chemicals such as therapeutic drugs .

Pre-clinical models of glioblastoma

GBM cell culture is a useful tool to study cell processes before using tumor behavior in animal models. Usually, a cell culture has optimized conditions for proliferation and survival of the cells. The medium used supply the cells with all metabolites, growth factors and cytokines. But tumor cells in culture have unlimited oxygen and optimal pH,

and that is not the reality *in vivo* due a hypoxic microenvironment. Furthermore, in culture the cells don't have a three-dimensional interaction with the other cells and matrix. To overcome this, there are spheroids models that mimetic it (37).

Due to selection pressure on cell culture, genetic alterations can occur and alter the genetic and phenotypic profile of the cancer cell lines in comparison to the original tumor (38). After a study between solid primary GBMs and GBM cell lines were identified 160 proteins gained and 60 proteins lost in culture, losing then the GBM heterogeneity and making difficult any comparation between *in vitro* and *in vivo*. One of this lost is EGFR overexpression (27–31).

The GBM cell lines are obtained from human brain diagnosed with GBM, astrocytoma grade IV. After the excision of the tumor, some cells are put into petri dishes. Here most of the cells die, and the ones which survived after a few passages become into an immortalized cell line. For glial cells, Pontén and Macintyre in 1968 were the first ones to optimize the culture conditions (39).

One of the usual GBM cell lines is U87. Genetically, U87 is hypodiploid human cell line, that easily forms tumors when injected in mice. These tumors have a huge vessels network (40).

The use of tumor initiating cell lines that are maintained in serum free conditions with growth factors (PDGF, bFGF, EGF) and growth as tumor spheroids are able to retain the tumor phenotype and tumor initiating capacity. But it was shown that growth of tumor initiating cells in adherent culture maintains highly pure stem cells populations (41,42).

Patient derived xenografts (PDX) are a tool to improve pre-clinical studies, since the tumor cells grow in an *in vivo* environment. PDX can be made using fresh tumor samples or cryopreserved ones (tissue cryopreserved at low temperature right after tumor excision). The single cell suspension can be implemented in the brain (orthotropic) or in the mice flank (heterotopic). But that was reported that heterotopic PDX do not demonstrate a local invasive profile compared to the orthotropic ones. This different can be explained by the different microenvironment in the two cases. But even in orthotropic xenograft, the murine brain microenvironment is different molecular and functionally from the human. The xenograft should be done in mice lacking immune system, since it was demonstrated that residual active immune system prevents tumor formation (43,44).

As we can see, GBM is a malignant and higly resistant tumor. Its biology needs to be better studied. One interesting therapeutic target in GBM is EGFR, since it is founded overexpressed in 40% of the cases. EGFR is a signaling receptor that is involved in the main signaling pathways that leads to cell migration and invasion, which are typical in GBM.

1.2 EGFR

EGFR and Glioblastoma

The discovery of EGFR in malignant transformation was made in the 80's by oncogenic viruses that showed EGFR as a cellular homolog of the avian erythroblastosis virus *v-erbB* oncogene (45).

The EGFR signaling network is critical for tumor progression because it promotes cancer cell survival, growth and invasion. In GBM, *erbB1* the gene encoding of the EGFR/ErbB1 protein is amplified is 40-60% after gene rearrangement and/or focal amplification. This amplification is often associated with mutations. These mutations can lead to ligand independent activity of the receptor, and are also reported to enhance motility and invasion by inducing genes of the extracellular matrix, metalloproteases and serine proteases. *erbB1* mutations in GBM are common, and they can be N-terminal truncation (EGFRvI), deletion of exons 14 – 15 (EGFRvII), deletion of exons 25 – 27 (EGFRvIV), C-terminal truncation (EGFRvV) and C-terminal duplications and truncations. The most common mutation in GBM is EGFRvIII (occured in more than 50% of the GBM cases). EGFRvIII is a truncated protein due to loss of exons 2-7, that gives arise to a 801 base pair deletion. The amino acids 6-273 are replaced by a glycine residue, and so the resulted protein is a 145 kDa glycoprotein with constitutive, ligand-independent activation. The constitutive activation is due the reduced interaction with E3-ligase Cbl, leading to a reduced degradation of the receptor which a negative feedback regulation system. EGFRVIII is also occurs in lung, breast, ovarian and prostate cancers (37–39,41,42).

As described above, EGFR overexpression has a relevant role in GBM progression. EGFR is a signaling receptor that is involved in diverse cellular processes, like cell migration and invasion (characteristics of GBM).

HER family

EGFR belongs to a family called HER family, which has four transmembrane receptors: EGFR (*HER1*), ERBB2 (*HER2*), ERBB3 (*HER3*) and ERBB4 (*HER4*) (50).

The EGFR is a 170 kDa glycoprotein, with 1186 amino acids that is composed by three main domains: an extracellular ligand-binding domain (ectodomain), a hydrophobic transmembrane domain and a cytoplasmic tyrosine kinase domain (46,47,50).

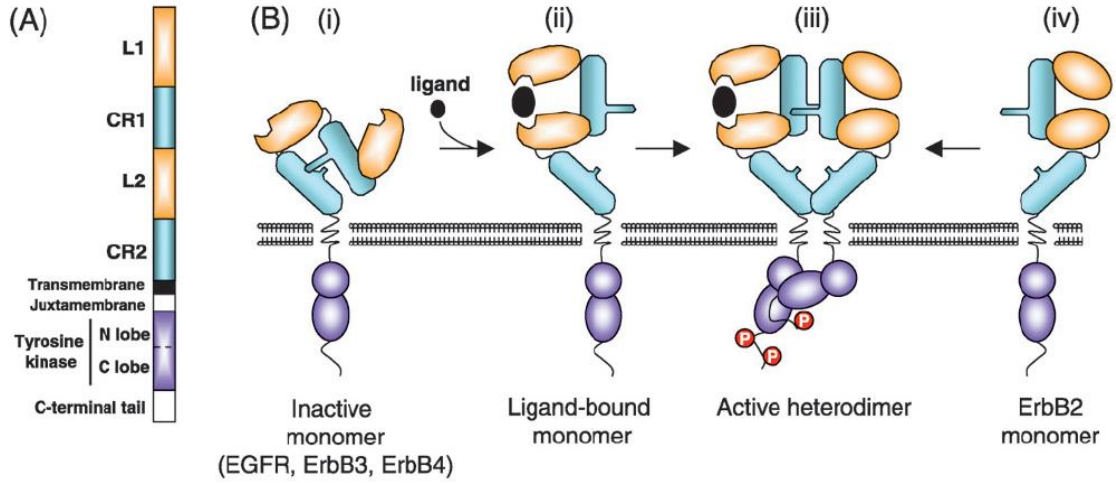

Figure 1.6: Schematic of ErbB receptor structure and its dimerization and activation. A – Schematic of ErbB receptor showing the different parts: ectodomain (L1,L2 – leucine-rich domains, CR1, CR2 – cysteine rich domains), transmembrane domain, tyrosine kinase domain and c-terminal tail. B- Schematic of dimerization and receptor activation: i- receptor in inactive state, ii- ligand binds to L1 and L2 changing receptor conformation, iii- receptor dimerize through cysteine domains, creating docking sites in tyrosine kinase domain, iv- ErB2 in is inactive state has the same conformation that the rest active receptors. Adapted from (47).

The ectodomain contains four subdomains: two leucine-rich subdomains (in figure 1.6 L1 and L2) and two cysteine-rich subdomains (in figure 1.6 CR1 and CR2). The leucine domains directly bind to ligand, while the cysteine domains are involved in interaction and dimerization with others receptor. The leucine domain is different between the family members, giving to them different ligand specificity.

While, the cytoplasmic domain is a highly conserved bilobed tyrosine kinase. Only HER3 does not have kinase activity. Between the two lobes there is a ATP binding site. The activation of the receptor by ligand binding (between L1 and L2) creates an extended conformation. This expose the dimerization loop present in CR1, allowing dimerization. In this moment, occurs the interaction between the N-lobe of one domain with the C-one of another, creating phosphorylated binding sites as docking sites (46,47,50).

The EGFR known ligands are EGF, TGFA/TGF-α, amphiregulin, epigen/EPGN, BTC/betacellulin, epiregulin/EREG and HBEGF/heparin-binding EGF. Some of them are cell membrane anchored proteins that are proteolytically disrupted to become soluble molecules that will induce EGFR activation. Their cleavage by metalloproteinases can be

activated by GPCR. The ligands can be overexpressed by active Ras or steroid hormones (47,50). EGFR can also be activated by ligand-independent mechanism. Ligand-independent activation can be induced by unphysiological stimuli (such as oxidative stress, UV, and irradiation), by others RTK (such as MET, IGFR) or by GPCR and adhesion receptors like integrins (51). In GBM, MET is also found dysregulated, being this a possible cause for anti-EGFR therapy resistance. EGFRvIII is described to be a activator of Met, and so the dual treatment is shown to reduce tumor growth (52,53).

EGFR activation is attenuated by tyrosine dephosphorylation of active receptor, by phosphatases such as density-enhanced phosphatase-1 and PTP1B. Their catalytic activities eliminate the sites in which signaling intermediates or adaptor proteins would bind and promote cell signaling (47). However little is known about the involvement of PTP1B in glioma progression and invasion.

EGFR signaling pathway

Receptor homo- and/or heterodimerization occurs after ligand binding, followed by activation of the tyrosine kinase activity with consequent tyrosine autophosphorylation on the cytoplasmic specific residues (Fig.1.6) (47,50).

These phosphorylated residues become docking sites for adaptor proteins such as Grb2 (binds to pY1068 and pY1086) or Shc (binds to binds pY1148 and pY1173), that can activate RAS/Raf/MAPK downstream signaling cascade (45,47). MAPK pathway is activated through the interaction between the Grb2 and SoS, leading to proliferation, migration, angiogenesis and differentiation. p38-MAPK in GBM is linked to invasion and angiogenic phenotypes (54,55). Its inhibition leads to decreased tumor growth in glioma xenografts (56). MAPK pathway is also involved in regulation of neural stemness (57).

EGFR activation leads to the stimulation of the PI3K/Akt pathway through the recruitment of the regulatory subunit p85. Whereas EGFR and ErbB2 receptors bind indirectly to p85 through adaptor proteins like Gab1, ErbB3 and ErbB4 directly bind to p85 (47,51). PI3K pathway is often dysregulated in GBM, since their negative regulators are frequently mutated, for example the loss of PTEN is founded in 45% of GBM cases. Studies targeting signaling pathways of this cascade such as mTOR are showing regression in GBM (58,59). In GBM, p85 can be also activated by direct interaction with cancer stem cell marker CD133, leading to PI3K activation (60).

All ligands and receptors of the family can activate the signaling cascade like Ras/Raf/MEK/MAPK, PI3K, PLC- γ and STAT. These signaling pathways are involved in glioma progression (fig.1.7).

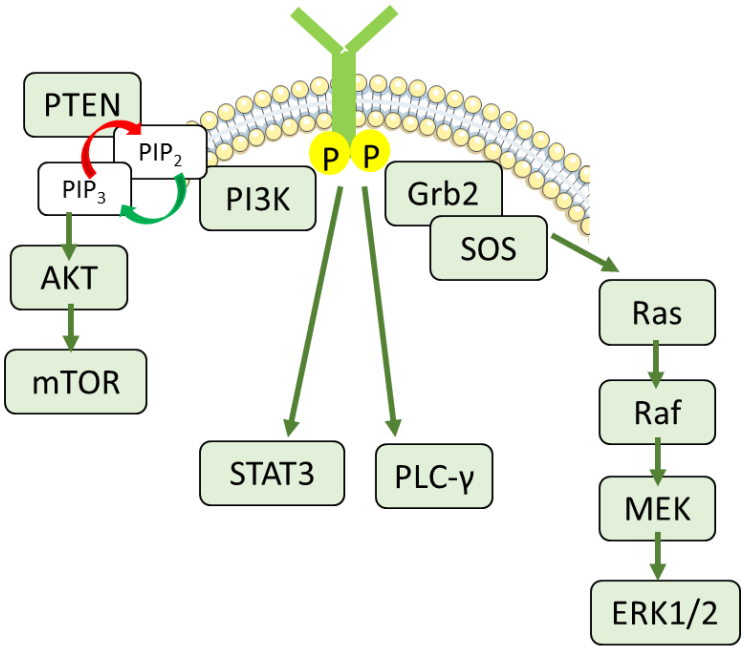

Figure 1.7: Schematic of some EGFR signaling pathways involved in glioma progression. After EGFR activation and auto phosphorylation are created docking sites for signaling molecules. EGFR interacts with Grb2 mediator to activate MAPK pathway. PI3K pathway is activated on the plasma membrane and the signal is controlled by PTEN. PTEN is usually mutated in GBM. EGFR can also activate directly STAT3 and PLC-γ pathways

The EGFR TK domain has numerous substrate proteins like STAT family members. STAT3 binding to activated EGFR leads to STAT3 dimerization and translocation into the nucleus (46,47,51). In GBM, the co-expression of EGFR and the mutant EGFRvIII activates STAT3/5 leading to glioma progression. EGFR phosphorylates the mutant receptor, allowing its nuclear entry where it forms a complex with STAT3. This study shows that EGFR not only function as a signaling receptor but also as a transcription factor (61). EGFR has a tyrosine residue (Tyr 992) that allows direct interaction with PLC-γ leading to actin reorganization and asymmetric motile phenotype (45,46). In GBM, was reported that the activation of PLC-γ and STAT3 leads to migration and invasion (62).

Endocytic pathway of EGFR

Internalization of the EGFR has contradictory results. Endocytosis of EGFR constitutes a regulatory mechanism of this signaling pathway, having different described functions. The internalization can attenuate the signal leads to receptor degradation, or also allows the continuation of the signal by endosomal signaling and/or recycling of the receptor back to the plasma membrane. Indeed, EGFR membrane trafficking is required for activation of specific transducers and has been shown to play critical role in cancer cell invasion, as described below. Two main steps compose the endocytic pathway: the internalization of the receptor and its trafficking in intracellular compartments (Fig.1.8) (63,64).

The internalization controls the levels of receptors that are present at the plasma membrane, regulating their accessibility to ligands.

There are described diverse endocytic pathways that lead to EGFR internalization, being the most important the clathrin-dependent pathway. Clathrin-independent pathway was described to be used in high levels of EGF environment. Also the internalization pathway can be chosen by the type of ligand bound to the receptor: EGF and TGFα induces clathrin-dependent pathway, while HB-EGF a clathrin-independent pathway. Inactive EGFR is usually associated with caveolae rafts. After ligand binding, EGFR moves out from there, dimerize and enter into the cell by clathrin-dependent endocytosis. The binding of Grb2 to EGFR allows its ubiquitination by E3 ubiquitin ligase Cbl on pY1045. Once ubiquinated, EGFR interacts with Eps15, allowing the binding to the clathrin-pit through AP-2 (65,66). The ubiquination of EGFR promotes its lysosomal degradation. There are also negative feedbacks produced after EGFR activation that lead to signal attenuation, such as the production of suppressor of cytokine signaling-5 (binds to EGFR and promotes its degradation), Sprouty-2 (modulates Ras/MAPK pathway), LRIG-1 (promotes Cbl binding and EGFR ubiquitination) and Mig6/RALT (binds to TK domain αI helix of EGFR, inhibiting its catalytic activity) (45,47,66). Sprouty-2 is a novel therapeutic marker in GBM, being usually expressed in commitment with EGFRvIII (67). Mig6 is a tumor suppressor that was described to regulate EGFR trafficking and suppress glioma progression (68).

After receptor endocytosis, this enters in a system of intracellular vesicles called endosomes. The first ones are the early endosomes where occurs the sorting of the receptor: unbounded receptor recycled quickly back to the plasma membrane, while ligand-bound receptor recycled slowly or are degraded in lysosomes (Fig.1.8) (64,69). Ligand dissociation can influenciate the fate of the receptor. The endosomal pH influenciates ligand dissociation since EGF remains bound to the receptor while TGFα dissociates. Because of that EGF leads to EGFR degradation and TGFα to EGFR recycling (70).

Ubiquitinated EGFR is sorted in the early endosomes by ESCRT machinery to intraluminal vesicles of maturating endosomes. From here the receptor is taken to lysosomal degradation (45,65).

Recycling of the receptor can occurs by the short loop (controlled mainly by Rab4) or by the long loop (controlled by Rab 11) (65).

Dysregulation in receptor trafficking has been described as a tumorigenesis promotor. Defects that leads to poor downregulation are associated with enhanced signaling. One described mechanism is the sustained PI3K signaling due the loss of SPRY2 that leads to EGFR/HER2 internalization and early endosomal signaling in a PTEN-dependent manner. This leads to proliferation and invasion in prostatic cancer (71). The interaction between EGFR and HER2 also overcomes ubiquitinated signaling attenuation, leading o recycling of the receptor (45,46). Increased EGFR recycling was described a mechanism that drives hepatocellular carcinoma metastasis (72).

Trafficking dysregulation involved in GBM progression has not been described so often. There was described a overexpression of NHE9 (Na(+)/H(+) exchanger) and its involvement in stemness, therapy resistance and invasion in GBM. NHE9 limits the luminal acidification of endosomes, promoting EGFR recycling and consequently signaling continuation (73).

EGFR endosomal signaling has also been reported. It was described AKT signaling in early endosomes through the APPL1, a Rab 5 effector. Rab 5 is the main characteristic protein of early endosomes. And also p38 MAPK sustain early endosomes signaling by promoting clathrin-mediated EGFR endocytosis and degradation evasion (65).

Therapies against EGFR

Since EGFR is involved in tumor progression, it becomes a promise target for therapy in hope to eradicate the tumor. There are different approaches used in target therapy against EGFR: the use of antibodies that block ligand binding or the use of small molecules that inhibit tyrosine kinase activity of the receptor (47,50).

Antibodies

The antibodies used against EGFR bind to the extracellular domain, induce the internalization of the receptor to try to inhibited the signaling pathway, but also is a potential stimulator of the immunological response. One of the most known is cetuximab, a chimeric antibody with high specificity for EGFR. Cetuximab is an EGF antagonist, and so it competes for the natural ligand-binding sites, preventing ligand binding and receptor activation. It was approved by FDA on February 2004 for colorectal cancer treatment. Panitumumab is a fully humanized antibody against EGFR, approved by FDA on September 2006 for treatment of colorectal cancer with *KRAS* wildtype. Both antibodies are given by intravenous injection (47,50).

Tyrosine kinase inhibitors

The small molecules called tyrosine kinase inhibitors (TKI) are synthetic molecules with low molecular weight, almost all are quinazoline-derived and they bind to intracellular domain of the receptor through a hydrogen bond (fig.1.9). TKI are homologous to adenosine triphosphate (ATP), competing for the ATP-binding domain of kinases (fig.1.10). In this way, TKI prevent the EGFR autophosphorylation, the activation of tyrosine kinase and the signaling pathway.

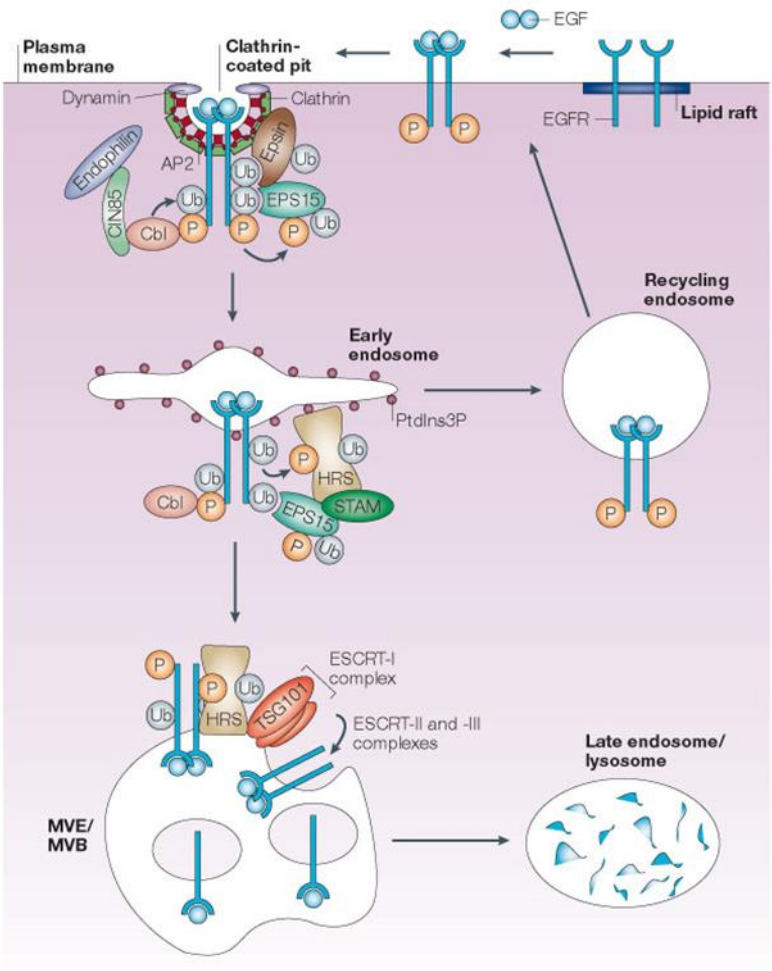

Figure 1.8: Schematic of clathrin-dependent EGFR internalization and consequent trafficking. After ligand binding, EGFR moves out from lipid rafts going to clathrin-coated pits. In this pit there are diverse proteins involved in the endocytic event. After internalization, the receptor goes to the early endosome where its fate is determined. The receptor can be recycling back to the plasma membrane or being degradated. The degradation is mediated by ESCRT complex that moves the receptor to multi vesicular endosomes (MVE) that after matures into late endosomes. These late endosomes then fuse with lysosomes. Adapted from (66).

One of the most known TKI is gefitinib that reversibly inhibits the TK activity of isolated EGFR with an IC_{50} in the nanomolar range. But *in vivo*, higher concentrations are required to block EGFR due the presence of intracellular ATP. It should be considered that in higher concentrations, gefitinib not also inhibit EGFR but also others RTK such as erbB2. Gefitinib has a half-life of about 28 hours. For that in clinic, gefitinib is administered daily, in a dose around 600mg/day. Gefitinib is metabolized by cytochrome P450 3A4 (CYP3A), being the inter-variability of this enzyme (expression and activity) one of the

reasons for different susceptibility to treatment. Gefitinib upregulates p27 (cell cycle inhibitor) and downregulates c-fos (transcription factor) and so gefitinib leads to a cell cycle arrest in G1 phase. In clinic, gefitinib is being used for treatment of locally advanced and metastatic non-small cell lung cancer (NSCLC) harboring EGFR-activating mutations (47,50,74–80).

Others TKI are also being used in clinic: erlotinib, an EGFR inhibitor, is being used in metastatic NSCLC and pancreatic cancer; lapatinib, an EGFR/erbB2 inhibitor, is being used in advanced or metastatic breast cancer. (81,82).

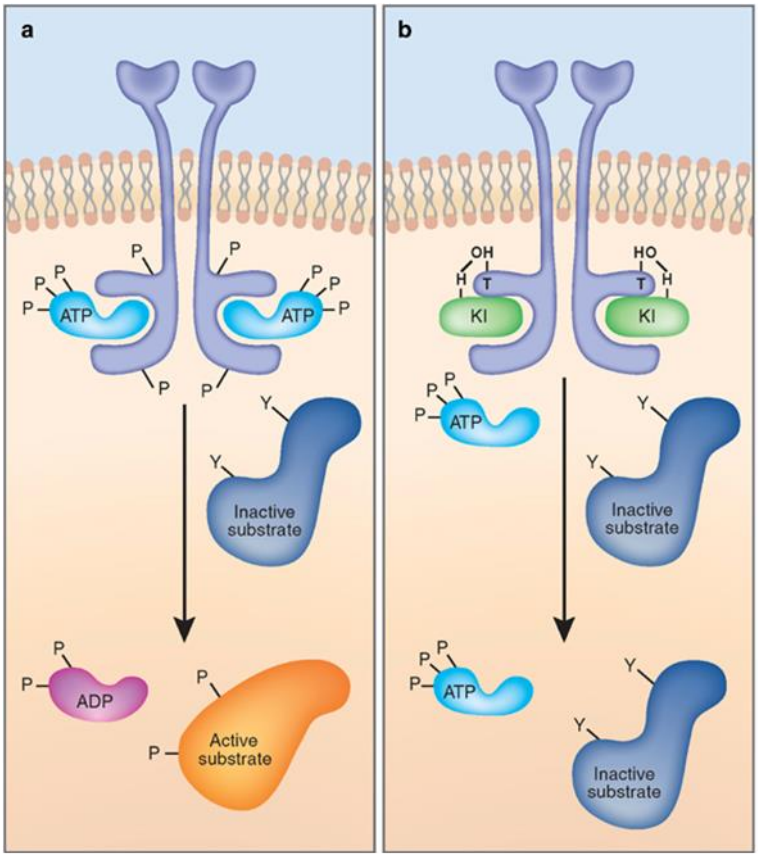

Figure 1.9: TKI mechanism of inhibition. a - Schematic of activated RTK bounded to ATP, b - inhibition by TKI (KI) that competes for ATP binding site and forms a hydrogen bond with the receptor. Adapted from (83).

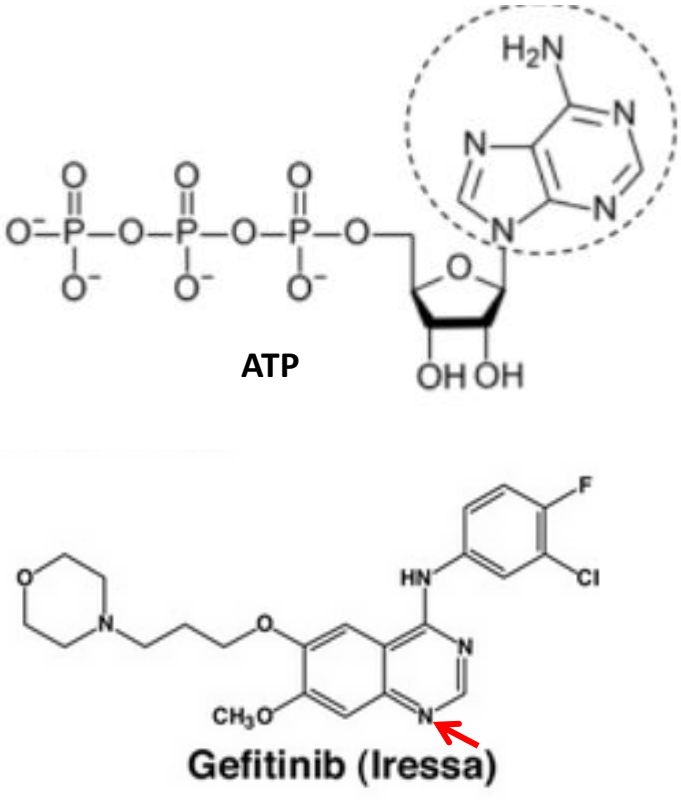

Figure 1.10: Structure of ATP and Gefitinib. ATP has adenine ring that is encircled and it is responsible for forming hydrogen bonds with the ATP-binding site on RTK. Gefitinib has a quinazoline group, where is founded the atom (indicated with red arrow) that form hydrogen-bonds with the kinase residues. Adapted from (79,80).

Secondary effect of EGFR therapies

Both ways of EGFR targeted therapy cause skin rash and diarrhea, due to direct biological effect of EGFR inhibition. So they are considered predictive factors of response to therapy. They have also a warning for pulmonary toxicity, in which cases 1% is fatal. And it should be controlled also the hepatic toxicity due to increase of liver transminases, normally asymptomatic (50).

Resistance to EGFR-targeted therapies

Despite the development of various therapeutic strategies and new compounds, the results of anti-EGFR targeted therapies remain somehow discouraging. Most of the tumors are resistance to therapies or relapse after a short period. In solid tumors, there is well documented mechanism of resistance to EGFR-targeted therapies. Some of these mechanisms are the acquisition of secondary EGFR point mutations and alterations or

redundancy in the signaling pathways. In NSCLC, the mutation T790M in exon 20 and the amplification of *MET*, another tyrosine kinase receptors are predictive biomarkers for a non-responsive profile of the patients to EGFR-targeted therapies. In colon carcinoma, the activating *KRAS* mutation leads to resistance and only patient bearing *KRAS*-wild type tumor are eligible to the cetuximab treatment (47,50,75).

Glioblastoma are refractory to EGFR targeted therapy and the resistance mechanisms are still not understood, and there is no predictive marker (49,81,83,84). Even if preclinical studies using anti-EGFR therapies in GBM were promising, the reality in clinical trials was very different, with no beneficial results compared with others therapies. Related to TKI, phase I/II of erlotinib as a single agent demonstrated promising disease control and response rate, while for gefitinib it seems to have clinical activity but no improvement in survival. The ability of TKI to enhance radiation sensivity observed *in vitro*, were not demonstrated in any clinical study. Related to EGFR antibodies, clinical trials using cetuximab or nimotuzumab in monotherapy or with other treatments showed a small or none activity and response rate (table 1.1). Another antibody (mAb 806) that targets the normal and the mutated receptor have promising pre-clinical results and seems having tolerance in phase I trials (81,85,86). Some of probable causes for resistance in GBM are compensatory activation with other ErbB family, tumor initiating cells, tumor heterogeneity, the BBB and the structure of the new vessels.

Table 1.1: Clinical trials using TKI in glioma. Adapted from (87).

Reference	Disease setting	Drug	Tumor response (PR or CR)
Rich JCO 2004	GBM, recurrent	Gefitinib 500 mg (no EIAED) or Gefitinib 1,000 mg (EIAED)	None (0/11)
Lieberman ASCO 2004	Malignant glioma, recurrent	Gefitinib 500 mg (no EIAED) or Gefiinib1,500 mg (EIAED)	13% (7/55)
Cloughesy ASCO 2005	GBM, recurrent	Erlotinib 200 mg (no EIAED) or Erlotinib 500 mg (EIAEDs)	8% (4/48)
Prados - Neuro Onc 2006	Malignant glioma, stable or progressive	Erlotinib 200 mg (no EIAED) or Erlotinib 500 mg (EIAED)	11% (6/57)
Franceschi Br J Cancer 2007	Malignant gioma, recurrent	Gefitinib 250 mg qd (regardless of EIAEDs)	None
Preusser J Neuroonc 2008	Malignant glioma, recurrent	Erlotinib 100–150 mg or Gefitinib 250 mg	14% (3/21)
Van den Bent JCO 2009	Malignant glioma, recurrent	Erlotinib 200 mg (no EIAED) or Erlotinib 500 mg (EIAED)	4% (2/54)
Yung Neuro Onc 2010	GBM, recurrent	Erlotinib 150 mg (no EIAED) or Erlotinib 300 mg (EIAEDs)	6% (3/48)
Raizer Neuro Onc 2010	Malignant glioma, recurrent	Erlotinib 150 mg (no EIAED)	

The BBB is a greater barrier against anti-cancer agents that were administrated systemically. The compounds to penetrate BBB should present higher lipophilicity. The tortuous vasculature also limits the drug penetration into the brain (83,87). The amount of gefitinib found in the brain is different among several studies. In NSCLC patients with brain metastasis, the ratio of gefitinib between cerebrospinal fluid and plasma was only 0.3-1.3% (88). This is in agreement with the prediction of low capacity to penetrate BBB since gefitinib is highly water-soluble. Also gefitinib is a substrate of the p-glycoprotein efflux pump that is expressed in brain tumors. But in some studies, there were observed penetration of gefitinib into the brain (89,90). This can be explained by the altered BBB integrity and the low level of CYP3A in brain (81,91) .

The tumor initiating cells (TIC) tend to be resistant to therapy by altering the checkpoint and DNA repair pathways. These cells are being associated with the presence of multiple drug resistant transporters. The existence of this transporters lead to the efflux of drugs, reducing their concentration in the brain (83). The activation of others receptors of the ErbB family were demonstrated as a mechanism of resistance for EGFR-targeted therapy in glioblastoma TIC (84).

Intra tumor heterogeneity is normally one of the most common reasons for therapy resistance. The heterogeneity can lead to redundancy and cross talk between signaling pathways. Besides EGFR overexpression, can also occur the mutation and amplification of others RTK and GPI-linked receptors (*IGFR1, MET, PDGFR α/β, uPAR*) which signaling compensates the EGFR inhibition. It has also been proposed that deletion of the tumor suppressor gene *PTEN*, leading to the continuous activation of PI3K pathway, prevent inhibition of EGFR signaling pathway by TKIs (81,83). In retrospective analysis association of EGFRvIII and wild-type *PTEN* was reported as a significant predictor of TKI response in GBM. But this predictive value was not observed in others studies (49,92,93).

Dysregulation of receptor trafficking can be stress-induced or a way to overcome cell death as described above. This dysregulation promotes tumor progression and can be also a mechanism of therapy resistance. But still few is known about that and so require further investigation (65,94,95).

As we can see there are molecular markers that predict the insensitivity of lung and colon tumors to EGFR targeted therapies. But in GBM there are not yet such biomarkers that can explain the failed clinical trials using first generation of EGFR TKI such as erlotinib and gefitinib (93).

The causes for resistance to EGFR therapies in GBM are unknown, but preclinical data in other cancer types correlate the crosstalk and bi-directional regulation of EGFR and integrins as one possible mechanism of therapy resistance (85,96–98).

1.3 Integrins

Integrins Family

Integrins are a family of heterodimeric cell surface receptors composed by non-covalent association of alpha and beta subunits. The family is composed by 18 α subunits (that determine ligand binding specificity) and 8 β subunits (that connects to cytoskeleton and signaling molecules), forming 24 different receptors that each binds to one or more ECM ligands (fig.1.11).

There are four families based on the evolutionary history of α subunits. The first group is composed by integrins that recognize the arginine-glycine-aspartic acid (RGD) motif on their ECM ligands such as fibronectin, vitronectin or fibrinogen. The second group is formed by laminin binding integrins. In this group, there is the special β4 that has a large intracellular domain and so function as a docking site due to its phosphorylation sites. The last two groups (leukocyte integrins (β2) and collagen integrins (β1) receptors) come from the same large group of integrins that are structurally different from the others groups due to an extra domain in their α subunit (96,99).

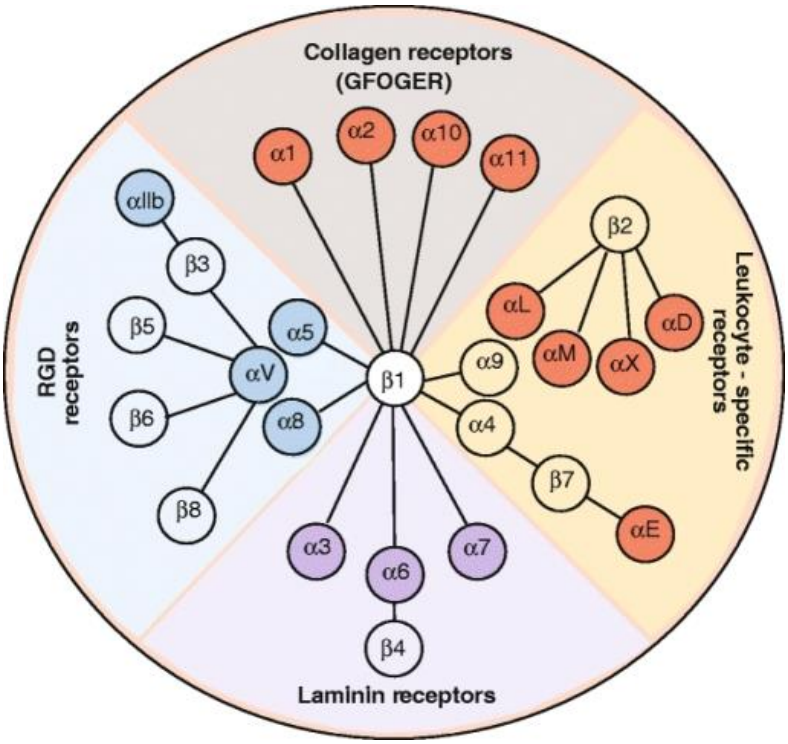

Figure 1.11: Family of integrins.Adapted from (93)

Integrin expression and function

Integrins are expressed in all cell types, however the profile of integrin vary from cell type to cell type. Integrins and their ligands are important in the early stages of embryonic development including in fertilization, implantation and in blastula formation. β1 integrin is one of the most important, since its homozygous knockout leads to early death of the embryo. It can be due to the fact that β1 is present in 12 of 24 combinations of integrins (99,100).

In the physiological development, maintenance and remodeling of tissues, stem cells have an important role. Stemness is regulated by signals from the stem cell niche microenvironment such as the ECM. In here, integrins have an important role, mainly β1 that is highly expressed in stem cells to maintain stemness and control the balance between renewal and differentiation. In this context, the role of integrins in cell fate is to give spatial cues to the cells, due to the interaction with ECM and their mechanosensor activity, while the temporal cues are given by growth factors (100,101).

Integrins regulate cellular processes such as survival, proliferation, differentiation, migration, adhesion, apoptosis, anoikis, polarity and in stemness (96–99).

Integrins signaling pathways

After ligand binding, the integrins as a surface receptors undergo a conformational change from inactive state to an active one that have a higher avidity for ligands. The inactive state is characterized by a bent conformation with a closed head piece, while the active one has an extended conformation and an open head-piece, so then the conformational change occurs in the extracellular β-subunit followed by the separation of the intracellular domains of both subunits (99,101–103).

Integrins have a mechanical and biochemical role.

The recognition of different ligands allows these receptors to sensitize different environments, forming so a physical connection between the inside and the outside of the cell. Integrins are relevant in attachment of cells to ECM but also in cell-cell interactions. This mechanical function of integrins is related mostly with their capacity of connecting with actin cytoskeleton through the formation of complexes with talin, paxilin, α-actinin, tensin and vinculin. The promotion and generation of contractile forces contributes to migration of cells (99,100).

Because integrins do not have enzymatic activity, they need to recruit cytoplasmic kinases to perform their signaling function. Integrins transmit signal through focal adhesion kinase (FAK), integrin linked kinase (ILK), talin, paxilin, Src, PI3K and Ras/MAPK. These interactions are mediated by the β subunit of integrin. This subunit has NPX/Y motif that allows the physical interaction with PTB domains. After ligand binding, FAK is recruited by the β subunit, and then it autophosphorylates (Tyr397), creating a docking site for Src. This active complex FAK/Src activates a lot of downstream pathways such as NF-kB, MAPK and PI3K. This recruitment of signaling molecules also potentiate the activity of tyrosine kinase receptors such as VEGF, FGFR and EGFR. ILK binds to β cytoplasmic tail and upregulates the activity of AKT. (99,101,104).

Integrins and Cancer

With playing so many roles in cell biology, mainly on proliferation, survival and migration, integrin defective signaling can result in a number of pathologies such as cancer (100).

In most cases integrins are overexpressed in cancer tissue compared to normal one (table 1.2). In some solid tumors, the epithelial cells that give arise to the tumor as the same integrins expression as the normal cells, normal and cancer cells express α2β1, α3β1, α6β1, α6β4. Integrin expression can be different between normal and tumors cells, like integrins αvβ3, α5β1 and αvβ6 which are almost undetectable on epithelia but their expression are upregulated in carcinomas, such as colon, breast, ovarian, lung and gastric (98,100,105).

Table 1.2: Integrin overexpression in cancers. α5β1 is overexpressed in various types of cancer. In glioblastoma are present the overexpression of α5β1, αvβ3 and αvβ5. In the table there are also represented integrin-targeted drugs. Volociximab is used against α5β1, etaracizumab against αvβ3, cilengitide and intetumumab against integrin αv, and ATN-161 against α5β1 and αvβ3. Adapted from (97,105).

Tumor	Overexpressed integrins	Drugs
Melanoma	**α5β1** αvβ3	Volociximab, Etaracizumab
Prostate	αvβ3	Intetumumab
Pancreas	**α5β1** αvβ3	Volociximab (IIA1) -
Ovarian	**α5β1** αvβ3	Volociximab (IIA1) -
GBM	**α5β1** αvβ3 αvβ5	ATN-161 Cilengitide Cilengitide
Colon	**α5β1** αvβ6	- Intetumumab
Lung	**α5β1**	Volociximab

Since expression and signalinf of integrins are cell-type dependent, there is not a consensual role of integrin overexpression in cancer as an anti- or pro- tumoral. Some integrins are also downregulated in tumors, such as α2β1 in breast cancer and α3β1 in melanoma (106,107).

Integrins expression in both tumor and stromal cells has an important role in metastasis. This expression promotes cell motility and anchorage-independent growth through activation of FAK/PAK/MAPK by integrin β1. Integrins were also associated with

metalloproteases and UPA, enhancing their activity. The interaction of integrins and GFR, described below, also promotes invasion through the enhancement of signaling pathways. Integrins signaling also influenciates cancer stemness, drug resistance and metastasis (101).The cancer stemness has a role in the initiation of tumor but also in resistance to therapy. (97,101,108). The altered expression of integrins in microenvironmental cells, such as endothelial cells, promotes angiogenesis, desmoplasia and immune responses (97,98,101,105). Integrins exert their oncogenic activity throught the crosstalk with tyrosine kinase receptor such as EGFR, MET or PDGFR. Integrin/grow factor receptor (GFR) cooperation can also lead to therapy resistance (97,101,108).

Studies of expression and function of integrins in glioma revealed an important role of these receptors in progression and survival of patients. Overexpression of ECM component like fibronectin (ligand of α5β1 and αvβ3) is associated with gliomagenesis and poor survival (109). Integrins αvβ3, αvβ5 and α5β1 were found highly expressed in human glioma explants (110). Integrin αvβ3 was demonstrated as a negative prognostic factor in GBM (111). Our laboratory demonstrated that α5β1 integrin is a diagnostic, prognostic and therapeutic factor in GBM. α5β1 integrin was found overexpressed in glioma grade IV compared with the low grades and normal tissue. This overexpression was associated with a more aggressive phenotype, in which patients had less survival rate when α5 was overexpressed. Also the expression of this integrin was associated with resistance to one of traditional treatment (TMZ). Moreover, our laboratory and others demonstrated the role of α5β1 integrin in glioma cell migration and dissemination (108,113–116).

All data mentioned above, show that integrins are potential therapeutic targets in GBM.

Currently, in clinical trials there is a cyclic peptide inhibitor of both integrins αvβ3/αvβ5, Cilengitide. Cilengitide seem to be well tolerated and to have a small anti-tumor efficacy (118). Unfortunately, a clinical trial phase III in GBM with combination of cilengitide with chemoradiotherapy did not show any increase of the overall survival of the patients (119).

Integrins and Growth Factor Receptors

Integrins and their ligands were demonstrated to collaborate with growth factor receptors (GFR). This collaboration is involved in aggressiveness of solid tumors.

Their interaction can be classified as concomitant or collaborative signaling, direct activation and amplification of signaling. The difference between concomitant and collaborative is that in the first they act independently, while in the second integrin are necessary to assist the proper GFR signaling. In direct activation, integrins activate GFR even without the presence of growth factors. While in the amplification of signaling, GFR increases the levels of integrins that *per se* can activate/promote GFR signaling (fig.1.12) (96).

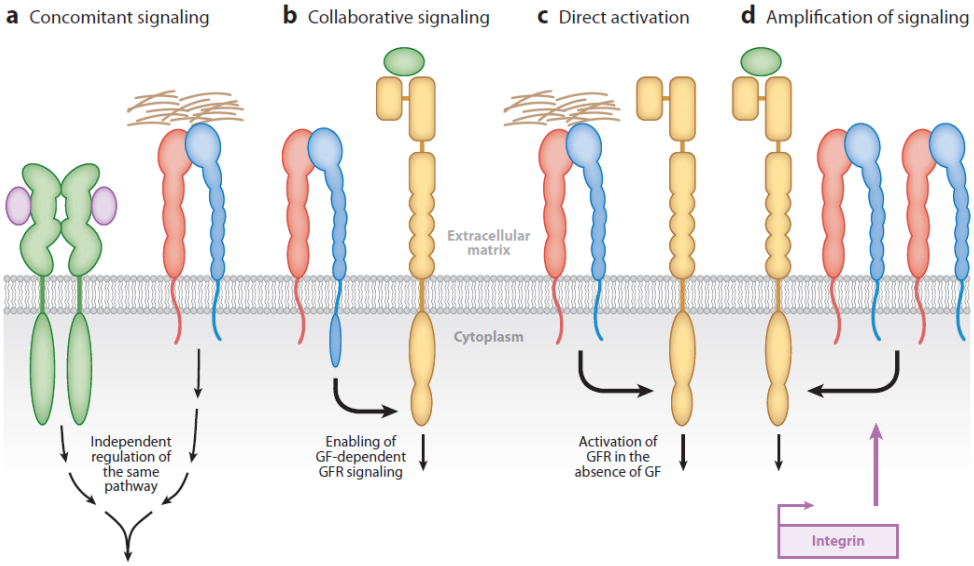

Figure 1.12: Mechanisms of interaction between integrins and growth factor receptors. Adapted from (96)

Integrins can positively regulate RTK signaling by directly phosphorylating them. This phosphorylation usually occurs in the same tyrosine residues, that are phosphorylated after EGF stimulation (120).

Integrins are not only positive regulators of RTK signaling. It was reported that the interaction between α1β1 and collagen, recruits T cell protein tyrosine phosphatase (TCPTP). TCPTP dephosphorylates EGFR, PDGFR and VEGFR, leading to signaling attenuation (121).

The interaction between EGFR and α5β1 integrin has been reported in *in vitro* and *in vivo* models of diverse cancers.

In epidermoid cancer, the inhibition of α5β1 integrin, reduces phosphorylation of EGFR (residues 1086 and 1148), leading to attenuation of PI3K and MAPK signaling pathways. The inhibition of both EGFR and α5β1 integrin suppresses the phosphorylation of downstream molecules that are involved in tumor proliferation (122).

In breast cancer the interaction between EGFR and β1 integrin is important to migration and invasion of cells, through the complex Src/EGFR/β1 integrin in the plasma membrane that recruits MMP and maturates invadopodia (123).

In Bronchial cancer, the regulation of EGFR signaling by β1 integrin is necessary to tumor migration (124).

Integrins/EGFR interaction can lead to resistance to EGFR-targeted therapies (table 1.3).

In breast cancer, a survival mechanism to lapatinib is β1 integrin dependent. Being this integrin also associated with low response rate to trastuzumab (125,126).

In lung cancer model, α5β1 integrin was associated with resistance to cetuximab. β1 integrin was found in erlotinib resistant lung cancer stem cells and associated with resistance to gefitinib treatment (124,127,128).

Table 1.3: Integrins involved in EGFR-targeted therapies resistance. Integrins and their ligands are found to be a cause of resistance to anti-EGFR drugs (antibodies and TKI) in diverse cancer types. Adapted from (97,101) .

Integrins	Cancers	Anti-EGFR drugs	Therapeutical class
fibronectin, α5β1	lung	cetuximab	mAb
β1	breast	trastuzumab	mAb
β1	lung	gefitinib	TKI
β3	breast, lung	erlotinib	TKI
β1, α5, α2	lung	erlotinib	TKI
β1	breast	lapatinib	TKI
β4	breast	trastuzumab	mAb

Integrins trafficking

Membrane trafficking of integrins has a role in regulation of cell-ECM contacts remodeling, being important during regulation of cell adhesion, on cell migration, invasion and so is involved in cancer progression. For example, the internalization of

integrin α5β1 through caveolin is important for fibronectin turnover, while the clathrin pathway has an important role in mitosis (96). The route chosen for integrins endocytosis is cell type- and microenvironment dependent. Usually integrins are endocytosed by clathrin- or caveolin- dependent pathways. There are also endocytosed by micropinocytosis from circular dorsal ruffles or by Rho-A dependent form. The nature of the ligands and the interactions with GFR modulate integrin endosomal trafficking (96,129,130).

After endocytosis, integrins undergo endosomal sorting on early endosomes, where their fate is decided (recycling or degradation). The movement of integrins to EEA1 positive early endosomes is mediated by Rab 21 and Rab5. The recycling of integrin can occur by the short/Rab4 loop or by the long/Rab11 loop. This choice depends on different factors: the activation state, the crosstalk with others integrins, GFR or downstream molecules. Some examples are described below. The inactive state usually recycle by the short loop while the active one by the long loop. Integrin αvβ3 suppresses recycling of α5β1 leading to migration. Src-mediated phosphorylation of syndecan-4 inhibits Arf6-dependent α5β1 recycling, stabilizing the focal adhesion and promoting cell migration. There are different molecules that promote integrin recycling. Rab 25 interacts with α5β1 integrin that are in endosomes to promote their recycling. Rab coupling proteins associate with α5β1 integrin and EGFR to promote their recycling after treatment with cilengitide (131). The receptor degradation into lysosomes, due to ubiquitin signal in the α chain of integrin, is a slow process that leads to a cytoplasmic localization of the receptor. Normally, this occurs to the active receptors that still have the ligand attached (96,105,129,130).

Trafficking of integrin and EGFR can regulate their signaling and response to therapy, being for that an interesting research subjet.

1.4 Objective

The group previously showed that during evasion from 3D stumor spheroids, loss of integrin α5 expression in glioblastoma cell line (U87) sensitizes cell to EGFR-targeted therapy (gefitinib) (fig. 1.13). The cooperation between EGFR and integrin happen at different levels, being one of which in the endocytic pathway.

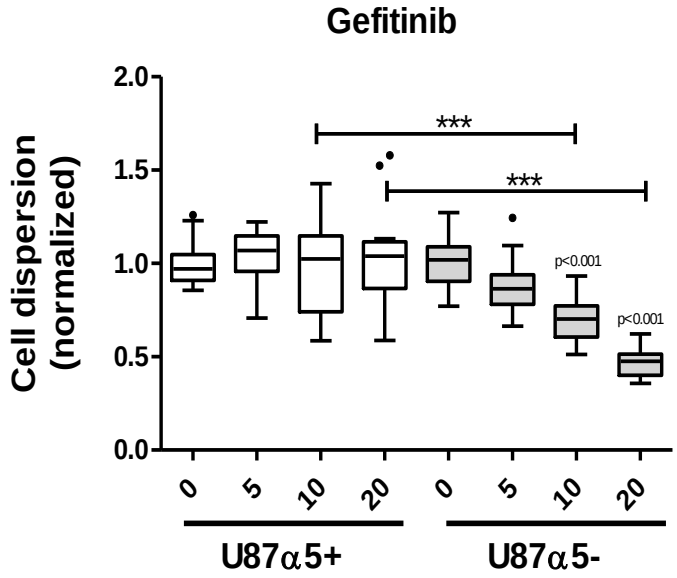

Figure 1.13: Loss of integrin α5 expression in glioblastoma cell line (U87) sensitizes cell to EGFR-targeted therapy (gefitinib). Dose effect of gefitinib (concentration in µM) on cell dispersion of U87 α5+ and U87 α5- cells. The number of dispersed cells was quantified after DAPI-labelling of their nucleus by a ImageJ macro and data were expressed as the ratio of dispersing cells compared to control (DMSO-treated) cells. Turkey-boxes represent data from 3 independent experiments. Statistical analysis was made using ANOVA ***p<0.001. Adapted from (unpublished data).

My objective was to determine if endocytosis is involved in integrin-dependent resistance to gefitinib.

As written above EGFR is internalized by clathrin-dependent pathway after activation (45). In the other hand, integrin are also described to be internalized by clathrin pathway (96). Clathrin pathway is dynamin-dependent, our strategy was thus to inhibit dynamin mediated endocytosis using chemical inhibitors (132).

2. Methods

2.1 Cell culture

The cell lines used are described on table 2.1. The U87 cell line was previously manipulated to have an overexpressed or downregulated integrin α5 expression level. U87 cells were previously stably transfected with pcDNA3.1 plasmid containing the human α5 integrin gene to overexpress the gene. The downregulation of the gene was obtained by transfecting the cells with a pSM2 plasmid coding a shRNA against α5 mRNA. The transfection was performed using jetPRIME (Polyplus transfection). The cell selection was made using cell sorting with PE-conjugated SAM-1 antibody, and after controlled by immunoblotting (108,114).

The brain tumor cells were cultured in EMEM with L-Glutamine (Lonza, Verviers, Belgium), supplemented with 1% sodium pyruvate (Lonza, Verviers, Belgium), 1% non-essential amino acids (Lonza, Verviers, Belgium), 1% of fetal bovine serum (FBS) (Dominique Dutscher, Brumath, France).

Cells were routinely cultured on 75cm^2 flask and maintained on an incubator at 37ºC and 5% of CO_2 under humidified atmosphere. Culture medium was changed every 3 days (10ml for a 75cm^2 flask). Cells were splited at 80% confluence. The medium was aspirated to avoid any serum residues because it inactivates trypsin due to the presence of protease inhibitors such α_1-antitrypsin and α_2-macroglobulin. Two ml of a trypsin/EDTA (Lonza, Verviers, Belgium) solution diluted ten-fold in DPBS (Lonza, Verviers, Belgium) was added. Cells flasks were placed at the incubator during five minutes. Cells detachment was controlled under the microscope. The trypsination was stopped with 2 ml of serum-complemented medium. The cell suspension was placed on a falcon tube and centrifugated during five minutes at 1000 rpm (300g). The cell concentration was determined on TC20^{TM} Automated Cell Counter (Bio-Rad, Hercules, USA) adding cell suspension and trypan blue dye 0.4% (Bio-Rad, Hercules, USA) at 1:1. The supernatant was aspirated and the pellet resuspended in complete culture medium. Cells were seeded at 500 000 cells in a 75cm^2 flask.

For long term storage, cells were freezed at -80ºC in cryovials in cell culture medium containing 20% serum and 10% of Dimethyl-sulfoxide (DMSO) (Sigma Aldrich, St.Louis, USA). DMSO acts as a cryoprotective agent. Cells were thawing by placing the

cryovials in a 37ªC water-bath and the cell suspension was transfer to a T-flask 25 cm^3 containing supplemented medium with 10% of FBS. To avoid cellular damage provoked by DMSO, the medium was replaced the day after.

All processes were performed under sterile conditions, under the PSMII Safe Fast Classic (Dassit, Ferrara, Italy).

2.2 Formation of tumoral spheroids

The formation of spheroids was performed using the hanging drop method, where cells are grown in a drop, allowing the formation of a single spheroid (fig.2.1). The method used was previously described by Blandin (114). Cell were suspended in culture medium containing 10% of methyl cellulose solution (Sigma, St.Louis, USA), at a density of 1,000 cells/20µl. Cell suspension was scattered throughout a petri dish in form of 20 µl drops. This plate was later inverted and maintained in a humid environment, at 37°C and 5% CO_2, for 48 hours.

The spheroids were then seeded on a fibronectin coated surface (fig.2.1) to evaluate the evasion of cells. This way for studying evasion resembles an *in vivo* situation where cells migrate from a small cluster.

24-well plates were coated for 2-3 hours with a 10 $\mu g.ml^{-1}$ fibronectin solution (250 µl per well). Excess fibronectin was aspirated and wells washed with cell culture medium. Each well was seeded with 3-5 spheroids. When indicated dynamin inhibitors (Dynasore (Santa Cruz Biotechonology, Dallas, USA) and Dyngo-4a (Selleckchem, Souffelweyersheim, France)) or EGFR tyrosine kinase inhibitor (Gefitinib (ChemiTek, Indianapolis, USA) were added in the culture medium when spheroids are plated on fibronectin coated surface.

Phase contrast image of the spheroids were obtained with 5x objective using microscope EVOS xl Core (Thermo Scientific, Braunschweig, Germany). After 24 hours of incubation, cells were fixed in glutaraldehyde 1% (Electron Microscopy Sciences, Hatfield, USA) for 30 minutes. Following, wells were washed with PBS and cells were stained for 30 minutes with DAPI (2.5 $\mu g.mL^{-1}$) (Santa Cruz Biotechonology, Dallas, USA). Nucleus were picturized under the objective 5x in the fluorescence microscope ZEISS-Axio (ZEISS, Oberkochen, Germany). Image analysis to evaluate the number of cells that migrated out of the spheroid was performed with ImageJ software using a homemade plugin (Romain Vauchelles, PIQ platform) (114).

Table 2.1: Glioma cell lines used.

Cell line	Characterists	References	Origin
U87	Glioblastoma with *PTEN* mutated (splice deletion of exon 3, intron 3 and codon 54), homozygous deletions in the *p16* and *p14ARF* genes, *TP53* and EGFR wild-type. ATCC provided cell line reported as different from the original U87 and also Uppsala U87MG.	(39,133–136)	Obtained from ATCC (Molsheim, France)
LN443	Glioblastoma with *PTEN* mutated (splice deletion exon 5), homozygous deletions in the *p16* and *p14ARF* genes and *TP53* wild-type. Cross contamination with LN-444.	(135,137)	Provided by Professor Hegi (Lausanne, Switzerland)
LN229	Glioblastoma with mutated *TP53* (codon 98 CCT(Pro)→CTT(Lys)), homozygous deletions in the *p16* and *p14ARF* genes, *EGFR* and *PTEN* wild-type.	(135,136)	Provided by Professor Hegi (Lausanne, Switzerland)
SF767	Anaplastic astrocytoma with *TP53, PTEN and p16* and *p14ARF* genes wild-type, and *EGFR* amplified.	(135,136,138)	Provided by Dr. Rigot (Marseille, France)
U373	Glioblastoma with *PTEN* deleted and *TP53* mutated (codon 273 CGT(Arg) →CAT(His)), and *EGFR* amplified.	(135–137,139)	Obtained from ATCC (Molsheim, France)
T98	Glioblastoma with mutated *TP53* (codon 237 ATG(Met)→ATA(Ile)), homozygous deletions in the *p16* and *p14ARF* genes, *PTEN* deleted and *EGFR* amplified.	(135–137,140)	Obtained from EACC (Saint Quentin Fallavier, France)
LN319	Human astrocytoma with mutated *TP53* (codon 175 CGC(Arg)→CAC(His)) and mutated *PTEN* (codon 15 AGA (Arg) → AGT (Ile)). Cross contamination witg LN-992.	(135,137,139)	Provided by Professor Hegi (Lausanne, Switzerland)
LNZ308	Glioblastoma with deleted *TP53*, and mutated *PTEN (*splice deletion of exon 6), and *EGFR* wild-type.	(135–137,139)	Provided by Professor Hegi (Lausanne, Switzerland)
SF763	Anaplastic astrocytoma with mutated *TP53* (codon 158 CGC (Arg)→CTC(Leu)), homozygous deletions in the *p16* and *p14ARF* genes and *PTEN wild-type.*	(135,138)	Provided by Dr. Rigot (Marseille, France)

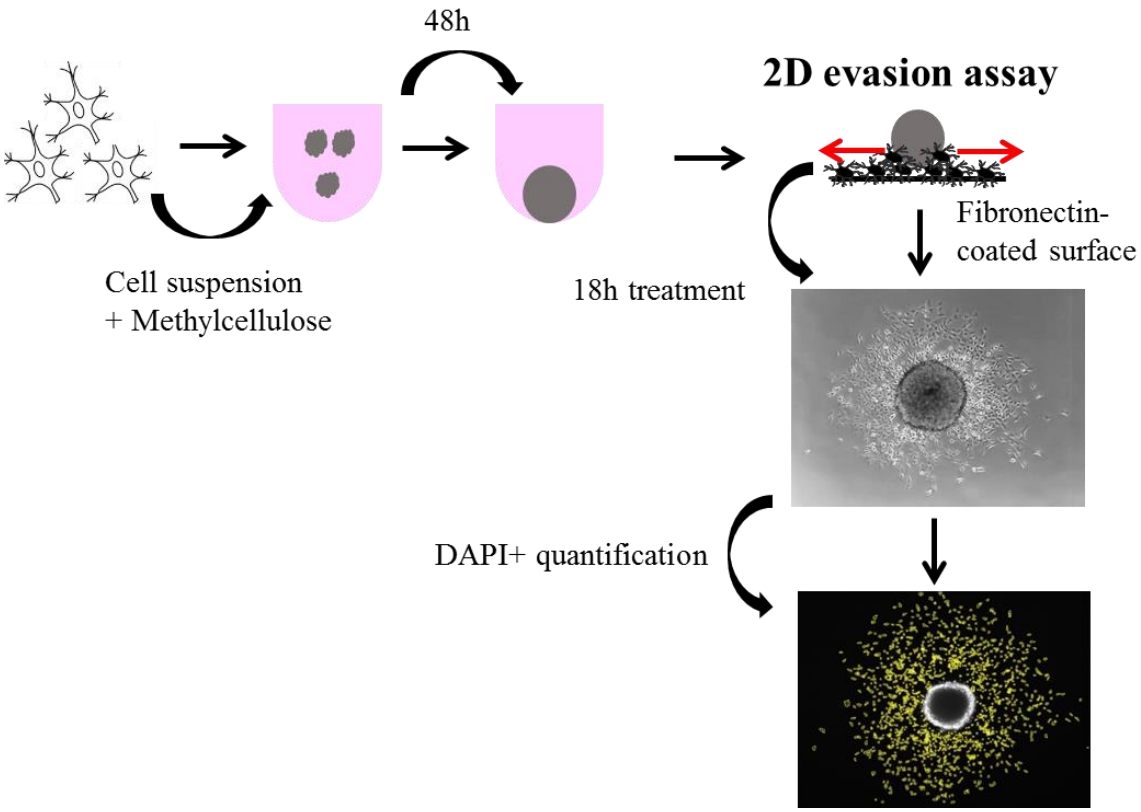

Figure 2.1: Schematics of spheroid evasion assay. Spheroid formation was performed using the hanging-drop method, where methylcellulose prevents non-specific interactions between cells and the plastic. After 48 hours, spheroids were plated on a previous fibronectin (FN)- coated surface and allow the evasion. DAPI stain was made and quantification of evading cells made by a home-made ImageJ plug-in.

2.3 Preparation of Methylcellulose solution

Six grames of methylcellulose are dissolved in 250 ml of EMEM medium without FBS. Then the solution is heated at 60°C during one hour. After, there is added 250 ml of EMEM medium supplemented with 20% of FBS, 2% of sodium pyruvate and 2% non-essential amino acids. The solution is mixed overnight at 4°C. The solution is centrifuged at 5000g during two hours. The supernadant is aliquoted and conserved at 4°C.

2.4 Immunofluorescence

Twelve mm coverslips (Thermo Scientific, Braunschweig, Germany) previously washed with an alcoholic acidic solution (1 M of HCl (Sigma Aldrich, St.Louis, USA) in 70% ethanol solution) were coated with 20 µg.ml^{-1} fibronectin (Promocell, Heidelberg, Germany) in PBS for 2 hours at 37°C and washed with PBS. Coverslips were distributed in 24-well plates. Cells were plated at cell density of 40,000 cells per well and cultured for 24 hours. When indicated cells were treated with drugs or the corresponding amount

of DMSO as control. After treatment, cells were fixed with a 3.7% paraformaldehyde (Electron Microscopy Sciences, Hatfield, USA) solution in PBS for ten minutes. Cells were washed three times for five minutes with PBS. Permeabilization was done using a 0.1% (w/v) Triton X-100/PBS solution for two minutes. This step facilitates cellular membrane disruption and antibody access entry into the cells. To avoid unspecific interactions, cells were incubated with a 3% (w/v) BSA/PBS solution (Euromedex, Souffelweyrsheim, France) for one hour. Coverslips were then incubated with the primary antibody (diluted on 3% (w/v) BSA/PBS) for three hours at room temperature or overnight at 4ºC and followed by three washes (five minutes each) with PBS. Cells were then incubated for 45 minutes in the presence of the appropriate Alexa 488- , Alexa 546- or Cy5- conjugated secondary antibodies diluted in 3% (w/v) BSA/PBS solution containing DAPI (2.5 $\mu g.ml^{-1}$). Cells were washed in PBS and the coverslips were mounted with fluorescence mounting medium (Dako, Carpinteria, USA), putting the cells in contact with the slide. All antibodies information and dilutions are presented on annex 1. Optical section (750 nm Z-resolution) were imaged using an immersion oil (Type F Immersion liquid (Leica, Nanterre, France) HCX PL APO CS 11506188 objective (magnification of 63x, numerical aperture of 1.4, pinhole of 1.00 airy unit and a zoom of 1.5) under the Leica TCS SPE II confocal microscope (Leica, Nanterre, France). Image analysis was performed using ImageJ software. The macro used for co-localization was JACOP, where the channels of interest are analyzed after performing a threshold to eliminate non-specific staining (background). The analysis determines the overlapping of the channels.

2.5 Stochastic Optical Reconstruction Microscopy (STORM)

STORM is a super-resolution microscopy technique that surpasses the diffraction limit by localization of individual fluorophores. Giving a lateral and axial resolution of 20 nm and 50 nm respectively, it allows the visualization of subcellular structures (141–143). STORM technique was used in our study to evaluate EGFR and β1 integrin co-localization in endomembrane vesicles after gefitinib treatment.

The immunofluorescence protocol of sample preparation was slightly modified for super-resolution experiments. Microscope coverslips (18 mm in diameter) were coated with a mixture of fibronectin (20 $\mu g.ml^{-1}$) and gold nanoparticles (3.8E+6 nanoparticles/ml, 100 nm diameter) (Sigma Aldrich, St. Louis, USA). These gold nanoparticles are used for a

drift correction after image acquisition (143). Then cells were seeded on a top of coverslips at a cell density of 40,000 cells per well (using 12-wells plate). After treatment with gefitinib, cells were fixed, permeabilized and stained against EGFR and β1 integrin. All antibodies information and dilutions are presented in Annex 1. For super-resolution microscopy experiments nucleus were not stained with DAPI. Cells were kept in PBS at 4°C until image acquisition.

Super-resolution imaging was performed on an inverted microscope Nikon Eclipse Ti-E (Nikon, Amsterdam, Netherlands) equipped with 100x, 1.49 N.A. oil-immersion objective. Fluorescence signal was collected using an EM-CCD camera (Hamamatsu, Massy, France). Imaging and data analysis were done by a collaborator PhD student Oleksandr Glushonkov.

2.6 Immunoblot Blot

Cells were seeded in a 6-well plate at a density of 200,000 cells per well for 24 hours. The plates were placed on ice, the medium from the wells was removed and the wells washed with PBS (Euromedex, Souffelweyrsheim, France). The PBS was removed and the total cell lysate was obtained by adding 100 µl of lysis buffer: 100 $mmol.l^{-1}$ NaF (Merck, Darmtadt, Germany), 1 $mmol.l^{-1}$ Sodium orthovanadate (Sigma Aldrich, St.Louis, USA), 1% Triton X-100 (Sigma Aldrich, St.Louis, USA), PBS (Euromedex, Souffelweyrsheim, France) 1X, 1 tablet/10 ml of Protease and Phosphatase Inhibitor EDTA-free (Thermo Scientific, Rockford, USA). Cell lysates were transferred to 1.5ml Eppendorf tube, vortex during 10 seconds and then placed on ice for 10 minutes. This process was performed three times. The lysates were then sonicated during 10 seconds at 100% of power amplitude and the steps on vortex and ice were repeated. After a 13,000 rpm centrifugation at 4ºC during 10 minutes, the supernatant was stored at -20ºC until used.

Total protein concentration was evaluated by DC™ protein assay (Bio-Rad,Hercules, USA). This is a modified and faster version of the colorimetric Lowry assay, where the reaction only takes 15 minutes. First occurs a reaction between the peptide bonds of the protein with the copper ions in alkaline environment. Then this complex protein/copper reduces Folin reagent, oxidating aromatic residues (tyrosine and tryptophan) than become blue with a maximum absorbance at 750nm. A standard curve was made using BSA standart sets (Bio-Rad, Hercules, USA) from 0.2 to 2 mg/ml. The protein samples were

diluted 1:5 in cell lysis buffer. For the samples and standards it was performed duplicates, and followed the manufacture instructions. The plates were read on iMark Microplate Reader (BioRad, Hercules, USA).

Before loading on the gel, the equivalent amount of proteins were diluted 1:1 in 2x Laemmeli Solution (Bio-Rad, Irvine, USA) mixed with β-mercaptoethanol (Roth, Karlsruhe, Germany) to have 10 µg of total protein in 13 µl. The samples were heated at 96ºC during seven minutes to denature the proteins and allow their movement through an electric field due to the no neutralized negative charge from the amino acids.

Proteins are separated based on their molecular weight on a sodium dodecyl sulfate polyacrylamide gel electrophoresis (SDS-PAGE). Electrophoresis was performed on a 4-20% Tris-HCl Criterion™ Precast Gel (Bio-Rad, Irvine, USA) (which allows the separation of proteins between 2-400kDa) submerged in running buffer (10% TG 10X (Euromedex, Souffelweyrsheim, France), 0.5% of SDS>99% (Euromedex, Souffelweyrsheim, France)). The molecular weight marker Precision Plus Protein standards on 4-20%Tris-HCl Criterion™ Gel (Bio-Rad, Hercules, USA) was used to allow the following of the samples. The electric field applied was 240 V.

Following this step, a wet transfer into a PVDF membrane (GE Healthcare Life Sciences, Freiburg, Germany) was performed. PVDF membranes compared to the nitrocellulose membranes have the advantage of later reprobing with an alternative antibody. The transfer was performed in a tank filled with transfer buffer (10% of TG 10X and 10% of absolute ethanol (Sigma-Aldrich, Steinheim, Germany)) for 32 minutes at 100 V.
After the transfer was complete, the PVDF membrane was blocked with 5% (w/v) of non-fat dried milk (Bio-Rad, Irvine, USA), diluted in washing buffer, for one hour at room temperature with agitation. The blocking step is crucial to prevent unspecific reactions from the primary antibody. The membrane was then incubated overnight at 4°C under agitation with the primary antibodies diluted in blocking buffer, followed by three washes of seven minutes using a washing buffer TBS/0.1% Tween 20 (Euromedex, Souffelweyrsheim, France). Secondary antibodies conjugated horseradish peroxidase (HRP) and diluted in blocking buffer were incubated for one hour at room temperature under agitation and followed by three washes of seven minutes using a washing buffer. Primary and secondary antibody references and dilutions are listed in detail on annex 1.

The antibody signal was revealed using Clarity TM western ECL substrate (Bio-Rad, Irvine, USA). This kit contains luminol and peroxidase, which in contact with HRP leads to emission of light. HRP when has its substrate peroxidase is able to oxidize luminol, creating them 3-aminophthalate dianion that emits light. Light emission was detected with LAS4000 imager (GEHealthCare) and quantify using ImageQuant analysis software (GEHealthCare). Data are presented as the mean +/- S.E.M of 3 independent experiments.

2.7 EGFR uptake assay

Cells were seeded at a cell density of 30,000 cells/wells on 12mm coverslips, previously coated with 20 $\mu g.ml^{-1}$ fibronectin solution for 24h. Cells were then serum-starved during one hour, at 37ºC and 5% CO_2, to remove all growth factors that can induce EGFR internalization, in a way to have the maximum number of receptors at the plasma membrane. Cells were placed on ice and washed with ice-cold Opti-MEM (Gibco, Paisley, UK). Cells were incubated at 4°C during 30 minutes with Alexa488-conjugated EGF (100 $ng.ml^{-1}$) (Invitrogen, Carlsbad, USA) diluted on Opti-MEM. Cells were washed with Opti-MEM. Some coverslips were fixed at this step using paraformaldehyde 3.7% during 10 minutes and then washed three times with PBS. The other coverslips were incubated with 37ºC pre-warmed Opti-MEM and placed at the incubator (37ºC, 5% CO_2) during one hour to allow the internalization of the ligands-bound receptors. Washing step with Opti-MEM was made, followed by fixation with paraformaldehyde 3.7% during 10 minutes and washing with PBS.

All coverslips were stained with DAPI, washed with PBS three times and mounted on slides using fluorescent mounting medium. Imaging was performed on the confocal microscope, in the mid-section of the cells. Image analysis to evaluate the number of vesicles was performed with ImageJ software using a homemade plugin (Romain Vauchelles, PIQ platform). Vesicles were counted after performing a threshold and was made a ratio between the number of vesicles and the number of cells (determined by the counting of the nucleus).

2.8 Statistical Analysis

Statistical analysis in more than two variables was done using one way ANOVA analysis, once the goal was to see if there was a significant difference between different conditions. Statistical analysis results were made using Bonferroni test with the software GraphPad

Prism. Statistical analysis in two variables was done using Student t-test. Data are represented as mean ± SEM (Standard error of the mean). The mean was obtained from independent experiments. The confidence interval of significance was stabilized at 95%.

3. Results

Using cell evasion from 3D spheroids, our team previously showed that in U87 cells loss of α5 integrin expression are more sensitive to gefitinib treatment. Published works showed that EGFR endocytosis and trafficking have been reported to have some influence in therapy resistance (65,144–146) and that integrin can regulate EGFR oncogenic activity during carcinoma invasion trought its trafficking. The aim of my master project was to determine if the endocytic pathway is involved in the integrin-mediated resistance to gefitinib.

3.1 Dynamin inhibition reverts negative effect of gefitinib in cell evasion

To determine if endocytic events are related with gefitinib resistance, endocytosis was blocked using pharmacacological inhibitors of dynamins. Dynamins (fig.3.1) are GTPase proteins involved in the budding of endocytic vesicles in the main endocytosis pathways, including clathrin-dependent route (fig.3.2). This route is described to be used by EGFR and integrins (45,96,132,147). Dynamins were blocked using two chemical inhibitors of its GTPase activity: dynasore (IC_{50} 80µM) which is a non competitive inhibitor inhibiting both dynamins (1 and 2) and dyngo4-a (IC_{50} 16µM), which bind to an allosteric site on the G domain and is more potent on dynamin 1 (0.4µM) than on dynamin-2 (3µM). There were evaluated using curve dose effect ranging from 6 to 50 $\mu mol.ml^{-1}$ for Dynasore and from 10 to 80 $\mu mol.ml^{-1}$ for Dyngo4-a. (45,96,132,147).

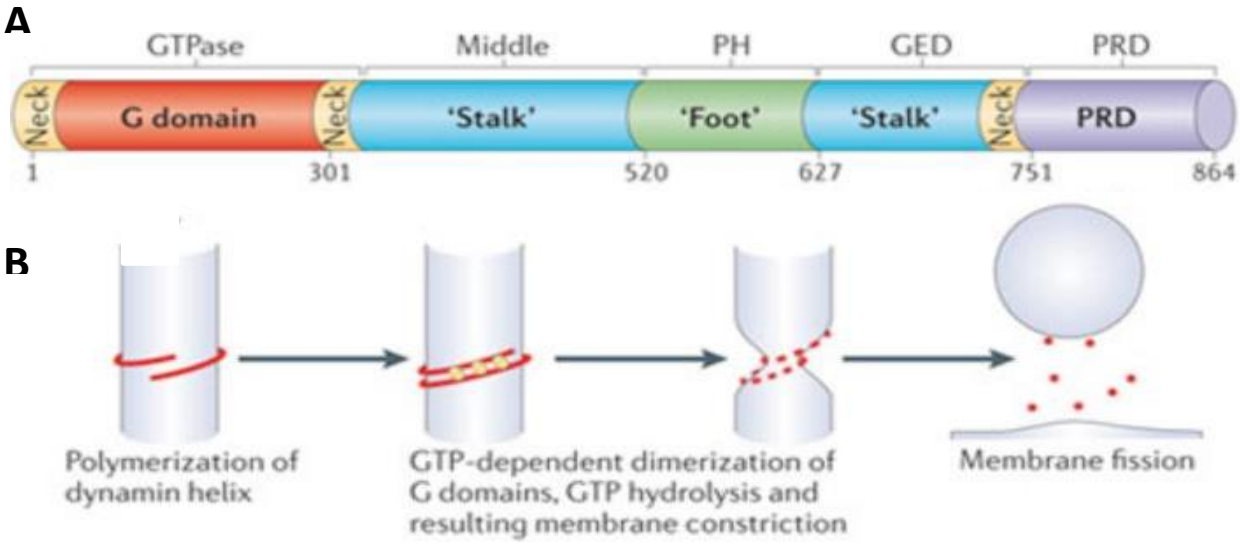

Figure 3.1: Dynamin struture and its role in membrane fission. A- Domain organization in human dynamin, where the number correspond to amino acid position on the gene. G domain is involved in GTP binding and consequent GTPase function, Middle and GED are involved in dynamin dimerization and oligomerization, PH and PRD domains are involved in dynamin interactions with other proteins. B – Mechanistic how dynamin after polymeration and consequent GTP hydrolysis leads to membrane fission. Adapted from (140).

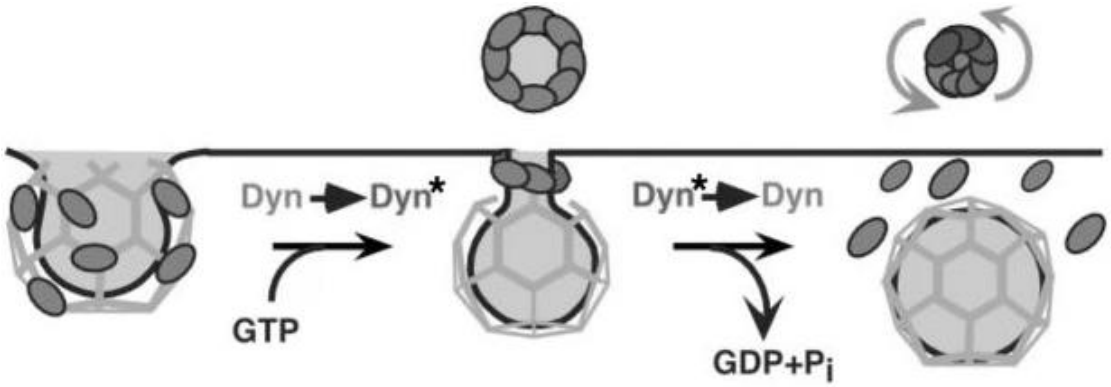

Figure 3.2: GTPase function of dynamin in clathrin-mediated endocytosis. After GTP binding, dynamin assembly in the neck of clathrin pit. GTP hydrolysis mediates dynamin conformation change that leads to vesicle fission. Adapted from (148).

Resistance to gefitinib was evaluated using cell evasion from a 3D small cluster of cells (spheroid). The assays were performed in two different cell lines (U87 α5+ and U87 α5-). The drugs were incubated alone or in combination with gefitinib during the 18 hours of cell evasion. The results are represented on figures 3.3 and 3.4 for dynasore, 3.5 and 3.6 for dyngo-4a.

When dynasore was incubated alone, we observed a significant decrease of cell evasion (number of cells out the spheroid) on the two highest concentrations (25 and 50 µmol.ml^{-1}) (for 25 µmol.ml^{-1} U87 α5+ 424.5±42.65, U87α5- 352.3±41.83; for 50 µmol.ml^{-1} U87 α5+ 342.0±24.55, U87α5- 324.2±33.95) in both cell lines compared with control cells (U87 α5+ 493.6±27.41, U87α5- 449.0±29.70) but no impact in the number of evading cells at lower concentrations (fig. 3.3, 3.4).

In agreement with previous results from the team, gefitinib used alone inhibited cell evasion in both cell lines but with more efficacy on U87a5- cells (133.1±11.34) than on U87a5+ (255.7±24.79).

Surprisingly, we observed that dynasore (12µM) completely blocked gefitinib-mediated evasion inhibition. Indeed, at a concentration of 12 µM of dynasore, we observed a significant increase in the number of evading cells when compared to gefitinib alone, both in U87a5+ cells (425.7±23.71 and 255.7±24.79, respectively) and in U87a5- cells (394.9±26.02 and 133.1±11.34, respectively). This event was statistically significant with the two lowest concentrations of dynasore (6 and 12 µmol.ml^{-1}) plus gefitinib (fig. 3.3, 3.4). As similar results were observed in both cell lines, this suggest that evasion stimulation by dynamin inhibition is α5 integrin- independent. Thus, dynamin inhibition by dynasore in low concentration has no impact on cell evasion of controlled cells but prevent gefitinib-induced inhibition of cell evasion. These results revealed an important function of dynamin in the activity of gefitinib.

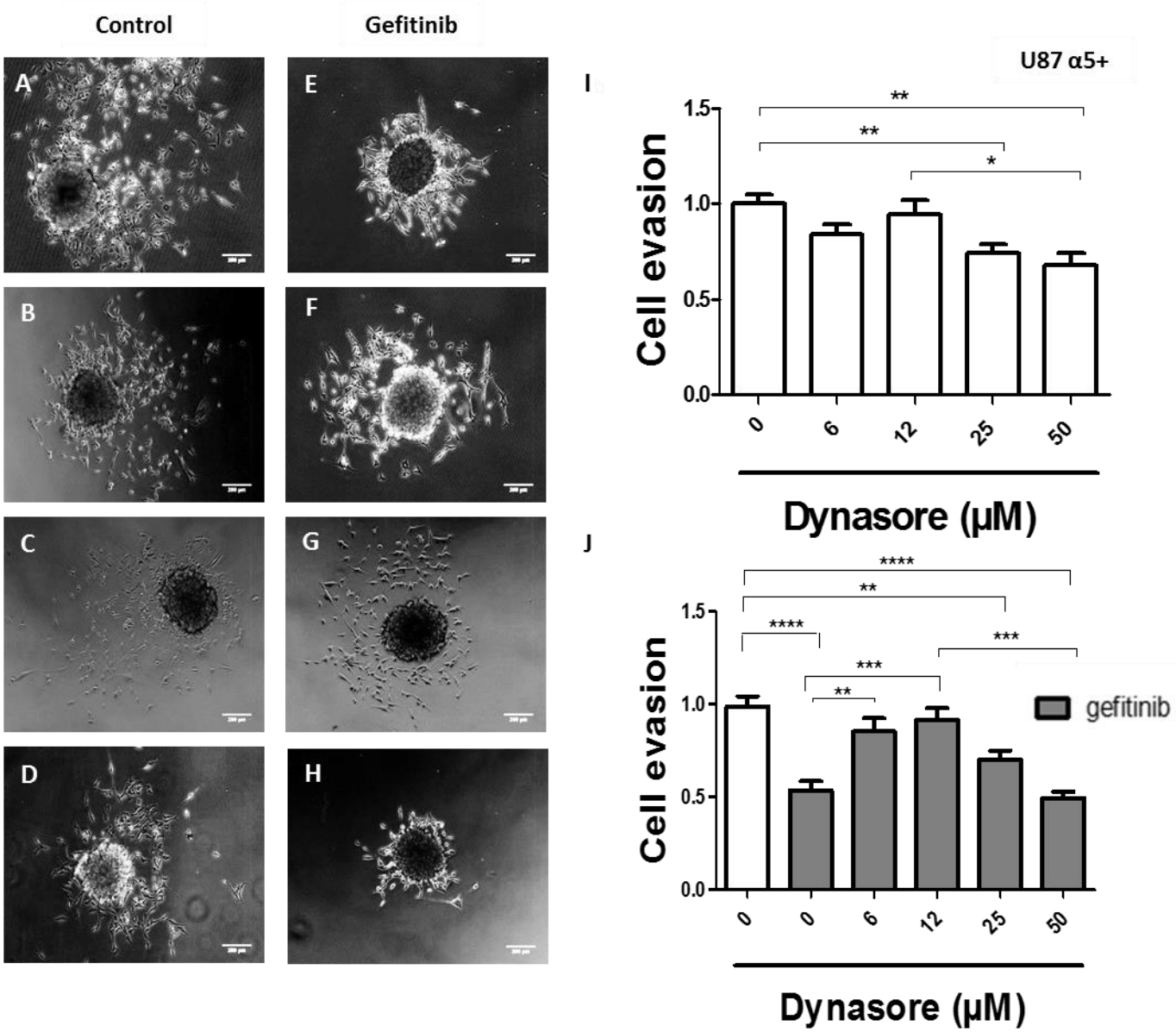

Figure 3.3: Cell evasion on U87 α5+ under treatment with dynasore and gefitinib. U87 α5+ spheroids were seeded on fibronectin-coated surface in the presence (20μM) or the absence of gefitinib and various concentration of dynasore for 18hours. A-H Phase Contrast images of spheroids under different incubation conditions (Scale bar 200 μm): A- Control, B- Dynasore 6 μmol.ml^{-1}, C- Dynasore 12 μmol.ml^{-1}, D- Dynasore 50 μmol.ml^{-1}, E-H – Gefitinib 20 μmol.ml^{-1} (E-alone, F- Dynasore 6 μmol.ml^{-1}, G- Dynasore 12 μmol.ml^{-1},H- Dynasore 50 μmol.ml^{-1}). I,J- The number of evading cells was quantified after DAPI-labelling of their nucleus and data were expressed as the ratio of evading cells compared to control (DMSO-treated) cells.Histograms represent mean±SEM of 3 independent experiments. Statistical analysis was made using ANOVA *p<0.05; **p<0.01; ***p<0.001; **** p<0.0001

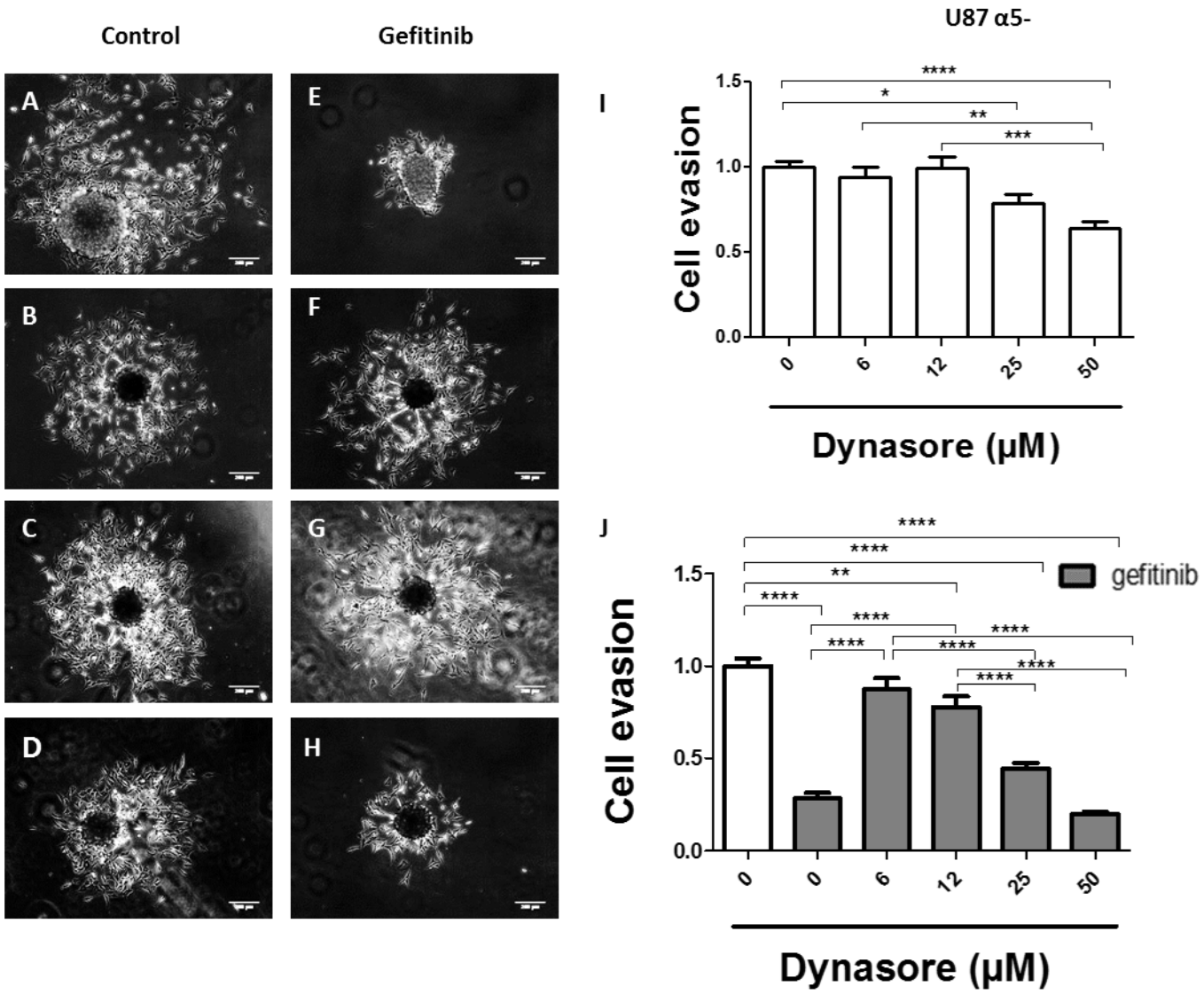

Figure 3.4: Cell evasion on U87 α5- under treatment with dynasore and gefitinib. U87 α5- spheroids were seeded on fibronectin-coated surface in the presence (20μM) or the absence of gefitinib and various concentration of dynasore for 18hours. A-H Phase Contrast images of spheroids under different incubation conditions (Scale bar 200 μm): A- Control, B- Dynasore 6 μmol.ml$^{-,1}$, C- Dynasore 12 μmol.ml$^{-,1}$, D- Dynasore 50 μmol.ml$^{-,1}$, E-H – Gefitinib 20 μmol.ml$^{-,1}$ (E-alone, F- Dynasore 6 μmol.ml$^{-,1}$, G- Dynasore 12 μmol.ml$^{-,1}$,H- Dynasore 50 μmol.ml$^{-,1}$). I,J- The number of evading cells was quantified after DAPI-labelling of their nucleus and data were expressed as the ratio of evading cells compared to control (DMSO-treated) cells. Histograms represent mean±SEM of 3 independent experiments. Statistical analysis was made using ANOVA *p<0.05; **p<0.01; ***p<0.001; **** p<0.0001

As pharmacological inhibitors in general and dynasore in particular have unspecific effects (149), we control the involvement of dynamin in gefitinib-mediated inhibition using another dynamin inhibitor, dyngo-4a (fig. 3.5, 3.6).

When cells were incubated with gefitinib alone, there was a significant decrease of the number of cells that goes out of the spheroid in both cell lines (fig. 3.5, 3.6). This decrease was more accentuated in the α5 - cell line (140.5±13.14) than in U87a5+ (173.8±12.14) compared with the control (U87 α5+ 372.3±17.30, U87α5- 477.7±23.68), as described before (fig. 3.6).

When cells were incubated with dyngo-4a and gefitinib there was observed an increase of cell evasion compared with only gefitinib incubation (for 10 μmol.ml^{-1} U87 α5+ 457.7±29.83, U87α5- 290.6±37.97; for 20 μmol.ml^{-1} U87 α5+ 361.8±22.33, U87α5- 348.3±35.85; for 40 μmol.ml^{-1} U87 α5+ 328.8±16.77, U87α5- 443.7±38.75) (fig. 3.5, 3.6). This event was statistically significant comparing gefitinib incubation with all concentrations of dyngo-4a except with the highest one. This phenotype occurred in both cell lines, demonstrating being α5 integrin independent. At 80 μmol.ml-1 of dyngo-4a plus gefitinib the cell evasion decreases comparing with the control but still is higher than the gefitinib condition (U87 α5+ 247.2±33.16, U87α5- 110.6±19.42). This decrease was more accentuated in α5 – cell line (fig.3.6).

Altogether, using two different pharmacological inhibitors, we showed that dynamin is involved in the gefitinib-mediated inhibition of U87 cell evasion regardless the a5 integrin expression level. This suggest that the endocytic pathway play a critical role in gefitinib mediated inhibition.

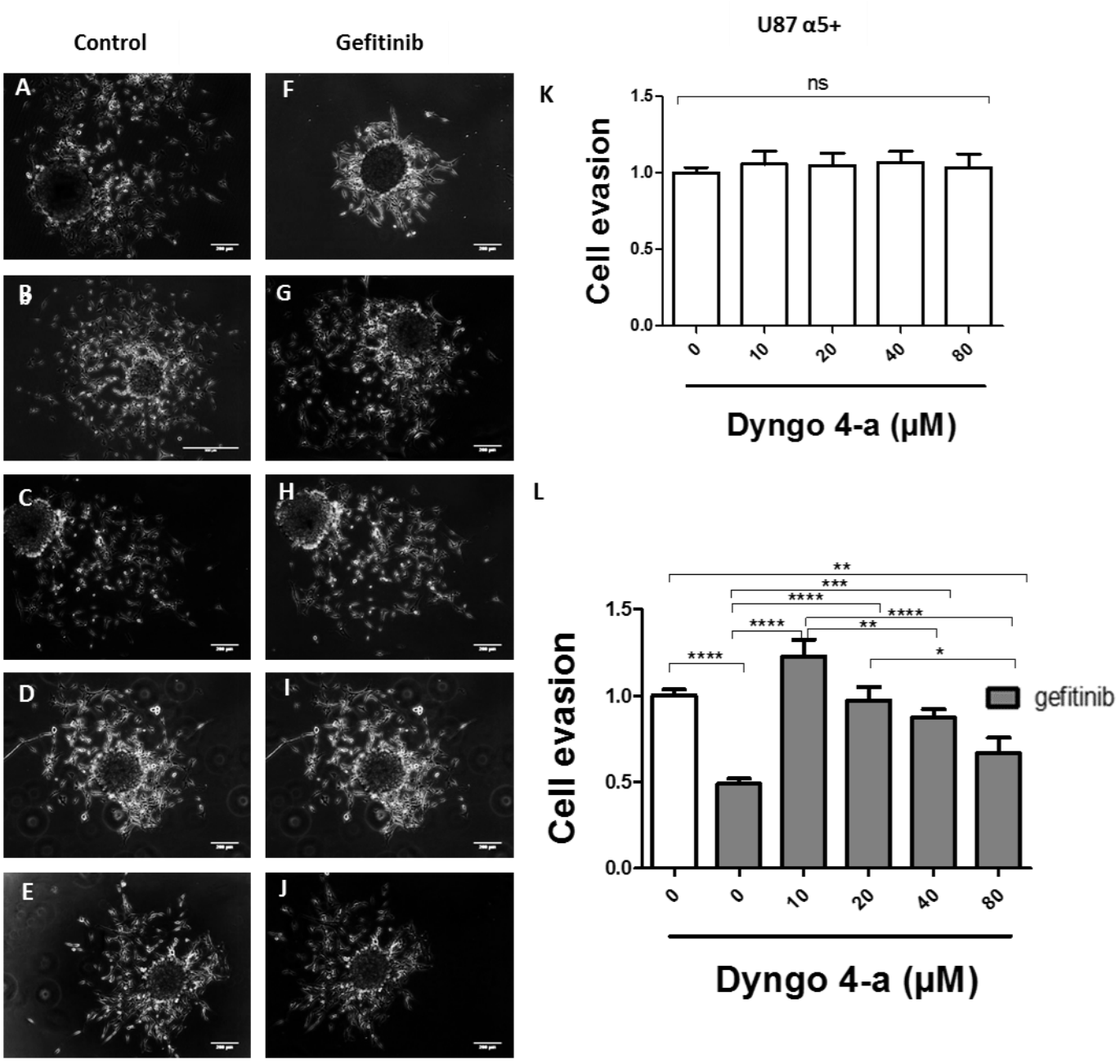

Figure 3.5: Cell evasion on U87 α5+ under treatment with dygo-4a and gefitinib.U87 α5+ spheroids were seeded on fibronectin-coated surface in the presence (20μM) or the absence of gefitinib and various concentration of dyngo-4a for 18 hours. A-J Phase Contrast images of spheroids under different incubation conditions (Scale bar 200 μm): A- Control, B- Dyngo-4a 10 μmol.ml^{-1}, C- Dyngo-4a 20 μmol.ml^{-1}, D- Dyngo-4a 40 μmol.ml^{-1}, E- Dyngo-4a 80 μmol.ml^{-1}F-J – Gefitinib 20 μmol.ml^{-1} (F-alone, G- Dyngo-4a 10 μmol.ml^{-1}, H- Dyngo-4a 20 μmol.ml^{-1},I- Dyngo-4a 40 μmol.ml^{-1} , J- Dyngo-4a 80 μmol.ml^{-1}). K,L- The number of evading cells was quantified after DAPI-labelling of their nucleus and data were expressed as the ratio of evading cells compared to control (DMSO-treated) cells. Histograms represent mean±SEM of 3 independent experiments. Statistical analysis was made using ANOVA *p<0.05; **p<0.01; ***p<0.001; **** p<0.0001

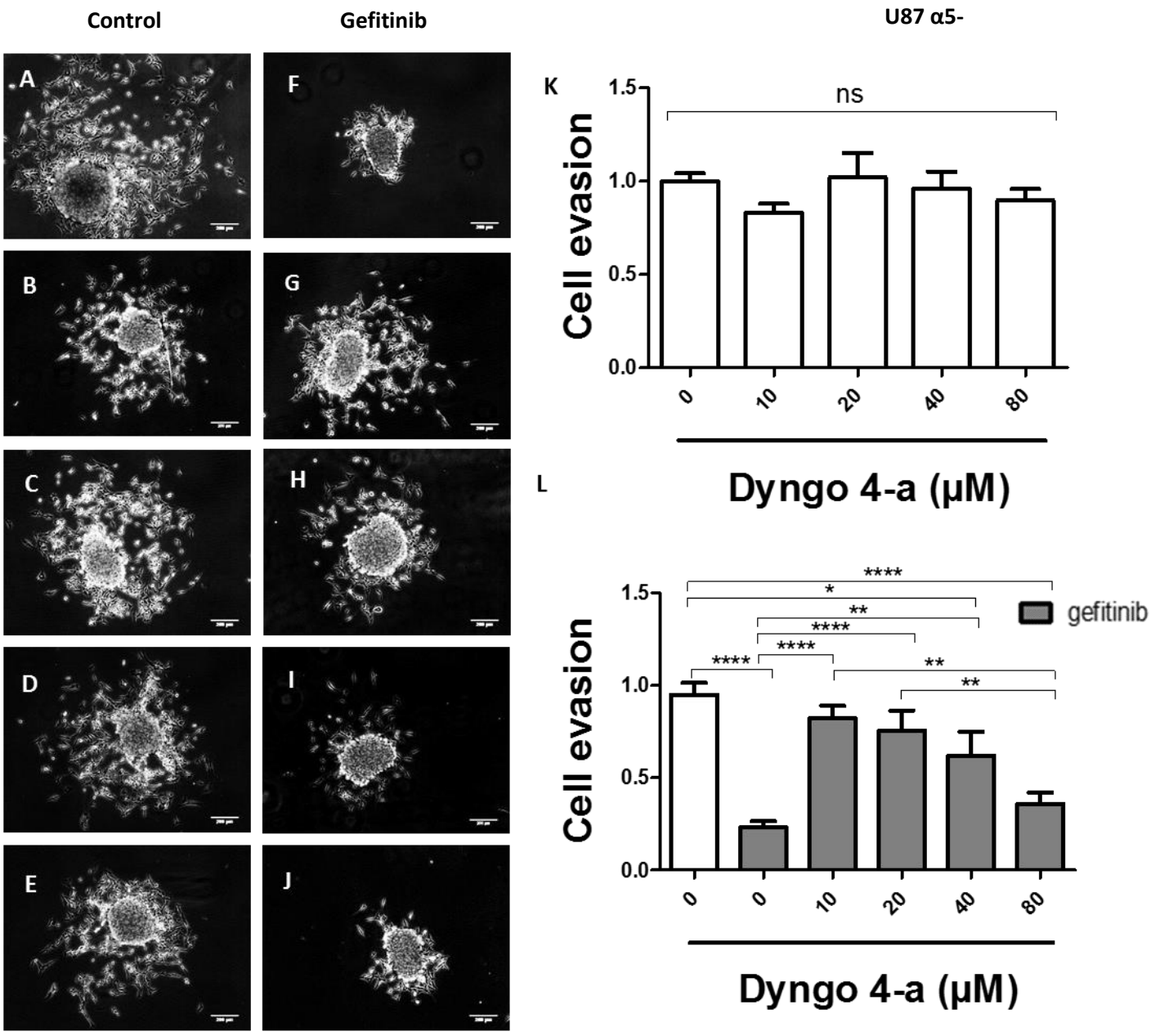

Figure 3.6: Cell evasion on U87 α5- under treatment with dygo-4a and gefitinib. U87 α5- spheroids were seeded on fibronectin-coated surface in the presence (20μM) or the absence of gefitinib and various concentration of dyngo-4a for 18 hours. A-J Phase Contrast images of spheroids under different incubation conditions (Scale bar 200 μm): A- Control, B- Dyngo-4a 10 μmol.ml$^{-,1}$, C- Dyngo-4a 20 μmol.ml$^{-,1}$, D- Dyngo-4a 40 μmol.ml$^{-,1}$, E- Dyngo-4a 80 μmol.ml$^{-,1}$F-J – Gefitinib 20 μmol.ml$^{-,1}$ (F-alone, G- Dyngo-4a 10 μmol.ml$^{-,1}$, H- Dyngo-4a 20 μmol.ml$^{-,1}$,I- Dyngo-4a 40 μmol.ml$^{-,1}$, J- Dyngo-4a 80 μmol.ml$^{-,1}$). K, L- The number of evading cells was quantified after DAPI-labelling of their nucleus and data were expressed as the ratio of evading cells compared to control (DMSO-treated) cells. Histograms represent mean±SEM of 3 independent experiments. Statistical analysis was made using ANOVA *p<0.05; **p<0.01; ***p<0.001; **** p<0.0001

3.2 Endocytosis is important in gefitinib treatment

As dynamin inhibition suggests a role for endocytosis in gefitinib effect, we thus seek to verify the impact of gefitinib on EGFR distribution in U87 cells. To this end, we performed confocal immunofluorescence microscopy against EGFR and one marker of early endosomes (EEA1). EEA1 is essential for early endosomes homotypic fusion being one of Rab5 protein effectors (150). The cells were treated with 20 $\mu mol.ml^{-1}$ of gefitinib in a time course experiment (zero to seven hours). In control U87 cells (fig.3.7 and 3.8), EGFR is localized mainly in the plasma membrane, while EEA1 is present in classical cytoplasmatic small vesicles. Only few early endosomes were immunolabelled by anti-EGFR antibodies. After gefitinib treatment, the presence of EGFR in early endosomes increased with time. This result demonstrates that gefitinib induces the localization of EGFR in early endosomes. We quantify the co-localization between EGFR and EEA1 at the different times using Pearson's correlation coefficient. As showed on figure 3.9, colocalization between the two proteins increased with time, in both cell lines (for 1 h U87 α5+ 44%, U87α5- 38%; for 2h30 U87 α5+ 68%, U87α5- 48%; for 7h U87 α5+ 68%, U87α5- 43%). Importantly, similar results were obtained in U8 a5+ and U87 a5-, indicating that gefitinib induced EGFR endocytosis independently of α5 integrin expression level.

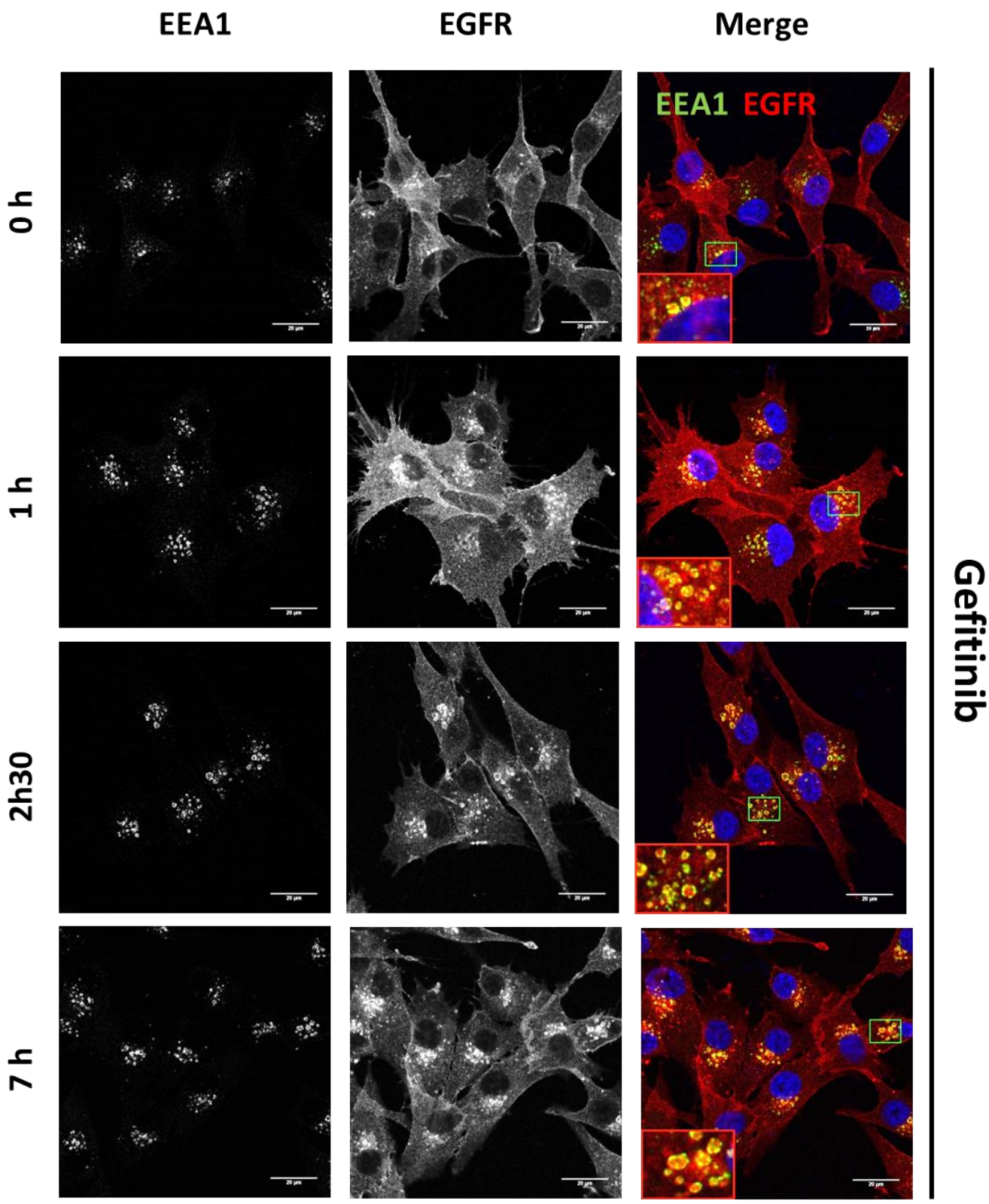

Figure 3.7: EGFR is localized in early endosomes in U87α5+.Confocal images of U87 cells α5+ in the presence of 20 µmol.ml^{-1} gefitinib at different times. Cells were fixed, permeabilized and stained against EGFR and early endosome marker (EEA1). The merge of the two images can be seemed on right column (Merge). Zoom in images was 3 x. Scale: 20 µm

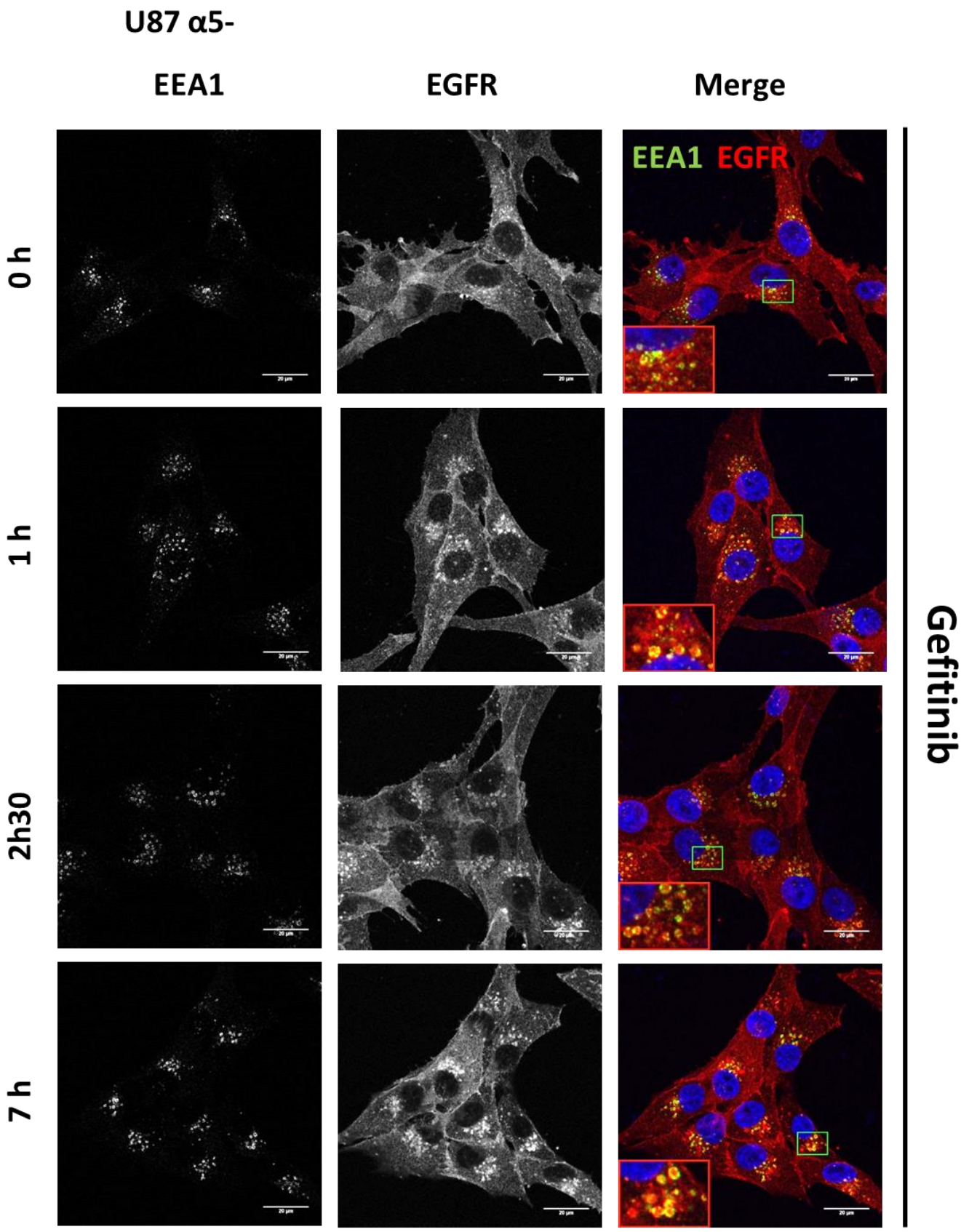

Figure 3.8: EGFR is localized in early endosomes in U87α5-.Confocal images of U87 cells α5- in the presence of 20 µmol.ml^{-1} gefitinib at different times. Cells were fixed, permeabilized and stained against EGFR and early endosome marker (EEA1). The merge of the two images can be seemed on right column (Merge). Zoom in images was 3 x Scale: 20 µm

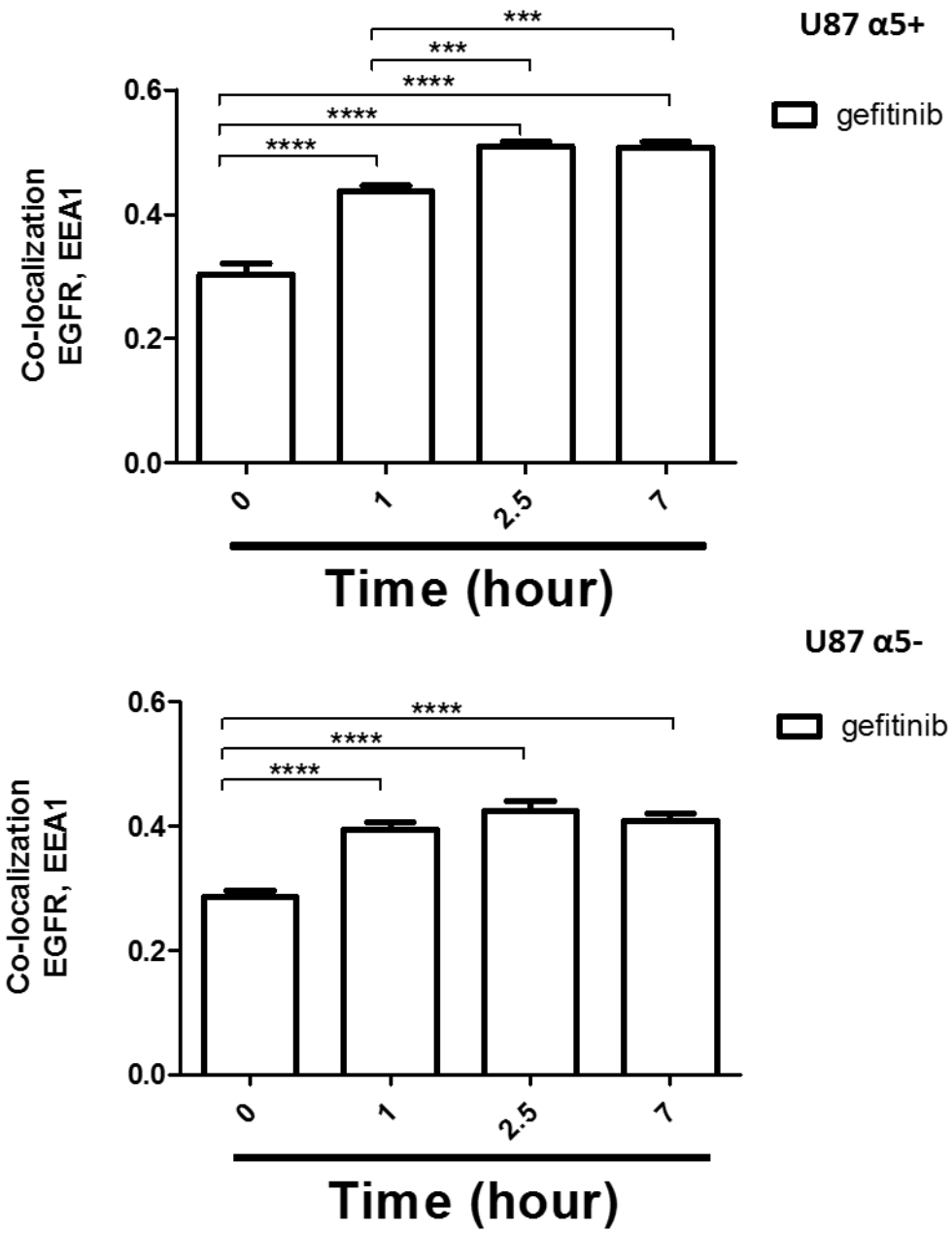

Figure 3.9: Co-localization of EGFR and EEA1 increases with the gefitinib incubation time.EGFR/EEA1 co-localization was evaluated using Pearson's correlation coefficient. Quantification was made at least from 6 different images from 2 independent experiments. Statistical analysis was performed using ANOVA ***p<0.001; **** p<0.0001

3.3 Gefitinib induces EGF uptake and dynasore impaired this phenotype

In order to determine if dynasore could impege gefitinib-mediated EGFR endocytosis, we then determine the influence of gefitinib and dynasore on ligand-induced EGFR internalization using fluorescent-tagged EGF.

To this end serum-starved U87 a5+ and U87 a5- cells were incubated at 4°C (a situation where endocytosis does not occur) in the presence of EGF-Alexa 488 (100 $ng.ml^{-1}$). Cells were then whashed and kept at 4°C (negative control) or placed at 37°C for various period of times (a situation where endocytosis occurs in normal conditions). In figure 3.10, at 4°C the staining is mainly at the plasma membrane, even if there are some cytoplasmic background. After one hour at 37°C, EGF is founded inside of the cells, in small vesicles.

To assess for the impact of gefitinib on EGFR internalization, we compared EGF uptake on control and gefitinib-treated U87 a5+ and U87a5- cells (Fig. 3.11), the number of EGF-positive vesicules were quantified using a home-made ImageJ plugin (Fig. 3.12).

As shown here, gefitinib significantly increased EGF internalization in both cells lines (for U87α5+ 12.52±2.281, for U87α5-10.14±1.868) compared with the positive control (for U87α5+ 8.071±0,7432 for U87α5-5.355±0.5567). We then measured EGF uptake on cells treated with dynasore. In the absence of gefitinib, dynasore (50µM) clearly inhibits EGF internalization in U87a5+ cells (4.384±0.9250) but not in U87a5-(6.187±0.7204). When cells are treated with 50 µM dynasore and gefitinib, dynamin inhibition significantly reduced gefitinib-mediated EGF endocytosis (for U87α5+ 5.211±0.8251, for U87α5- 4.344±0.6354). This impairment is visualized in both cell lines and so it is α5 integrin independent. This result shows a similar pattern to the one obtained in cell evasion assay. Together with the evasion assays, our experiments indicate that blocking dynamin-mediated endocytosis of EGFR prevent this action of gefitinib on cell evasion, independently of a5 integrin expression level.

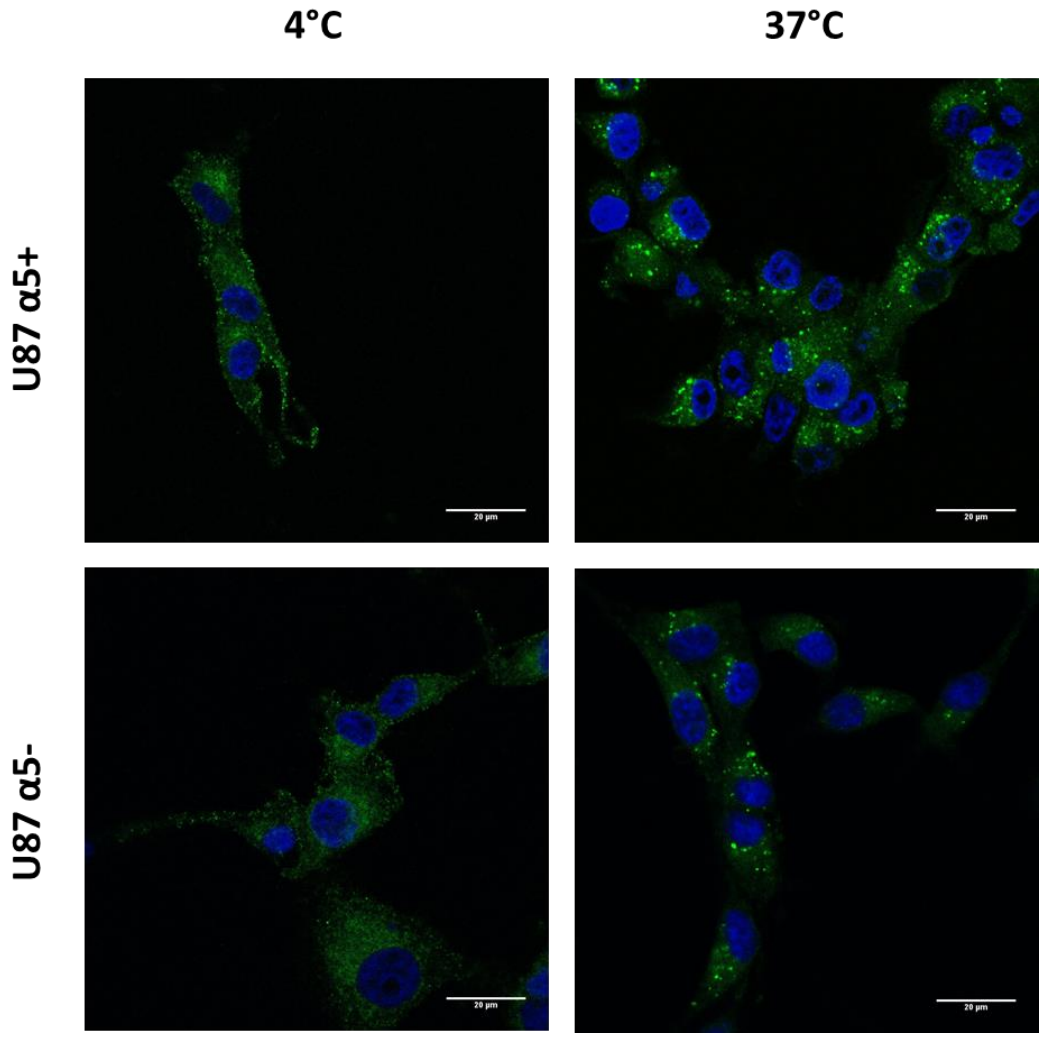

Figure 3.10: Negative (4°C) and Positive (37°C) controls of EGF uptake assay. Serum-starved cells were incubated with Alexa 488-EGF (100 ng.ml^{-1}) at 4°C for 30 minutes. Cells were then placed at 37°C for one hour. to allow internalization or kept at 4°C as control. At the end of the time course, cells were fixed and stained with DAPI and confocal images were performed Scale: 20 µm

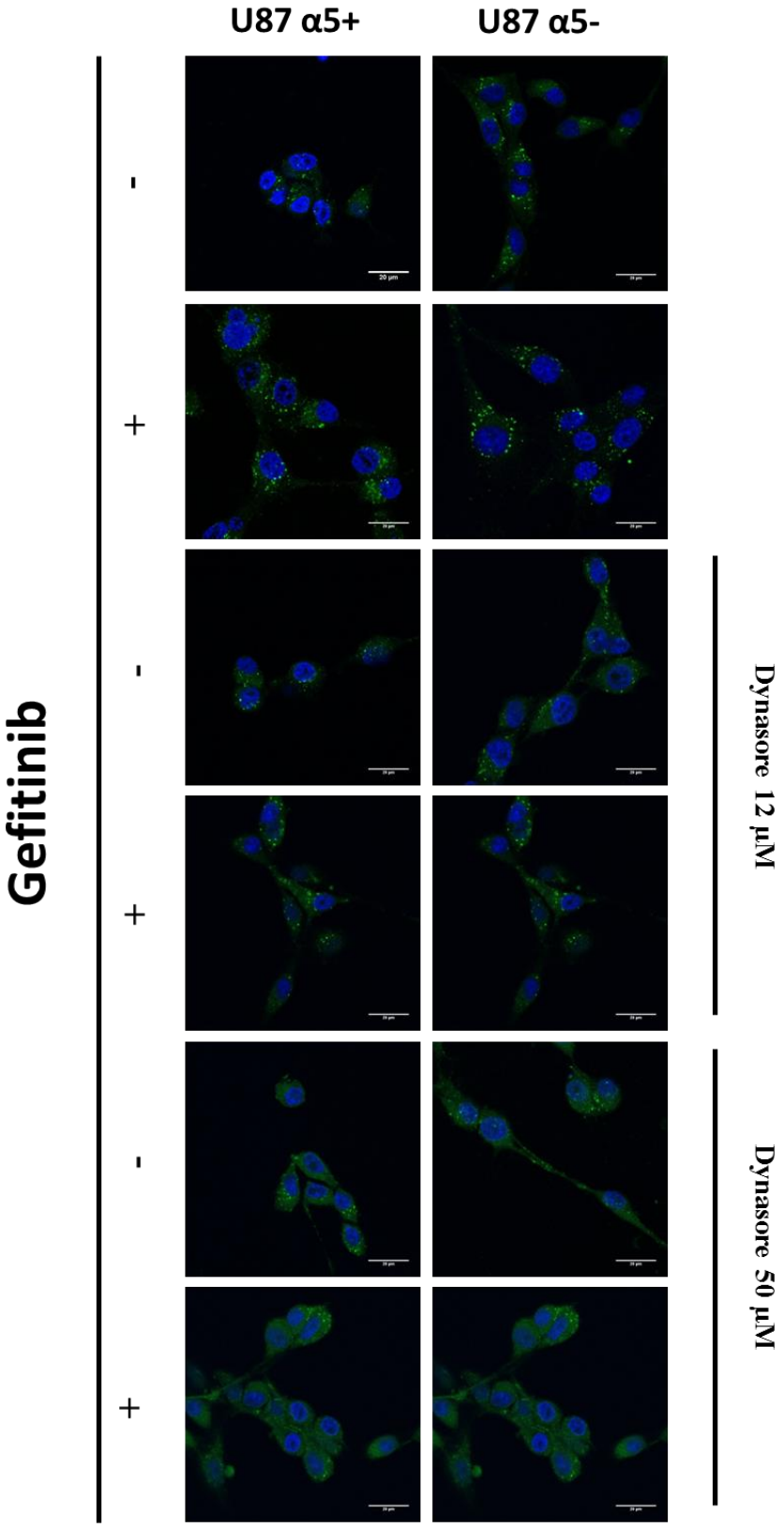

Figure 3.11: EGF uptake after treatment with dynasore and/or gefitinib. Serum-starved cells were incubated with Alexa 488-EGF (100 ng.ml^{-1}) at 4°C for 30 minutes. Cells were then placed at 37°C with 20 µM of gefitinib and/or 12 or 50 µM of dynasore for one hour to allow EGF internalization. At the end of the time course, cells were fixed and stained with DAPI and confocal images were performed Scale: 20 µm

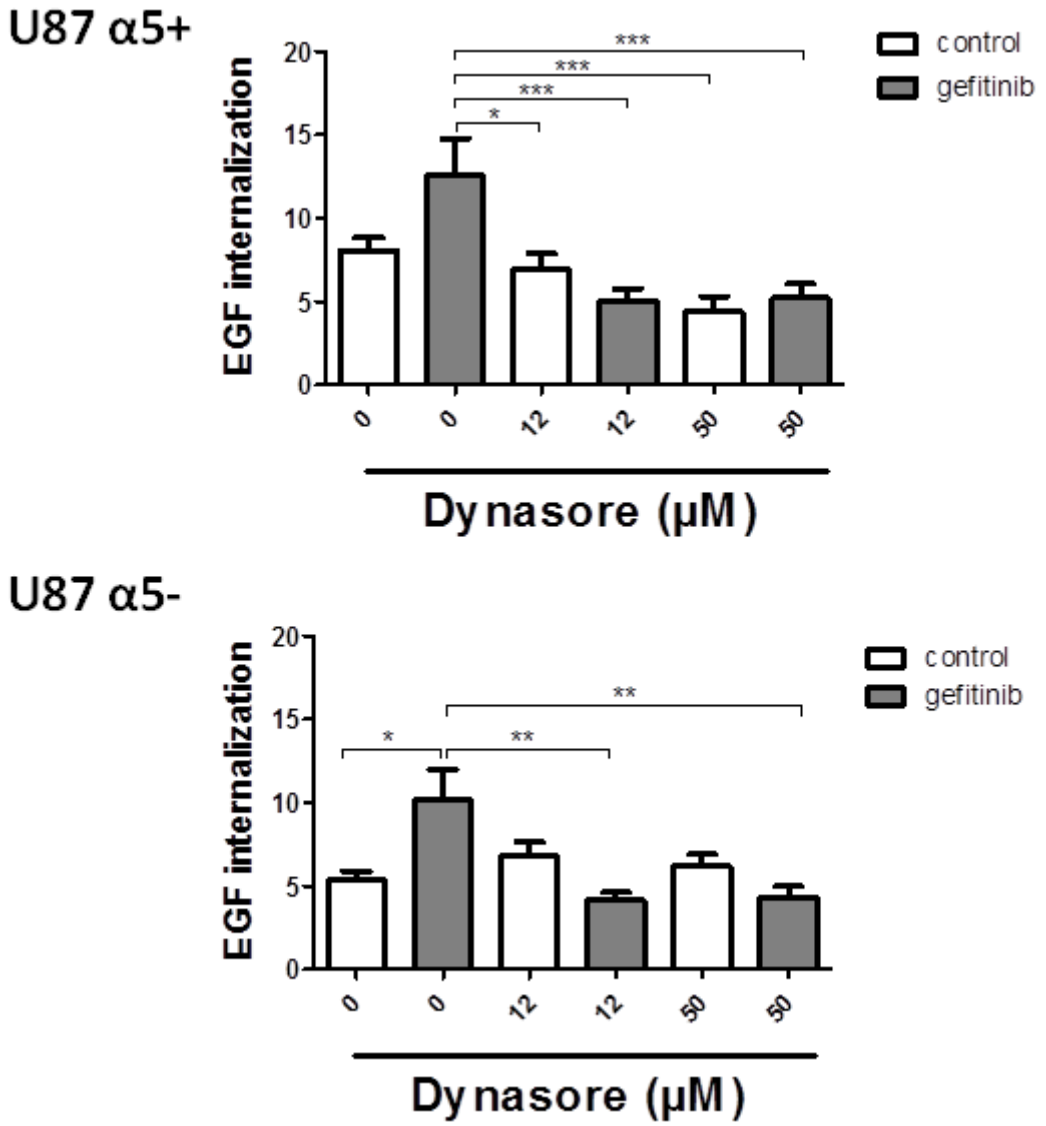

Figure 3.12: Quantification of EGF uptake after treatment with dynasore and/or gefitinib. After fixation, confocal images were analysed with a home-made ImageJ plugin to quantify the number of EGF-containing intracellular vesicules per cells. Histograms represent mean±SEM of at least 12 cells from 2 independent experiments. Statistical analysis was made using ANOVA *p<0.05; **p<0.01; ***p<0.001

3.4 β1 integrin and EGFR co-localized in endomembranar strutures after gefitinib treatment.

In our cell evasion assays, α5 expression is a resistant factor to gefitinib. However, we observed that gefitinib can induce EGFR internalization independently of integrin expression level. It has been published that α5 integrin can traffic with EGFR to promote carcinoma cell invasion (131,151). Our interpretation is that α5β1 integrin may impact on EGFR trafficking and function during membrane trafficking after endocytosis. We thus first seek to determine if β1 and α5 integrins were also internalized with EGFR after gefitinitb treatment. To this end we used confocal immunofluorescence microscopy. It can be observed (fig.3.13) that β1 integrin and EGFR in control cells are mostly present at the plasma membrane. Surpringly, after gefitinib treatment, β1 integrin is also internalized and found in EGFR-positive endosomes. These results occured in both cell lines, U87 α5+ and U87 α5-. Related to α5 integrin (fig.3.14), the integrin is mainly localized at cell/ECM adhesion structures in U87 α5+, while is almost inexistent in the U87 α5- cells. In focal adhesion level, co-localization between active α5 integrin and EGFR did not occur. After gefitinib treatment, EGFR and α5 integrin are internalized and in some cases found in the same vesicules.

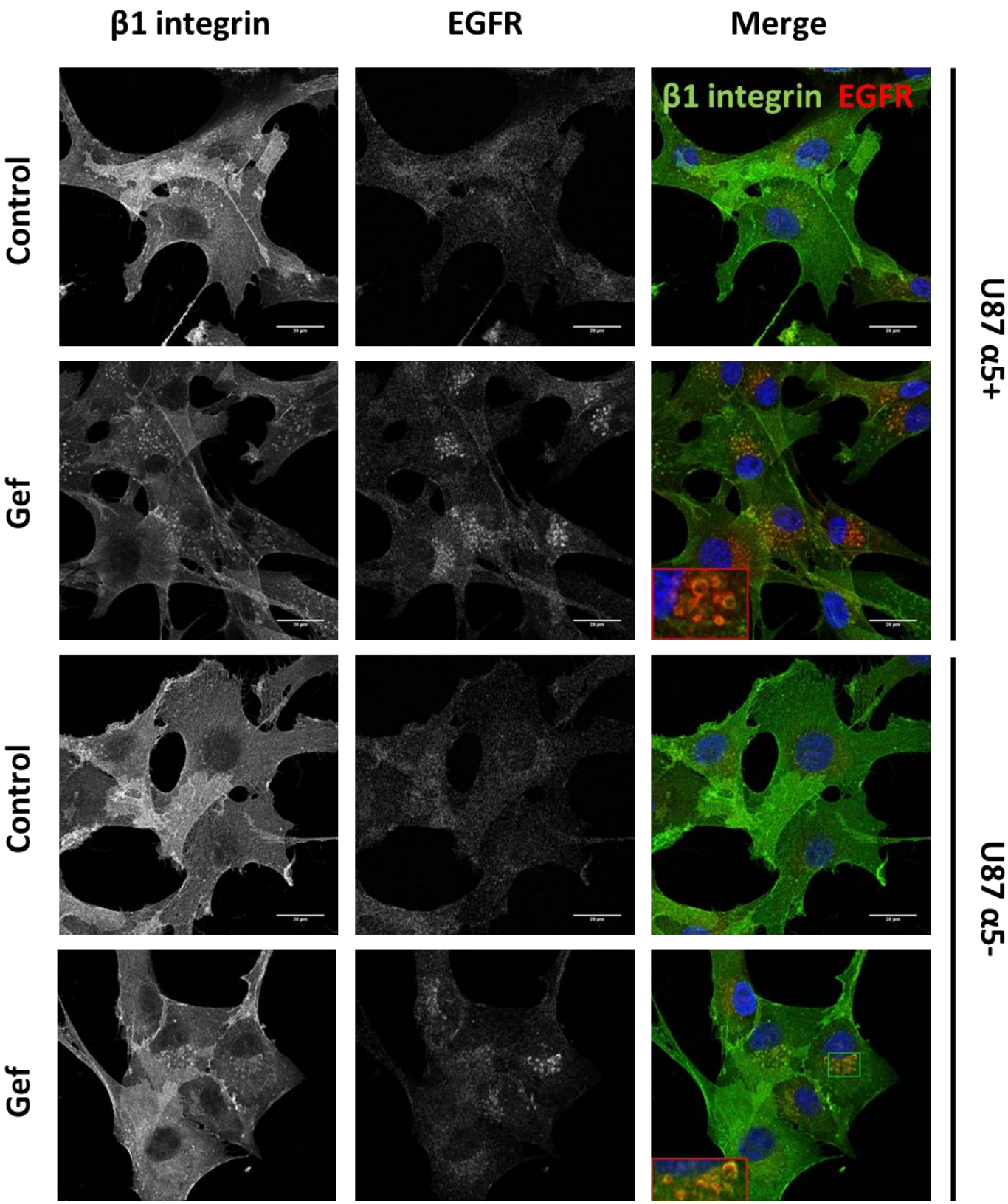

Figure 3.13: β1 integrin and EGFR are co-internalized after gefitinib treatment. Confocal images of U87 cells α5+ and α5- in the absence (Control) and presence of 20 µmol.ml^{-1} gefitinib (Gef). Cells were fixed, permeabilized and stained against β1 integrin and EGFR. The merge of the two images can be seemed on right column (Merge). Zoom in images was 3 x. Scale: 20 µm

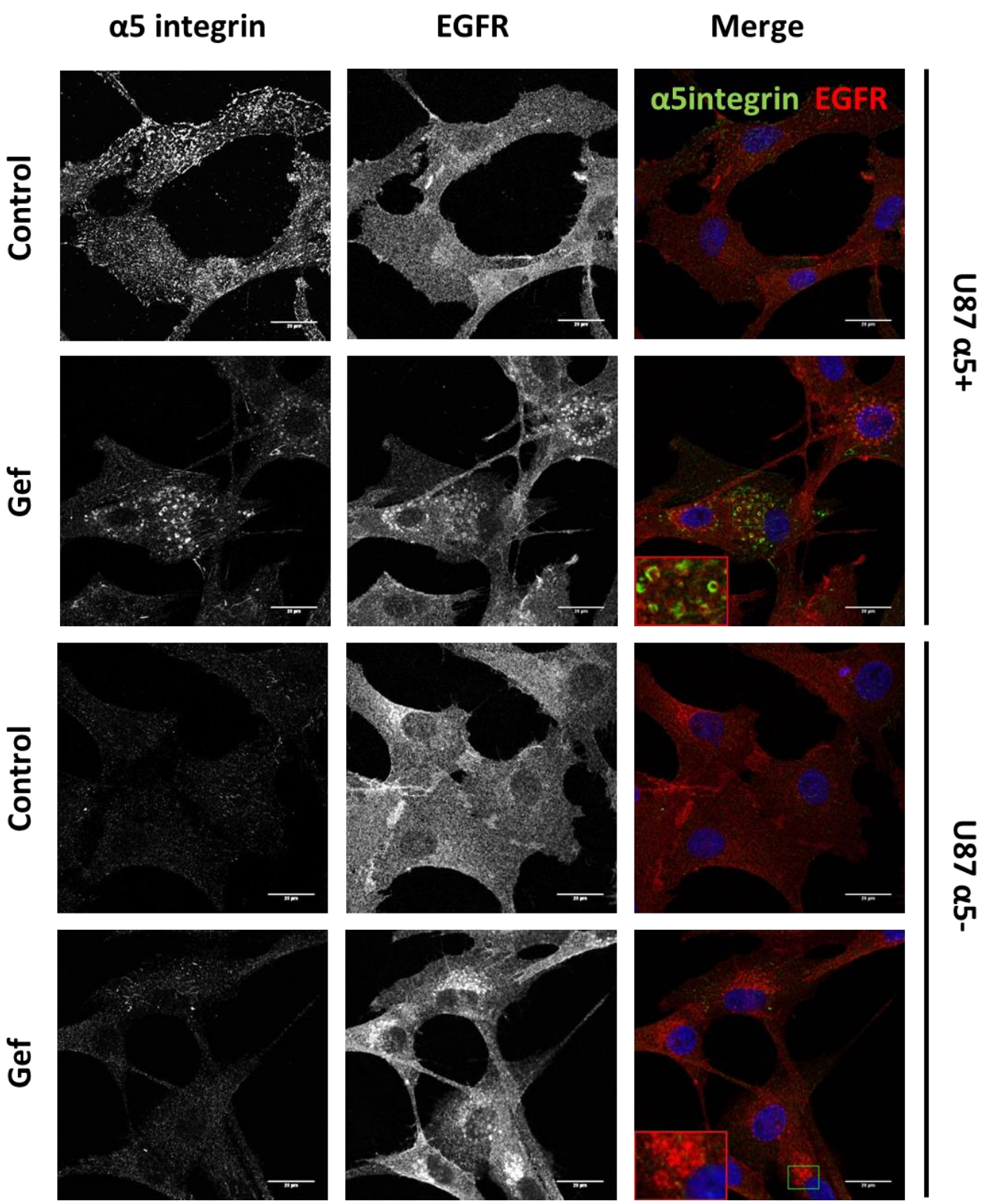

Figure 3.14: α5 integrin and EGFR are co-internalized after gefitinib treatment in U87α5+.Confocal images of U87 cells α5+ and α5- in the absence (Control) and presence of 20 µmol.ml^{-1} gefitinib (Gef). Cells were fixed, permeabilized and stained against α5 integrin and EGFR. The merge of the two images can be seemed on right column (Merge). Zoom in images was 3 x. Scale: 20 µm

Due to diffraction-limited resolution, confocal fluorescence microscopy can only distingue two proteins that distant from each other more than 300 nm (x-y plane). To overcome this fault, we used a super-resolution technique, PALM- STORM imaging, in order to determine with more precision, the proximity between β1 integrin and EGFR (spatial resolution around 20-30 nm in x-y plane). After gefitinib treatment (fig.3.15), both proteins are closed to each other in endosomal compartment. This experiment demonstrates that after geftinib treatment, β1 integrin and EGFR may physically be in endosomes.

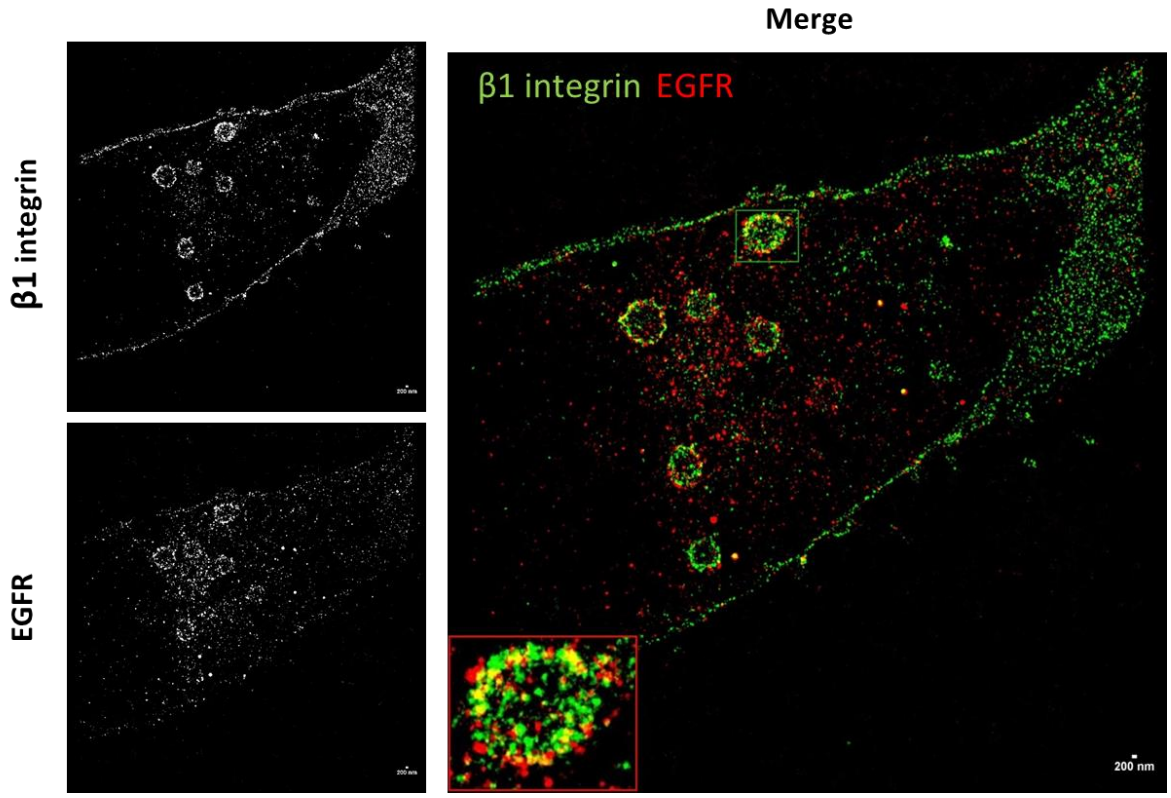

Figure 3.15: β1 integrin and EGFR are co-localized after gefitinib treatment. PALM-STORM images of U87 cells α5+ in and presence of 20 µmol.ml^{-1} gefitinib. Cells were fixed, permeabilized and stained against β1 integrin and EGFR. The merge of the two images can be seemed on right side (Merge). Zoom in images was 3 x. Scale: 200 nm

3.5 Gefitinib-induced EGFR and β1 integrin internalization occurs in others glioma cell lines

To verify what occurs in others glioma cell lines, protein levels of α5 integrin and EGFR and gefitinib induced endocytosis were evaluated. First of all, α5 integrin and EGFR protein levels were analyzed to confirm the presence of these proteins in glioma phenotype. It was demonstrated that different cell lines presented different protein levels patterns (fig. 3.16 and table 3.1). There are two cell lines with high levels of α5 integrin (LN443 and U87) and three cell lines with high levels of EGFR (SF767, SF763 and T98). Both SF 767 and SF 763 present low levels of α5 integrin. LN319 presents low levels of both proteins.

Confocal microscopy was performed in different glioma cell lines after gefitinib treatment (fig.3.17 and 3.18). In control condition, EGFR and β1 integrin are mainly localized in the plasma membrane. After treatment with 20 $\mu mol.ml^{-1}$ of gefitinib during 24 hours, there were also verified internalization of EGFR and β1 integrin in diverse glioma cell lines. The occurence of internalization is described on table 3.1. These results provide information for the strong contribution of gefitinib in this phenotype in glioma cells, being this α5 integrin independent since the strong internalization occured in cell lines with low α5 integrin level.

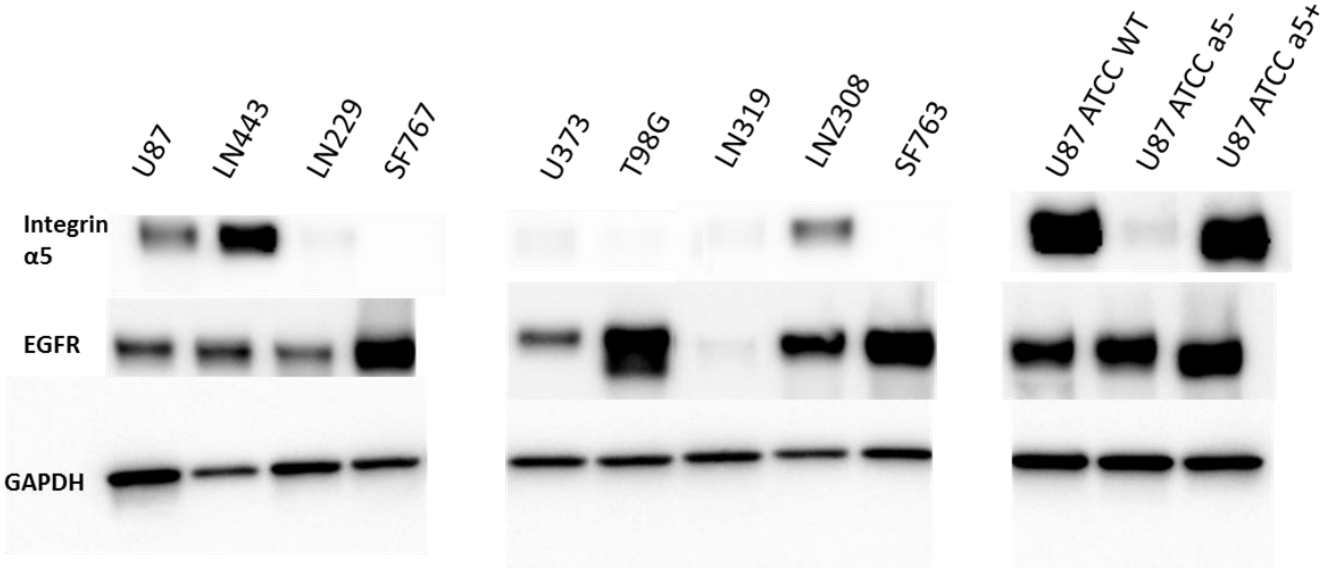

Figure 3.16: Protein expression of α5 integrin and was analyzed by immunoblotting using GAPDH as a loading control.

Table 3.1 - Characteristics of different glioma cell lines. Protein expression of α5 integrin and was analyzed by immunoblotting using GAPDH as a loading control. Each value represents the mean±SEM, *n* = 3. β1 Integrin and EGFR internalization after gefitinib treatment was evaluated with confocal immunofluorescence microscopy

	Protein expression level		**Internalization**	
Cell line	**α5 integrin**	**EGFR**	**β1 integrin**	**EGFR**
LN443	4.18±0.79	0.79±0.53	Medium Weak	Medium Strong
LN229	0.20±0.22	0.31±0.32	Strong	Strong
SF767	Below 0.01	1.08±1.09	Strong	Strong
U373	0.02±0.01	0.38±0.23	Medium	Medium
T98	0.10±0.09	1.81±1.40	Medium Strong	Strong
LN319	0.05±0.04	0.07±0.05	Weak	Medium
LNZ308	0.53±0.45	0.86±0.60	Medium	Medium Strong
SF763	Below 0.01	2.24±1.36	Strong	Strong
U87 ATCC WT	4.83±2.38	0.77±0.52	Strong	Strong
U87 ATCC α5-	0.11±0.04	0.85±0.67	Medium Strong	Strong
U87 ATCC α5+	4.24±1.94	1.17±0.86	Strong	Strong

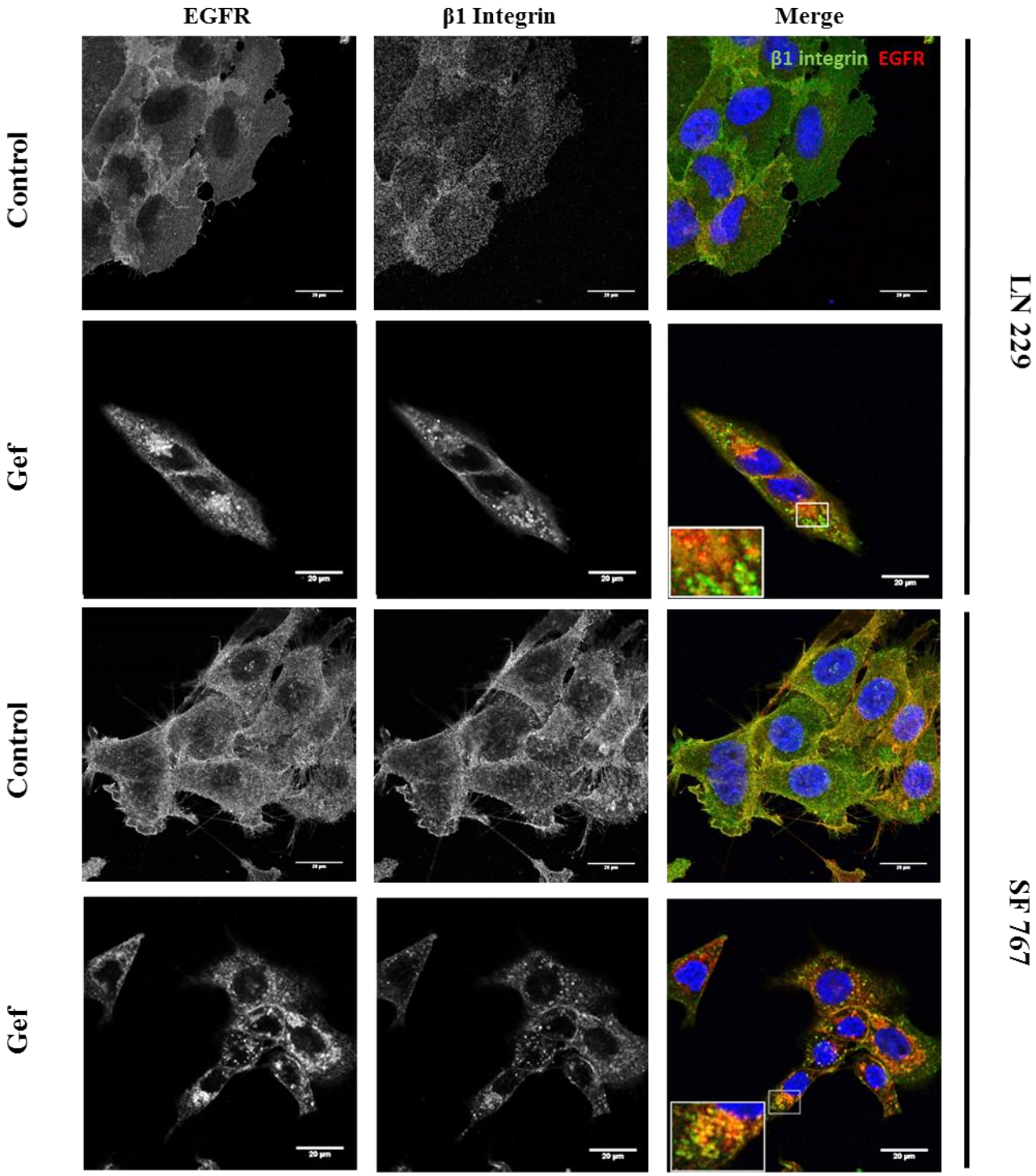

Figure 3.17: EGFR and β1 integrin localization in absence (Control) and presence (Gef) of 20µmol.ml-1of gefitinib. Cells were fixed, permeabilized and stained against EGFR and β1 integrin. The merge of the two images can be seemed on the right column (merge). Zoom in gefitinib images was 3 x. Scale: 20 µm

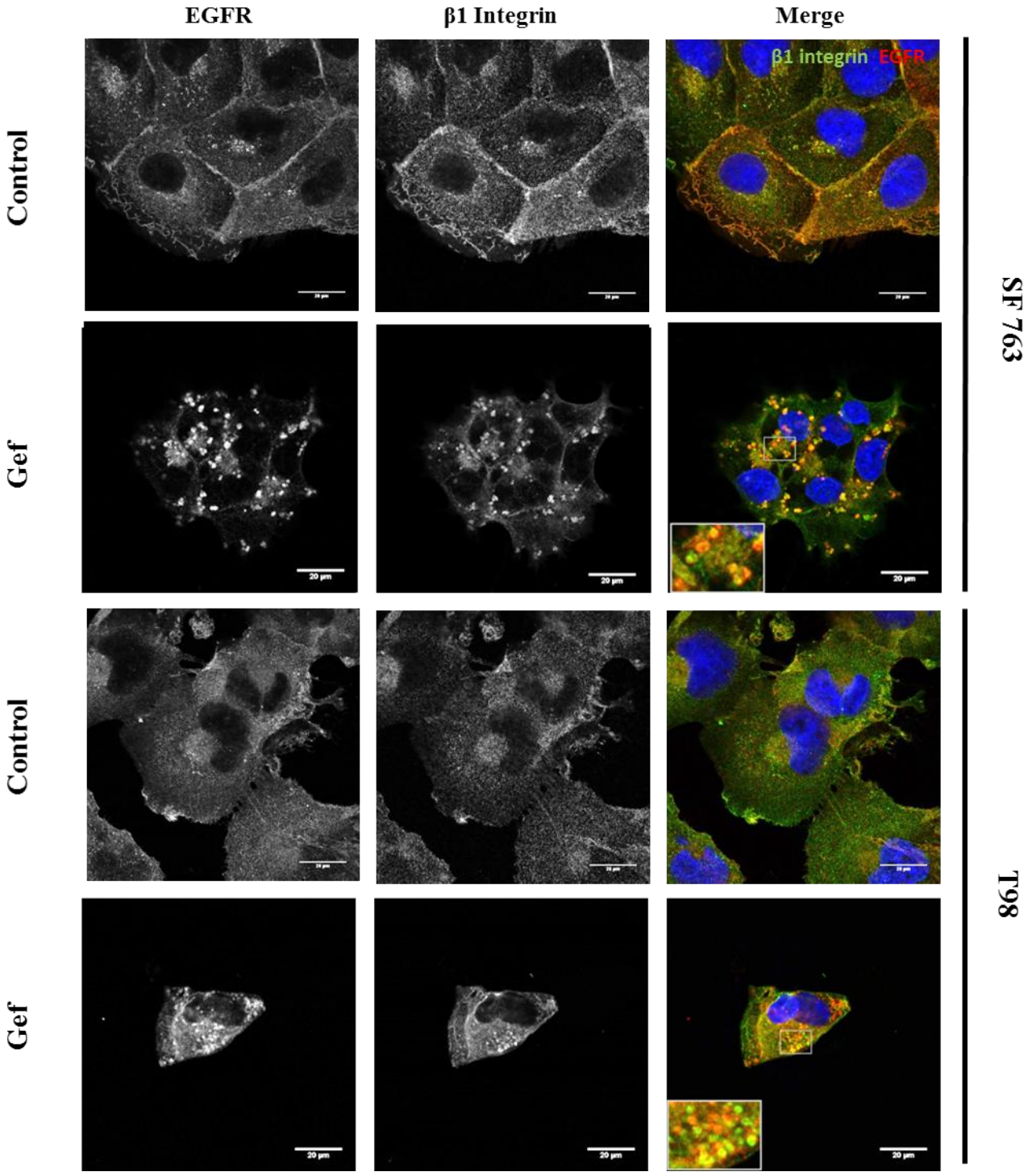

Figure 3.18: EGFR and β1 integrin localization in absence (Control) and presence (Gef) of 20µmol.ml-1of gefitinib.Cells were fixed, permeabilized and stained against EGFR and β1 integrin. The merge of the two images can be seemed on the right column (merge). Zoom in gefitinib images was 3 x. Scale: 20 µm

4. Discussion

Glioblastoma is the most aggressive brain cancer, being characterized by its resistance to therapy.EGFR is involved in gliomagenesis, being a very interesting therapeutic target. Anti-EGFR targeted-therapies are effective in other cancers. But in glioblastoma the clinical trials with antibodies and TKI failed. Until now, there is not a consensus related to predictive factors in EGFR-targeted therapies, even the co-existence of the mutated EGFRVIII and *PTEN* deletion is not a predictive factor (92). To try to uncover the nature of this resistance, the group started studying the relationship between EGFR and α5 integrin. Indeed, integrins are known to enhance oncogenic EGFR function and can trigger resistance to anti-EGFR therapy in carcinoma preclinical models (131). α5 integrin was described as a diagnostic, prognostic and predictive factors and is a new pertinent therapeutic factor in glioblastoma (108,113,116,117). α5 integrin was also associated with migration in GBM (114,115). So, migration and its is important to study regulation of migration and invasion in GBM. Co-trafficking between EGFR and α5β1 integrin are described during carcinoma invasion (131).

The objective I had was to determine if endocytic pathway is important for resistance to a clinical approved anti-EGFR TKI (gefitinib) during GBM cell dissemination.

During my master, using 2 differents pharmacological inhibitors of dynamin, a critical protein of clathrin-dependent endocytosis, we completely blocked gefitinib-induced inhibition of cell evasion from 3D spheroids. This observation was made either on cell expressing high or low level of α5 integrin. By confocal microscopy we showed that gefitinib-treatment induced the EGFR endocytosis. EGFR endocytosis was independent of α5 expression level. Using EGF-induced internalization we confirmed that gefitinib enhances EGFR endocytosis and that dynamin inhibitors prevent EGFR internalization. We hypothesis thus that, when endocytosis is impaired, cells become resistant (with a more evading behaviour) to gefitinib independently of α5 level. Gefitinib-mediated EGFR endocytosis happen together with α5β1 integrin endocytosis. And we used super-resolution microscopy (PALM-STORM) to show that the two proteins may physically interact in endosomes. Thus, we speculate that when endocytosis occured normally, α5β1 integrin may impact on EGFR trafficking and function during membrane trafficking downstream of endocytosis to confer resistance towards gefitinib treatment.

In the endocytic trafficking, the first step is the protein internalization. Different pathways are described for internalization, the clathrin-dependent pathway isthe most common for both EGFR and integrin.

The clathrin-mediated endocytosis has the following steps: putative nucleation, cargo selection, clathrin coat assembly, vesicle scission, uncoating and recycling of clathrin. Putative nucleation corresponds to the formation of a pit (membrane invagination) that will be recognized by protein such as Eps15. Eps15 binds to EGFR, being involved in the receptor endocytosis. The cargo selection is mediated by AP2, another protein that interacts with EGFR, to recruit it for the pit. When cargo is bound to the pit, clathrin stars to assembly, being recruited by AP2 to the plasma membrane. Proteins in the neck of the vesicle recruit dynamin. Dynamin is a GTPase protein that allows membrane fission. After vesicle detachment from the membrane clathrin starts to disassemble.

The role internalization in gefitinib activity could be studied through the manipulation of diverse proteins like clathrin and dynamin. Dynamin was the chosen one, because it affects only the internalization process and not the plasma membrane invagination and protein contain. It was already described the need of clathrin microdomain for EGFR signaling pathways independetly of receptor endocytosis (152). Also, dynamin is involved in more than one endocytic pathways, and the goal of this objective was not to specifically characterize the endocytic mechanism but only see its role in gefitnib treatment.

Dynamin is a GTPase protein involved in cell membrane remodeling. Mammalian dynamin family has three isoforms, which are very homologous between each other but with different expression patterns. Dynamin 1 is expressed only in neurons, dynamin 2 is ubiquitously expressed and dynamin 3 is present in the brain and testis. There are different models to explain membrane fission but all are mechanoenzyme- and GTPase activity-dependent. The GTP hydrolysis provokes a conformation change of dynamin, generating forces that results in fission by constriction or stretching (147,153).

To impair the role of dynamin, we used two chemical inhibitors: dynasore and dyngo-4a. Both dynasore and dyngo-4a block dynamin GTPase activity after the recruitment and self-assembly. They are both small interfering molecules that allow fast impact on biological processes, being also most of the time reversible. This confers an advantage of

chemical inhibitory molecules over dominant-negative mutants or dynamin knockdown by small interfering RNA (siRNA) (153).

Dynasore is a reversible noncompetitive inhibitor of GTPase activity of dynamin, preventing the scission of vesicles from the plasma membrane. Dynasore inhibits dynamin 1 and 2 regardless of their assembly state with GTP, so it interferes with the catalytic step. At 80µM, dynasore seems to inhibit also the mitochondrial dynamin Drp1(153). Dyngo-4a is a more potent dynamin inhibitor, being 37 times stronger that dynasore, and also less toxic to the cells. Dyngo-4a shows more selectivity towards dynamin 1 and it binds to allosteric site of G domain. The usual concentrations used for these two inhibitors are 80 µM for dynasore and 30 µM for dyngo-4a. Endocytic blockage of dynasore was maximum at 80 µM and half-maximum at 30 µM. However, these concentrations were often used serum-free medium and for short period of times (1-3 hours). To avoid dynasore unspecific effects and extreme toxicity (due to also incubation with gefitinib in some conditions), we performed a dose effect between 6 and 50 µM (154). Dyngo-4a is known to be more effective and less toxic than dynasore. But it also has a higher affinity towards dynamin 1 (only expressed in brain) versus dynamin 2 (ubiquitous expressed). Dynamin 2 is involved in cell migration in glioblastoma and others cancers (155–158). To try to potentiate also dynamin 2 inhibition, to study the toxic effects and possible off targets of the drugs and/or dynamin inhibition, there were used a dyngo-4a concentrations range between 10 and 80 µM. But it is important to have in mind that these results were obtained while inhibiting dynamin with chemical inhibitors that have some disadvantages. A chemical inhibitor unables one protein function while leaving unchanged all others. These inhibitors, dynasore and dyngo-4a, were reported to have some off targets (149,159). Using dynamin triple knock out mice were revealed off targets of Dynasore, not related with dynamin, such as inhibition of both fluid-phase endocytosis and peripheral membrane ruffling. These inhibitors are involved in inhibition of membrane ruffling and it can happen by the destabilization of F-actin. Both inhibition of fluid-phase endocytosis and membrane ruffling are related since in the first the extracellular material is engulfed by plasma membrane extensions. Dynasore seems to affect in a dynamin-independent way the lipid rafts, by reducing cellular levels of cholesterol but also turning its distribution more dispersed on plasma membrane. This phenotype can also be involved in the ruffling. Dynamin is involved in the delivery of cholesterol from endosomal compartment to endoplasmic reticulum, but its

downregulation using RNA interference does not give the same phenotype as dynasore regarding to cholesterol (149,159,160). Also chemical inhibitors have some troubles regarding stability and efficiency. Dynasore was reported to become unstable with time and to lost activity with high cellular density (more than 70% confluency), with the use of detergents such as Tween and with the use of serum (153,161). Also, due to possible non-specific effect of dynasore and dyngo-4a, dynamin 1 and 2 depletion by siRNA is required to confirm the role of dynamin proteins in gefitinib activity.

The biological assay used to evaluate the gefitinib resistance was the cell evasion from a small cluster of cells (spheroids). Spheroids are widely used to better characterize cellular events then the normal 2D cell culture. Spheroids assays resemble some physiological characteristics present *in vivo* such as cell-cell interactions, cell-ECM interactions, and the accessibility in gradient to oxygen, nutrients, drugs and signals (162,163). We focused on cell evasion because cell migration is one of the main characteristics of GBM and also previous work from the team showed that α5 expression had no impact on gefitinid inhibitory activity on cell growth and survival (data not shown). GBM are highly invasive tumors. This glioma cell migration and invasion make difficult the total tumor resection (first therapy line in this cancer). Also, migrating cells are more resistant to therapy (164). Migration was studied by plating spheroids on fibronectin-coated surface. Fibronectin was used as ECM protein because it was described to be overexpressed in glioblastoma and it is the ligand of α5β1 integrin. The activation of α5β1 integrin after fibronectin binding was described as a activator of beta-catenin pathway that leads to migration in glioma cells (113,165). Migration can also be evaluated using other assays, using mainly monolayer culture. It can be evaluated by a boyden chamber anda wound healing assay for example (166).

We first showed that dynamin inhition completly blocked gefitinib action on U87 cells, whatever the level of α5 integrin expression (Figures 3.3-3.6). This result suggest that endocytosis is required for an efficient inhibition of EGFR. Dysregulation of EGFR trafficking is involved in therapy resistance toward anti-EGFR TKI (167,168). In our experience, after plating the spheroids on fibronectin, there were incubated with dynamin inhibitors, gefitinib or both during almost one day. When dynasore was incubated alone, it affected cell evasion only at the highest concentrations studied (25 and 50 µM) while dyngo4-a did not affect cell evasion whatever the concentrations used. Since dyngo 4-a is more potent than dynasore and it was used at higher concentrations, it can be supposed

that the decrease of cell evasion observed in dynasore was due to its toxicity or specific off-target effects of this drug. When cells were incubated with the lowest concentrations of dynasore (6 and 12 µM) and gefitinib, there were observed a reversion of the cell evasion impairment caused by gefitinib. This event was α5 integrin independent. In the highest concentrations of dynasore the cell evasion was slightly higher than gefitinib alone or in the same range. Related to dyngo-4a all concentrations revert gefitinib-induced inhibition of cell evasion, with more strength at the lowest concentrations. Like for dynasore, this phenotype was α5 integrin independent. To complete this work, we should evaluate the toxicity of the drugs by studying the cell viability with MTT test or trypan blue exclusion test or by studying cell death by annexin V/ propidium iodide assay.

To confirm that endocytosis is important in gefitinib treatment, we evaluated if EGFR is present in early endosomes, that are the first endosomal vesicles after internalization. The nature of the vesicle was verified using confocal immunofluorescence microscopy with EGFR and EEA1 antibodies. EEA1 as described above is an early endosome marker. We also performed co-localization quantification using the macro JACOP by overlapping the channels of EGFR and EEA1 before and after gefitinib treatment. We observed a strong increase in the co-localization between these two proteins after gefitinib treatment. This result clearly show that gefitinib stimulate endocytosis in U87 cells.

To confirm that dynamin inhibitors trigger resistance to gefitinib by control of endocytic pathway, we used ligand-bound EGFR internalization assay. The data presented on figures 3.11 and 3.12 confirmed that gefitinib stimulated EGFR dynamin-dependent endocytosis and that this event occurs independently of the α5 integrin level of expression. Moreover, dynasore efficiently blocks the increased EGF uptake induced by gefitinib.

The assay used was based on the internalization of Alexa 488-EGF. EGF bounds to EGFR, inducing its endocytosis as described for ligand-bound receptor (47). Before starting the assay, cells were serum-starved to remove all growth factors present in the medium solution. This allows themaximal expression of EGFR at the plasma membrane level. This experiment has its faults that can be improved. On cells kept at 4°C, EGF localization was mainly at the plasma membrane. But we also observed some intracellular fluorescence. The problem likely came from autofluorescence of the cell becauseEGF-Alexa 488 concentration was quite low. To improve this, we will need a control with unlabeled cells and also to increase EGF-Alexa 488 concentration. Dynasore alone did

not have an effect in control untreated cells. These is surprising because in the literature ligand-induced EGFR endocytosis is dynamin dependent (169). However, in these experiences higher concentration (80μM) of dynasore were required to effectively block EGF internalization. Also, it should be used a positive control for clathrin-dependent endocytosis as transferrin, a wide used control (170). To remove non-endocyitozed EGF and enhance quantification of endocytosed EGFR, it should be made an acidic wash after the incubation at 37°C (for example sodium acetate buffer, pH 4.5). This step does not affect EGFR properties (171,172). The protocol needs to be optimized to the cell line used due to all stresses (serum-starvation, differences of temperatures). There is also an alternative technique to quantify ligand-induced endocytosis of EGFR based on biochemical approaches (131). It is important to have in mind, that in here it is only evaluated the ligand-bound EGFR internalization, but gefitinib can also induce unbounded-EGFR internalization. To verify this the same experiment can be reproduced using an anti-human EGFR antibody directly conjugated with fluorophore. With this type of protocol, EGFR internalization is stimulated by ligand binding. It still needs to be evaluated the role of dynamin inhibition on EGFR gefitinib-induced. To this end EGFR distribution can be analyzed on cells treated by gefitinib and dynamin inhibitors.The internalization profiling can be done with a time course experiment on living cells. To this end cells expressing EGFR-GFP are treated with gefitinib and live imaging can be performed with Total Internal Reflection Fluorescence Microscopy. This technique only allows the visualization of a limited sample region (until 200 nm of depth), allowing the visualization of the plasma membrane and the first steps of internalization processes.

Because α5 expression protects cells from gefitinib, we thought that this must happen after the endocytosis. We thus analyzed α5 and β1 distribution in cells treated with gefitinib. We clearly found by confocal immunofluorescence microscopy that β1 integrin is internalized after gefitinib treatment and found in EGFR-positive endosomes. This co-internalization happened in both U87 α5+ and U87 α5- cells, demonstrating it is independent of α5 expression level. To better assess if α5 expression affect gefitinib-induced endocytosis of β1, we should performed antibody-mediated integrin endocytosis assays as performed with EGFR. Also we should performed triple staining against EGFR, β1 integrin and early endosome markers (EEA1 or Rab5) and focal adhesion markers (paxillin, FAK), to compare the co-localization of the 2 receptors at the plasma membrane and in the endosomes. This can be achieved using labelled-primary antibodies. It can be

done also by expressing EEA1-GFP or paxillin-GFP and performing indirect immunofluorescence for the others integrin and EGFR. The other proteins should be labelled using fluorophores with compatible fluorescent spectra than GFP (excitation peak at 395 nm, emission peak at 488nm).

Measurement of protein proximity and thus possible physical interaction is crucial for biological systems knowledge. Multi-protein complexes are around 20-50 nm of diameter. This value is below the optical resolution limit (minimal distance between two points so they can be visualized independently) obtained with conventional fluorescence microscopy. Usually, the technique used is fluorescence microscopy imaging by overlapping images obtained for each protein of interest. Proteins are labeled with fluorescent-label antibodies, with different excitation spectra. After imaging acquisition, channels are overlap and it is formed a composite image. Unfortunately, diffraction-limited resolution of this technique only allow the discrimination of two different proteins at the minimal distance between each other of 200-300 nm in the xy-plane and 500-700 nm in the z-axis (141,142,173).

To overcome this problem, super resolution techniques such as stochastic optical reconstruction microscopy (STORM) were built. In this technique photo-switchable fluorophores are sequentially activated, imaged and deactivated, in order to determinate with high precision the position of the fluorophore in a given moment. In the end, all the positions acquired allow a resolution of 20-25 nm along the *xy*-plane and less than 50 nm in the *z*-axis (fig.4.1) (174).

With STORM it could be observed that after gefitinib treatment, EGFR and β1 integrin are both localized in vesicle structures, being closed to each other. This in support of a physical interaction between the 2 proteins in the endosomes. Another techinique of choice to measure protein interaction is FRET (Fluorescence resonance energy transfer). FRET is based on a energy transfer system between two chromophores. The donor is excited with a lower energy unable to excitate the acceptor. When the two proteins are apart, the signal obtained is from the donor. When they are closed to each other, occurs a energy transfer and in thi time is the acceptor that emits light (175,176).

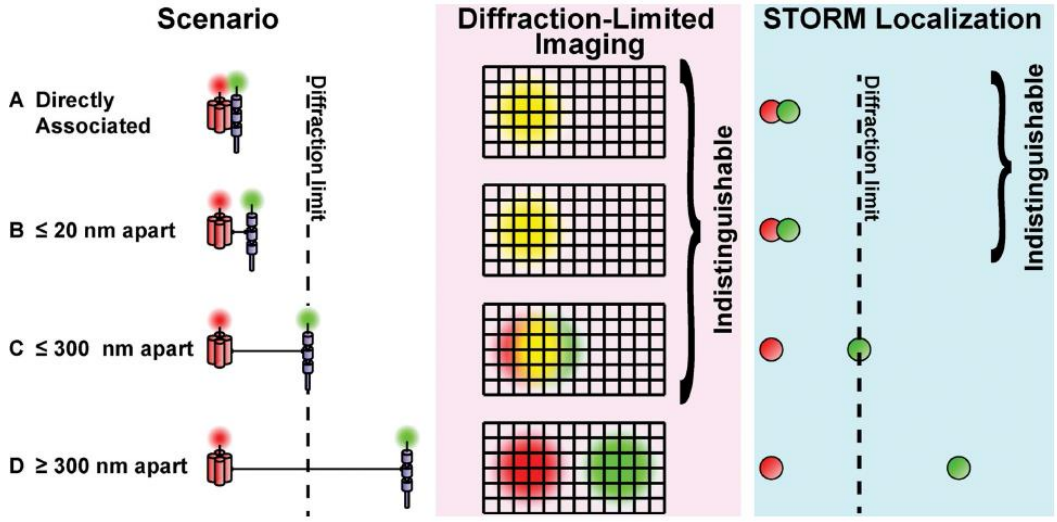

Figure 4.1: STORM versus diffraction-limited imaging techniques. When proteins that are directly associated (A) or located less than 20 nm apart (B) are indistinguishable by both types of techniques. However, STORM is able to distinguish proteins located over than 20 nm apart (C, D), while diffraction-limited imaging techniques are only able to distinguish when this distance is over 300 nm (D). Adapted from (173).

We also observed that EGFR is internalized after gefitinib treatment in different cell lines. In most of them, there is also β1 internalization. This phenotype seems to be α5 independent as cell lines with low integrin expression levels, seem to have strong internalization (SF763 and SF767 for example). Internalization characterization was made by evaluating in different cells, the occurrence or not of internalized proteins (founded inside of the cytoplasm in endomembranar-like strutures). More rigourous image analysis are required to confirmed these results, as describe above. In this experiment, we used the same gefitinib incubation condition as the one used with U87 cell line. But the cells are different, so it should be done a gefitinib dose effect on these cell lines regarding concentration and time of incubation. This evaluation should contain a toxicity test and an internalization profiling. For toxicity it can be studied the cell viability by MTT test or trypan blue exclusion test or the cell death by annexin V or caspases levels, in different drug concentrations and time of incubation. Cell evasion in these cell lines still needs to be evaluated, so it can be made a correlation between EGFR internalization and gefitinib treatment.

It can be concluded that during gefitinib treatment, EGFR endocytosis occurs and cell evasion decreases. Integrin α5 influences the response profile of cells to gefitinib, since its downregulation sensitizes the cells to treatment, but do not have influence in the

endocytic phenotype. Dynamin inhibitors do not influence cell evasion alone, but, impaired gefitinib-induced inhibition of U87 cell evasion. Dynamin inhibitors impair gefitinib-induced endocytosis. Endocytosis was reported to be a novel therapeutic target. In several studies, growth factor receptor endocytosis was reported to not be the signal attenuation mechanism. Endosomal EGFR signaling was able to activate the major signaling pathways and suppress cell death after serum-deprivation (177,178). ERK activation at plasma membrane and inside of endosomes activates different downstream targets (179). Altered growth factor receptors trafficking processes are involved in tumorigenesis, like signaling from endosomes, recycling and dysregulation of degradation (180). It is also involved in therapy resistance, since lung cancer cells were resistant to gefitinib treatment by having impaired the trafficking of the phosphorylated receptor from early endosomes to late endosomes (181). Pro-survival autophagy mechanisms are also involved in surviving mechanisms to gefitinib (144,182,183). Further experiments, like immundetection of autophagosomes are required to test the role of autophagy in our model.

But the role of endocytosis in gefitinib sensitivity is controversial in the scientific community. There is evidence that endocytosisimpairment increases gefitinib inhibition (145), but others showed the opposite, that endocytosis attenuates the signal (155).

In our study, endocytosis impairment conferes total resistance to gefitinib. While gefitinib induces endocytosis probably to attenuate the EGFR signal. This attenuation should be evaluated by immunoblotting of the main downstream proteins of EGFR signaling pathway (AKT and ERK, total protein and phosphorylated one).

But it remains to explain why U87 α5+ in the presence of gefitinib migrates more than the U87 α5-, while after endocytosis impairment both present the same phenotype. Importantly, in our different experiments we found that gefitinib activates β1 integrin endocytosis together with EGFR even in cells that express very low level of α5. This suggest that β1 is associated in other α subunit. It will be important in future to identify this α subunit and to understand why they are not able to trigger resistance to gefitinib. Integrin α5 can have a role in EGFR trafficking after endocytosis. Its role can be related to the recycling of EGFR back to the plasma membrane, where the signal can continue. There are already studies reporting the influence of integrin and EGFR recycling, and its role in promoting migration and invasion due to constitutive signaling activation

(131,184,185). But also integrin recycling (through endosomal and retrograde recycling) by itself is already described as an invasion promotor by reprogramming actin cytoskeleton and also by promoting the correct lamellipodia formation (151,186–189). EGFR recycling is involved in cellular migration in others physiological context, besides cancer as in keratinocytes and corneal epithelia (190,191). For that it should be interesting to study the receptors recycling in our model, or by using chemical inhibitors such as primaquine or using interference RNA against Rab 4 or 11(192,193).

Even with still a lot of work ahead, this study allowed the highlight for endocytosis and trafficking importance in therapy resistance, in one of the most aggressive cancers

5. Conclusion

Glioblastoma is an aggressive tumor without an effective therapy. Although EGFR is involved in glioma progression, targeted therapies failed in clinical trials. The cooperation between EGFR and integrin in the TK receptor trafficking is described as a potential therapy resistance mechanism.

The main objective of this work was to determine if endocytosis has a role in gefitinib treatment, using for that dynamin inhibitors, impairing vesicle fission and consequently endocytosis.

Using cell evasion assays, our team showed that U87 cells with higher levels of α5 integrin are more resistant to gefitinib treatment. During my master, we showed that dynamin inhibition completely protects cells from gefinib activity in a α5 integrin independent way. Increase of EGFR endocytosis can be described as an important event in gefitinib treatment since EGFR is co-localized inside of early endosomes after treatment. This event is α5 independent even if α5 and β1 integrins are also internalized with gefitinib treatment in U87. Importantly we found that gefitinib induced EGFR and β1 endocytosis in several GBM cells lines.

This work highlights endocytosis and trafficking importance in resistance to TKI targeting EGFR, in one of the most aggressive cancers. It remains to determine how α5β1 can trigger resistance to gefitinib, likely during membrane trafficking downstream of endocytosis.

6. Bibliography references

1. Ferlay J, Steliarova-Foucher E, Lortet-Tieulent J, Rosso S, Coebergh JWW, Comber H, et al. Cancer incidence and mortality patterns in Europe: estimates for 40 countries in 2012. Eur J Cancer Oxf Engl 1990. 2013;49(6):1374–403.

2. Collins VP. Cellular mechanisms targeted during astrocytoma progression. Cancer Lett. 2002;188(1–2):1–7.

3. Thakkar JP, Dolecek TA, Horbinski C, Ostrom QT, Lightner DD, Barnholtz-Sloan JS, et al. Epidemiologic and Molecular Prognostic Review of Glioblastoma. Cancer Epidemiol Biomark Prev Publ Am Assoc Cancer Res Cosponsored Am Soc Prev Oncol. 2014;23(10):1985–96.

4. DeAngelis LM. Brain Tumors. N Engl J Med. 2001;344(2):114–23.

5. Gaillard F. Glioblastoma. In: Radiopaedia [Internet]. Available from: https://radiopaedia.org/articles/glioblastoma

6. Louis DN, Perry A, Reifenberger G, Deimling A von, Figarella-Branger D, Cavenee WK, et al. The 2016 World Health Organization Classification of Tumors of the Central Nervous System: a summary. Acta Neuropathol (Berl). 2016;131(6):803–20.

7. Behin A, Hoang-Xuan K, Carpentier AF, Delattre J-Y. Primary brain tumours in adults. The Lancet. 2003;361(9354):323–31.

8. Kitange GJ, Templeton KL, Jenkins RB. Recent advances in the molecular genetics of primary gliomas. Current Opinion in Oncology. 2003; 15(3):197-203

9 Verhaak RGW, Hoadley KA, Purdom E, Wang V, Qi Y, Wilkerson MD, et al. Integrated genomic analysis identifies clinically relevant subtypes of glioblastoma characterized by abnormalities in PDGFRA, IDH1, EGFR, and NF1. Cancer Cell. 2010;17(1):98–110.

10. Parker NR, Khong P, Parkinson JF, Howell VM, Wheeler HR. Molecular heterogeneity in glioblastoma: potential clinical implications. Front Oncol. 2015;5:55.

11. Romaguera-Ros M, Peris-Celda M, Oliver-De La Cruz J, Carrión-Navarro J, Pérez-García A, García-Verdugo JM, et al. Cancer-initiating enriched cell lines from human glioblastoma: preparing for drug discovery assays. Stem Cell Rev. 2012;8(1):288–98.

12. Teng J, Carla da Hora C, Kantar RS, Nakano I, Wakimoto H, Batchelor TT, et al. Dissecting inherent intratumor heterogeneity in patient-derived glioblastoma culture models. Neuro-Oncol. 2017;now253

13. Bellail AC, Hunter SB, Brat DJ, Tan C, Van Meir EG. Microregional extracellular matrix heterogeneity in brain modulates glioma cell invasion. Int J Biochem Cell Biol. 2004;36(6):1046–69.

14. Vehlow A, Cordes N. Invasion as target for therapy of glioblastoma multiforme. Biochim Biophys Acta. 2013;1836(2):236–44.

15. Alves TR, Lima FRS, Kahn SA, Lobo D, Dubois LGF, Soletti R, et al. Glioblastoma cells: a heterogeneous and fatal tumor interacting with the parenchyma. Life Sci. 2011;89(15–16):532–9.

16. Hagemann C, Anacker J, Ernestus R-I, Vince GH. A complete compilation of matrix metalloproteinase expression in human malignant gliomas. World J Clin Oncol. 2012;3(5):67–79.

17. Badiga AV, Chetty C, Kesanakurti D, Are D, Gujrati M, Klopfenstein JD, et al. MMP-2 siRNA inhibits radiation-enhanced invasiveness in glioma cells. PloS One. 2011;6(6):e20614.

18. Kesanakurti D, Chetty C, Rajasekhar Maddirela D, Gujrati M, Rao JS. Functional cooperativity by direct interaction between PAK4 and MMP-2 in the regulation of anoikis resistance, migration and invasion in glioma. Cell Death Dis. 2012;3(12):e445.

19. Hirata E, Yukinaga H, Kamioka Y, Arakawa Y, Miyamoto S, Okada T, et al. In vivo fluorescence resonance energy transfer imaging reveals differential activation of Rho-family GTPases in glioblastoma cell invasion. J Cell Sci. 2012;125(Pt 4):858–68.

20. Mirimanoff R-O, Gorlia T, Mason W, Van den Bent MJ, Kortmann R-D, Fisher B, et al. Radiotherapy and Temozolomide for Newly Diagnosed Glioblastoma: Recursive Partitioning Analysis of the EORTC 26981/22981-NCIC CE3 Phase III Randomized Trial. J Clin Oncol. 2006;24(16):2563–9.

21. Ferraro N, Barbarite E, Albert TR, Berchmans E, Shah AH, Bregy A, et al. The role of 5-aminolevulinic acid in brain tumor surgery: a systematic review. Neurosurg Rev. 2016;39(4):545–55.

22. Stupp R, Mason WP, van den Bent MJ, Weller M, Fisher B, Taphoorn MJB, et al. Radiotherapy plus Concomitant and Adjuvant Temozolomide for Glioblastoma. N Engl J Med. 2005;352(10):987–96.

23. Newton H. Innovative Approaches to Chemotherapy Delivery. In: Handbook of Brain Tumor Chemotherapy. 1st ed. California: Academic Press; 2006.

24. Agarwala SS, Kirkwood JM. Temozolomide, a novel alkylating agent with activity in the central nervous system, may improve the treatment of advanced metastatic melanoma. The Oncologist. 2000;5(2):144–51.

25. Zhu W, Zhou L, Qian J-Q, Qiu T-Z, Shu Y-Q, Liu P. Temozolomide for treatment of brain metastases: A review of 21 clinical trials. World J Clin Oncol. 2014;5(1):19–27.

26. Stupp R, Brada M, van den Bent MJ, Tonn J-C, Pentheroudakis G, ESMO Guidelines Working Group. High-grade glioma: ESMO Clinical Practice Guidelines for diagnosis, treatment and follow-up. Ann Oncol Off J Eur Soc Med Oncol. 2014;25 Suppl 3:iii93-101.

27. Kreisl TN, Kim L, Moore K, Duic P, Royce C, Stroud I, et al. Phase II Trial of Single-Agent Bevacizumab Followed by Bevacizumab Plus Irinotecan at Tumor Progression in Recurrent Glioblastoma. J Clin Oncol. 2009;27(5):740–5.

28. Mehta S, Shelling A, Muthukaruppan A, Lasham A, Blenkiron C, Laking G, et al. Predictive and prognostic molecular markers for cancer medicine. Ther Adv Med Oncol. 2010;2(2):125–48.

29. Oldenhuis CNAM, Oosting SF, Gietema JA, de Vries EGE. Prognostic versus predictive value of biomarkers in oncology. Eur J Cancer. 2008;44(7):946–53.

30. Seymour T, Nowak A, Kakulas F. Targeting Aggressive Cancer Stem Cells in Glioblastoma. Front Oncol [Internet]. 2015;5.

31. Rahman M, Deleyrolle L, Vedam-Mai V, Azari H, Abd-El-Barr M, Reynolds BA. The cancer stem cell hypothesis: failures and pitfalls. Neurosurgery. 2011;68(2):531–545

32. Lobo NA, Shimono Y, Qian D, Clarke MF. The biology of cancer stem cells. Annu Rev Cell Dev Biol. 2007;23:675–99.

33. Singh SK, Hawkins C, Clarke ID, Squire JA, Bayani J, Hide T, et al. Identification of human brain tumour initiating cells. Nature. 2004;432(7015):396–401.

34. On N, Mitchell R, Savant SD, Bachmeier CJ, Hatch GM, Miller DW. Examination of Blood-Brain Barrier (BBB) Integrity In A Mouse Brain Tumor Model. J Neurooncol. 2013;111(2):133–43.

35. Schneider SW, Ludwig T, Tatenhorst L, Braune S, Oberleithner H, Senner V, et al. Glioblastoma cells release factors that disrupt blood-brain barrier features. Acta Neuropathol (Berl). 2004;107(3):272–6.

36. Weiss N, Miller F, Cazaubon S, Couraud P-O. The blood-brain barrier in brain homeostasis and neurological diseases. Biochim Biophys Acta BBA - Biomembr. 2009;1788(4):842–57.

37. Vogel TW, Zhuang Z, Li J, Okamoto H, Furuta M, Lee Y-S, et al. Proteins and Protein Pattern Differences between Glioma Cell Lines and Glioblastoma Multiforme. Clin Cancer Res. 2005;11(10):3624–32.

38. Torsvik A, Stieber D, Enger PØ, Golebiewska A, Molven A, Svendsen A, et al. U-251 revisited: genetic drift and phenotypic consequences of long-term cultures of glioblastoma cells. Cancer Med. 2014;3(4):812–24.

39. Pontén J, Macintyre EH. Long term culture of normal and neoplastic human glia. Acta Pathol Microbiol Scand. 1968;74(4):465–86.

40. Jaworski S, Sawosz E, Grodzik M, Kutwin M, Wierzbicki M, Włodyga K, et al. Comparison of tumour morphology and structure from U87 and U118 glioma cells cultured on chicken embryo chorioallantoic membrane. Bull Vet Inst Pulawy. 2013;57(4):593–598.

41. Lee J, Kotliarova S, Kotliarov Y, Li A, Su Q, Donin NM, et al. Tumor stem cells derived from glioblastomas cultured in bFGF and EGF more closely mirror the phenotype and genotype of primary tumors than do serum-cultured cell lines. Cancer Cell. 2006;9(5):391–403.

42. Pollard SM, Yoshikawa K, Clarke ID, Danovi D, Stricker S, Russell R, et al. Glioma stem cell lines expanded in adherent culture have tumor-specific phenotypes and are suitable for chemical and genetic screens. Cell Stem Cell. 2009;4(6):568–80.

43. Joo KM, Kim J, Jin J, Kim M, Seol HJ, Muradov J, et al. Patient-specific orthotopic glioblastoma xenograft models recapitulate the histopathology and biology of human glioblastomas in situ. Cell Rep. 2013;3(1):260–73.

44. William D, Mullins CS, Schneider B, Orthmann A, Lamp N, Krohn M, et al. Optimized creation of glioblastoma patient derived xenografts for use in preclinical studies. J Transl Med. 2017;15(1):27.

45. Sebastian S, Settleman J, Reshkin SJ, Azzariti A, Bellizzi A, Paradiso A. The complexity of targeting EGFR signalling in cancer: From expression to turnover. Biochim Biophys Acta BBA - Rev Cancer. 2006;1766(1):120–39.

46. Normanno N, De Luca A, Bianco C, Strizzi L, Mancino M, Maiello MR, et al. Epidermal growth factor receptor (EGFR) signaling in cancer. Gene. 2006;366(1):2–16.

47. Wieduwilt MJ, Moasser MM. The epidermal growth factor receptor family: Biology driving targeted therapeutics. Cell Mol Life Sci. 2008;65(10):1566–84.

48. Lal A, Glazer CA, Martinson HM, Friedman HS, Archer GE, Sampson JH, et al. Mutant Epidermal Growth Factor Receptor Up-Regulates Molecular Effectors of Tumor Invasion. Cancer Res. 2002;62(12):3335–9.

49. Azuaje F, Tiemann K, Niclou SP. Therapeutic control and resistance of the EGFR-driven signaling network in glioblastoma. Cell Commun Signal CCS. 2015;13:23.

50. Harari PM. Epidermal growth factor receptor inhibition strategies in oncology. Endocr Relat Cancer. 2004;11(4):689–708.

51. Sheng Q, Liu J. The therapeutic potential of targeting the EGFR family in epithelial ovarian cancer. Br J Cancer. 2011;104(8):1241–5.

52. Pillay V, Allaf L, Wilding AL, Donoghue JF, Court NW, Greenall SA, et al. The plasticity of oncogene addiction: implications for targeted therapies directed to receptor tyrosine kinases. Neoplasia N Y N. 2009;11(5):448–458, 2 p following 458.

53. Guo G, Narayan RN, Horton L, Patel TR, Habib AA. The Role of EGFR-Met Interactions in the Pathogenesis of Glioblastoma and Resistance to Treatment. Curr Cancer Drug Targets. 2017;17(3):297–302.

54. Li Z, Chang C-M, Wang L, Zhang P, Shu H-KG. Cyclooxygenase-2 Induction by Amino Acid Deprivation Requires p38 Mitogen-Activated Protein Kinase in Human Glioma Cells. Cancer Invest. 2017;1–11.

55. Sangpairoj K, Vivithanaporn P, Apisawetakan S, Chongthammakun S, Sobhon P, Chaithirayanon K. RUNX1 Regulates Migration, Invasion, and Angiogenesis via p38 MAPK Pathway in Human Glioblastoma. Cell Mol Neurobiol.;1-13.

56. Campbell RM, Anderson BD, Brooks NA, Brooks HB, Chan EM, De Dios A, et al. Characterization of LY2228820 dimesylate, a potent and selective inhibitor of p38 MAPK with antitumor activity. Mol Cancer Ther. 2014;13(2):364–74.

57. Riddick G, Kotliarova S, Rodriguez V, Kim HS, Linkous A, Storaska AJ, et al. A Core Regulatory Circuit in Glioblastoma Stem Cells Links MAPK Activation to a Transcriptional Program of Neural Stem Cell Identity. Sci Rep. 2017;7:43605.

58. Fan Q, Aksoy O, Wong RA, Ilkhanizadeh S, Novotny CJ, Gustafson WC, et al. A Kinase Inhibitor Targeted to mTORC1 Drives Regression in Glioblastoma. Cancer Cell. 2017;31(3):424–35.

59. Zhang X, Ding Z, Mo J, Sang B, Shi Q, Hu J, et al. GOLPH3 promotes glioblastoma cell migration and invasion via the mTOR-YB1 pathway in vitro. Mol Carcinog. 2015;54(11):1252–63.

60. Wei Y, Jiang Y, Zou F, Liu Y, Wang S, Xu N, et al. Activation of PI3K/Akt pathway by CD133-p85 interaction promotes tumorigenic capacity of glioma stem cells. Proc Natl Acad Sci U S A. 2013;110(17):6829–34.

61. Fan Q-W, Cheng CK, Gustafson WC, Charron E, Zipper P, Wong RA, et al. EGFR phosphorylates tumor-derived EGFRvIII driving STAT3/5 and progression in glioblastoma. Cancer Cell. 2013;24(4):438–49.

62. Ou Y, Ma L, Dong L, Ma L, Zhao Z, Ma L, et al. Migfilin protein promotes migration and invasion in human glioma through epidermal growth factor receptor-mediated phospholipase C-γ and STAT3 protein signaling pathways. J Biol Chem. 2012;287(39):32394–405.

63. Citri A, Yarden Y. EGF-ERBB signalling: towards the systems level. Nat Rev Mol Cell Biol. 2006;7(7):505–16.

64. Le Roy C, Wrana JL. Clathrin- and non-clathrin-mediated endocytic regulation of cell signalling. Nat Rev Mol Cell Biol. 2005;6(2):112–26.

65. Tomas A, Futter CE, Eden ER. EGF receptor trafficking: consequences for signaling and cancer. Trends Cell Biol. 2014;24(1):26–34.

66. Hampton KK, Craven RJ. Pathways driving the endocytosis of mutant and wild-type EGFR in cancer. Oncoscience. 2014;1(8):504–12.

67. Walsh AM, Kapoor GS, Buonato JM, Mathew LK, Bi Y, Davuluri RV, et al. Sprouty2 Drives Drug Resistance and Proliferation in Glioblastoma. Mol Cancer Res MCR. 2015;13(8):1227–37.

68. Ying H, Zheng H, Scott K, Wiedemeyer R, Yan H, Lim C, et al. Mig-6 controls EGFR trafficking and suppresses gliomagenesis. Proc Natl Acad Sci U S A. 2010;107(15):6912–7.

69. Roepstorff K, Grøvdal L, Grandal M, Lerdrup M, van Deurs B. Endocytic downregulation of ErbB receptors: mechanisms and relevance in cancer. Histochem Cell Biol. 2008;129(5):563–78.

70. Longva KE, Blystad FD, Stang E, Larsen AM, Johannessen LE, Madshus IH. Ubiquitination and proteasomal activity is required for transport of the EGF receptor to inner membranes of multivesicular bodies. J Cell Biol. 2002;156(5):843–54.

71. Gao M, Patel R, Ahmad I, Fleming J, Edwards J, McCracken S, et al. SPRY2 loss enhances ErbB trafficking and PI3K/AKT signalling to drive human and mouse prostate carcinogenesis. EMBO Mol Med. 2012;4(8):776–90.

72. Ye Q-H, Zhu W-W, Zhang J-B, Qin Y, Lu M, Lin G-L, et al. GOLM1 Modulates EGFR/RTK Cell-Surface Recycling to Drive Hepatocellular Carcinoma Metastasis. Cancer Cell. 2016;30(3):444–58.

73. Kondapalli KC, Llongueras JP, Capilla-González V, Prasad H, Hack A, Smith C, et al. A leak pathway for luminal protons in endosomes drives oncogenic signalling in glioblastoma. Nat Commun. 2015;6:6289.

74. Rich JN, Reardon DA, Peery T, Dowell JM, Quinn JA, Penne KL, et al. Phase II Trial of Gefitinib in Recurrent Glioblastoma. J Clin Oncol. 2004;22(1):133–42.

75. Dziadziuszko R, Jassem J. Epidermal growth factor receptor (EGFR) inhibitors and derived treatments. Ann Oncol Off J Eur Soc Med Oncol. 2012;23 Suppl 10:x193-196.

76. Reck M, Gatzemeier U. Gefitinib ("Iressa"): a new therapy for advanced non-small-cell lung cancer. Respir Med. 2005;99(3):298–307.

77. Segovia-Mendoza M, González-González ME, Barrera D, Díaz L, García-Becerra R. Efficacy and mechanism of action of the tyrosine kinase inhibitors gefitinib, lapatinib and neratinib in the treatment of HER2-positive breast cancer: preclinical and clinical evidence. Am J Cancer Res. 2015;5(9):2531–61.

78. Tiseo M, Bartolotti M, Gelsomino F, Bordi P. Emerging role of gefitinib in the treatment of non-small-cell lung cancer (NSCLC). Drug Des Devel Ther. 2010;4:81–98.

79. Gotink KJ, Verheul HMW. Anti-angiogenic tyrosine kinase inhibitors: what is their mechanism of action? Angiogenesis. 2010;13(1):1–14.

80. Arora A, Scholar EM. Role of Tyrosine Kinase Inhibitors in Cancer Therapy. J Pharmacol Exp Ther. 2005;315(3):971–9.

81. Lo H-W. EGFR-targeted therapy in malignant glioma: novel aspects and mechanisms of drug resistance. Curr Mol Pharmacol. 2010;3(1):37–52.

82. Smyth LA, Collins I. Measuring and interpreting the selectivity of protein kinase inhibitors. J Chem Biol. 2009;2(3):131–51.

83. Taylor TE, Furnari FB, Cavenee WK. Targeting EGFR for treatment of glioblastoma: molecular basis to overcome resistance. Curr Cancer Drug Targets. 2012;12(3):197–209.

84. Clark PA, Iida M, Treisman DM, Kalluri H, Ezhilan S, Zorniak M, et al. Activation of multiple ERBB family receptors mediates glioblastoma cancer stem-like cell resistance to EGFR-targeted inhibition. Neoplasia N Y N. 201;14(5):420–8.

85. Roth P, Weller M. Challenges to targeting epidermal growth factor receptor in glioblastoma: escape mechanisms and combinatorial treatment strategies. Neuro-Oncol. 2014;16 Suppl 8:viii14-19.

86. Voelzke WR, Petty WJ, Lesser GJ. Targeting the epidermal growth factor receptor in high-grade astrocytomas. Curr Treat Options Oncol. 2008;9(1):23–31.

87. Proto C, Imbimbo M, Gallucci R, Brissa A, Signorelli D, Vitali M, et al. Epidermal growth factor receptor tyrosine kinase inhibitors for the treatment of central nervous system

metastases from non-small cell lung cancer: the present and the future. Transl Lung Cancer Res. 2016;5(6):563–78.

88. Zeng Y-D, Liao H, Qin T, Zhang L, Wei W-D, Liang J-Z, et al. Blood-brain barrier permeability of gefitinib in patients with brain metastases from non-small-cell lung cancer before and during whole brain radiation therapy. Oncotarget. 2015;6(10):8366–76.

89. Cappuzzo F, Ardizzoni A, Soto-Parra H, Gridelli C, Maione P, Tiseo M, et al. Epidermal growth factor receptor targeted therapy by ZD 1839 (Iressa) in patients with brain metastases from non-small cell lung cancer (NSCLC). Lung Cancer Amst Neth. 2003;41(2):227–31.

90. Heimberger AB, Learn CA, Archer GE, McLendon RE, Chewning TA, Tuck FL, et al. Brain tumors in mice are susceptible to blockade of epidermal growth factor receptor (EGFR) with the oral, specific, EGFR-tyrosine kinase inhibitor ZD1839 (iressa). Clin Cancer Res Off J Am Assoc Cancer Res. 2002;8(11):3496–502.

91. Lin K-H, Hong S-T, Wang H-T, Lo Y-L, Lin AM-Y, Yang JC-H. Enhancing Anticancer Effect of Gefitinib across the Blood-Brain Barrier Model Using Liposomes Modified with One α-Helical Cell-Penetrating Peptide or Glutathione and Tween 80. Int J Mol Sci. 2016;17(12).

92. Thiessen B, Stewart C, Tsao M, Kamel-Reid S, Schaiquevich P, Mason W, et al. A phase I/II trial of GW572016 (lapatinib) in recurrent glioblastoma multiforme: clinical outcomes, pharmacokinetics and molecular correlation. Cancer Chemother Pharmacol. 2010;65(2):353–61.

93. Mellinghoff IK, Lassman AB, Wen PY. Signal transduction inhibitors and antiangiogenic therapies for malignant glioma. Glia. 2011;59(8):1205–12.

94. Wheeler DL, Huang S, Kruser TJ, Nechrebecki MM, Armstrong EA, Benavente S, et al. Mechanisms of acquired resistance to cetuximab: role of HER (ErbB) family members. Oncogene. 2008;27(28):3944–56.

95. Tan X, Lambert PF, Rapraeger AC, Anderson RA. Stress-Induced EGFR Trafficking: Mechanisms, Functions, and Therapeutic Implications. Trends Cell Biol. 2016;26(5):352–66.

96. Cooperation Between Integrins and Growth Factor Receptors in Signaling and Endocytosis. Annu Rev Cell Dev Biol. 2011;27(1):291–320.

97. Blandin A-F, Renner G, Lehmann M, Lelong-Rebel I, Martin S, Dontenwill M. β1 Integrins as Therapeutic Targets to Disrupt Hallmarks of Cancer. Front Pharmacol [Internet]. 2015;6.

98. Desgrosellier JS, Cheresh DA. Integrins in cancer: biological implications and therapeutic opportunities. Nat Rev Cancer. 2010;10(1):9–22.

99. Barczyk M, Carracedo S, Gullberg D. Integrins. Cell Tissue Res. 2010;339(1):269–80.

100. Anderson LR, Owens TW, Naylor MJ. Integrins in development and cancer. Biophys Rev. 2014;6(2):191–202.

101. Seguin L, Desgrosellier JS, Weis SM, Cheresh DA. Integrins and cancer: regulators of cancer stemness, metastasis, and drug resistance. Trends Cell Biol. 2015;25(4):234–40.

102. Arnaout MA, Goodman SL, Xiong J-P. Structure and mechanics of integrin-based cell adhesion. Curr Opin Cell Biol. 2007;19(5):495–507.

103. Askari JA, Buckley PA, Mould AP, Humphries MJ. Linking integrin conformation to function. J Cell Sci. 2009;122(Pt 2):165–70.

104. McDonald PC, Oloumi A, Mills J, Dobreva I, Maidan M, Gray V, et al. Rictor and integrin-linked kinase interact and regulate Akt phosphorylation and cancer cell survival. Cancer Res. 2008;68(6):1618–24.

105. Schaffner F, Ray AM, Dontenwill M. Integrin α5β1, the Fibronectin Receptor, as a Pertinent Therapeutic Target in Solid Tumors. Cancers. 2013;5(1):27–47.

106. Zutter MM, Santoro SA, Staatz WD, Tsung YL. Re-expression of the alpha 2 beta 1 integrin abrogates the malignant phenotype of breast carcinoma cells. Proc Natl Acad Sci U S A. 1995;92(16):7411–5.

107. Owens DM, Watt FM. Influence of beta1 integrins on epidermal squamous cell carcinoma formation in a transgenic mouse model: alpha3beta1, but not alpha2beta1, suppresses malignant conversion. Cancer Res. 2001;61(13):5248–54.

108. Janouskova H, Maglott A, Leger DY, Bossert C, Noulet F, Guerin E, et al. Integrin α5β1 Plays a Critical Role in Resistance to Temozolomide by Interfering with the p53 Pathway in High-Grade Glioma. Cancer Res. 2012;72(14):3463–70.

109. Bredel M, Bredel C, Juric D, Harsh GR, Vogel H, Recht LD, et al. Functional network analysis reveals extended gliomagenesis pathway maps and three novel MYC-interacting genes in human gliomas. Cancer Res. 2005;65(19):8679–89.

110. Mattern R-H, Read SB, Pierschbacher MD, Sze C-I, Eliceiri BP, Kruse CA. Glioma cell integrin expression and their interactions with integrin antagonists: Research Article. Cancer Ther. 2005;3A:325–40.

111. Schittenhelm J, Schwab EI, Sperveslage J, Tatagiba M, Meyermann R, Fend F, et al. Longitudinal expression analysis of αv integrins in human gliomas reveals upregulation of integrin αvβ3 as a negative prognostic factor. J Neuropathol Exp Neurol. 2013;72(3):194–210.

112. Kita D, Takino T, Nakada M, Takahashi T, Yamashita J, Sato H. Expression of dominant-negative form of Ets-1 suppresses fibronectin-stimulated cell adhesion and migration through down-regulation of integrin alpha5 expression in U251 glioma cell line. Cancer Res. 2001;61(21):7985–91.

113. Renner G, Noulet F, Mercier M-C, Choulier L, Etienne-Selloum N, Gies J-P, et al. Expression/activation of α5β1 integrin is linked to the β-catenin signaling pathway to drive migration in glioma cells. Oncotarget. 2016;7(38):62194–207.

114. Blandin A-F, Noulet F, Renner G, Mercier M-C, Choulier L, Vauchelles R, et al. Glioma cell dispersion is driven by α5 integrin-mediated cell–matrix and cell–cell interactions. Cancer Lett. 2016;376(2):328–38.

115. Ray A-M, Schaffner F, Janouskova H, Noulet F, Rognan D, Lelong-Rebel I, et al. Single cell tracking assay reveals an opposite effect of selective small non-peptidic α5β1 or

αvβ3/β5 integrin antagonists in U87MG glioma cells. Biochim Biophys Acta. 2014;1840(9):2978–87.

116. Martinkova E, Maglott A, Leger DY, Bonnet D, Stiborova M, Takeda K, et al. alpha5beta1 integrin antagonists reduce chemotherapy-induced premature senescence and facilitate apoptosis in human glioblastoma cells. Int J Cancer. 2010;127(5):1240–8.

117. Maglott A, Bartik P, Cosgun S, Klotz P, Rondé P, Fuhrmann G, et al. The small alpha5beta1 integrin antagonist, SJ749, reduces proliferation and clonogenicity of human astrocytoma cells. Cancer Res. 2006;66(12):6002–7.

118. Reardon DA, Fink KL, Mikkelsen T, Cloughesy TF, O'Neill A, Plotkin S, et al. Randomized phase II study of cilengitide, an integrin-targeting arginine-glycine-aspartic acid peptide, in recurrent glioblastoma multiforme. J Clin Oncol Off J Am Soc Clin Oncol. 2008;26(34):5610–7.

119. Stupp R, Hegi ME, Gorlia T, Erridge SC, Perry J, Hong Y-K, et al. Cilengitide combined with standard treatment for patients with newly diagnosed glioblastoma with methylated MGMT promoter (CENTRIC EORTC 26071-22072 study): a multicentre, randomised, open-label, phase 3 trial. Lancet Oncol. 2014;15(10):1100–8.

120. Moro L, Dolce L, Cabodi S, Bergatto E, Boeri Erba E, Smeriglio M, et al. Integrin-induced epidermal growth factor (EGF) receptor activation requires c-Src and p130Cas and leads to phosphorylation of specific EGF receptor tyrosines. J Biol Chem. 2002;277(11):9405–14.

121. Mattila E, Marttila H, Sahlberg N, Kohonen P, Tähtinen S, Halonen P, et al. Inhibition of receptor tyrosine kinase signalling by small molecule agonist of T-cell protein tyrosine phosphatase. BMC Cancer. 2010;10:7.

122. Morozevich GE, Kozlova NI, Ushakova NA, Preobrazhenskaya ME, Berman AE. Integrin α5β1 simultaneously controls EGFR-dependent proliferation and Akt-dependent pro-survival signaling in epidermoid carcinoma cells. Aging. 2012;4(5):368–74.

123. Williams KC, Coppolino MG. SNARE-dependent interaction of Src, EGFR and β1 integrin regulates invadopodia formation and tumor cell invasion. J Cell Sci. 2014;127(Pt 8):1712–25.

124. Morello V, Cabodi S, Sigismund S, Camacho-Leal MP, Repetto D, Volante M, et al. β1 integrin controls EGFR signaling and tumorigenic properties of lung cancer cells. Oncogene. 2011;30(39):4087–96.

125. Lesniak D, Xu Y, Deschenes J, Lai R, Thoms J, Murray D, et al. Beta1-integrin circumvents the antiproliferative effects of trastuzumab in human epidermal growth factor receptor-2-positive breast cancer. Cancer Res. 2009;69(22):8620–8.

126. Huang C, Park CC, Hilsenbeck SG, Ward R, Rimawi MF, Wang Y-C, et al. β1 integrin mediates an alternative survival pathway in breast cancer cells resistant to lapatinib. Breast Cancer Res BCR. 2011;13(4):R84.

127. Eke I, Storch K, Krause M, Cordes N. Cetuximab attenuates its cytotoxic and radiosensitizing potential by inducing fibronectin biosynthesis. Cancer Res. 2013;73(19):5869–79.

128. Kanda R, Kawahara A, Watari K, Murakami Y, Sonoda K, Maeda M, et al. Erlotinib resistance in lung cancer cells mediated by integrin β1/Src/Akt-driven bypass signaling. Cancer Res. 2013;73(20):6243–53.

129. De Franceschi N, Hamidi H, Alanko J, Sahgal P, Ivaska J. Integrin traffic – the update. J Cell Sci. 2015;128(5):839–52.

130. Arjonen A, Alanko J, Veltel S, Ivaska J. Distinct Recycling of Active and Inactive β1 Integrins. Traffic Cph Den. 2012;13(4):610–25.

131. Caswell PT, Chan M, Lindsay AJ, McCaffrey MW, Boettiger D, Norman JC. Rab-coupling protein coordinates recycling of alpha5beta1 integrin and EGFR1 to promote cell migration in 3D microenvironments. J Cell Biol. 2008;183(1):143–55.

132. Weng L, Enomoto A, Miyoshi H, Takahashi K, Asai N, Morone N, et al. Regulation of cargo-selective endocytosis by dynamin 2 GTPase-activating protein girdin. EMBO J. 2014;33(18):2098–112.

133. Allen M, Bjerke M, Edlund H, Nelander S, Westermark B. Origin of the U87MG glioma cell line: Good news and bad news. Sci Transl Med. 2016;8(354):354re3.

134. Clark MJ, Homer N, O'Connor BD, Chen Z, Eskin A, Lee H, et al. U87MG decoded: the genomic sequence of a cytogenetically aberrant human cancer cell line. PLoS Genet. 2010;6(1):e1000832.

135. Ishii N, Maier D, Merlo A, Tada M, Sawamura Y, Diserens AC, et al. Frequent co-alterations of TP53, p16/CDKN2A, p14ARF, PTEN tumor suppressor genes in human glioma cell lines. Brain Pathol Zurich Switz. 1999;9(3):469–79.

136. Cowley GS, Weir BA, Vazquez F, Tamayo P, Scott JA, Rusin S, et al. Parallel genome-scale loss of function screens in 216 cancer cell lines for the identification of context-specific genetic dependencies. Sci Data. 2014;1:140035.

137. Bady P, Diserens A-C, Castella V, Kalt S, Heinimann K, Hamou M-F, et al. DNA fingerprinting of glioma cell lines and considerations on similarity measurements. Neuro-Oncol. 2012;14(6):701–11.

138. Berens ME, Rief MD, Loo MA, Giese A. The role of extracellular matrix in human astrocytoma migration and proliferation studied in a microliter scale assay. Clin Exp Metastasis. 1994;12(6):405–15.

139. Torsvik A, Røsland GV, Svendsen A, Molven A, Immervoll H, McCormack E, et al. Spontaneous malignant transformation of human mesenchymal stem cells reflects cross-contamination: putting the research field on track - letter. Cancer Res. 2010;70(15):6393–6.

140. Stein GH. T98G: An anchorage-independent human tumor cell line that exhibits stationary phase G1 arrest in vitro. J Cell Physiol. 1979;99(1):43–54.

141. MacDonald L, Baldini G, Storrie B. Does Super Resolution Fluorescence Microscopy Obsolete Previous Microscopic Approaches to Protein Co-localization? Methods Mol Biol Clifton NJ. 2015;1270:255–75.

142. Liu Z, Xing D, Su QP, Zhu Y, Zhang J, Kong X, et al. Super-resolution imaging and tracking of protein–protein interactions in sub-diffraction cellular space. Nat Commun. 2014;5:4443.

143. Bon P, Bourg N, Lécart S, Monneret S, Fort E, Wenger J, et al. Three-dimensional nanometre localization of nanoparticles to enhance super-resolution microscopy. Nat Commun. 2015;6:7764.

144. Bokobza SM, Jiang Y, Weber AM, Devery AM, Ryan AJ. Combining AKT inhibition with chloroquine and gefitinib prevents compensatory autophagy and induces cell death in EGFR mutated NSCLC cells. Oncotarget. 2014;5(13):4765–78.

145. Cardoso ACF, Andrade LN de S, Bustos SO, Chammas R. Galectin-3 Determines Tumor Cell Adaptive Strategies in Stressed Tumor Microenvironments. Front Oncol. 2016;6.

146. Shaughnessy R, Retamal C, Oyanadel C, Norambuena A, López A, Bravo-Zehnder M, et al. Epidermal growth factor receptor endocytic traffic perturbation by phosphatidate phosphohydrolase inhibition: new strategy against cancer. FEBS J. 2014;281(9):2172–89.

147. Ferguson SM, De Camilli P. Dynamin, a membrane remodelling GTPase. Nat Rev Mol Cell Biol. 2012;13(2):75–88.

148. Mettlen M, Pucadyil T, Ramachandran R, Schmid SL. Dissecting dynamin's role in clathrin-mediated endocytosis. Biochem Soc Trans. 2009;37(Pt 5):1022.

149. Park RJ, Shen H, Liu L, Liu X, Ferguson SM, De Camilli P. Dynamin triple knockout cells reveal off target effects of commonly used dynamin inhibitors. J Cell Sci. 2013;126(Pt 22):5305–12.

150. Jovic M, Sharma M, Rahajeng J, Caplan S. The early endosome: a busy sorting station for proteins at the crossroads. Histol Histopathol. 2010;25(1):99–112.

151. Jacquemet G, Green DM, Bridgewater RE, von Kriegsheim A, Humphries MJ, Norman JC, et al. RCP-driven α5β1 recycling suppresses Rac and promotes RhoA activity via the RacGAP1-IQGAP1 complex. J Cell Biol. 2013;202(6):917–35.

152. Garay C, Judge G, Lucarelli S, Bautista S, Pandey R, Singh T, et al. Epidermal growth factor-stimulated Akt phosphorylation requires clathrin or ErbB2 but not receptor endocytosis. Mol Biol Cell. 2015;26(19):3504–19.

153. Kirchhausen T, Macia E, Pelish HE. Use of dynasore, the small molecule inhibitor of dynamin, in the regulation of endocytosis. Methods Enzymol. 2008;438:77–93.

154. Newton AJ, Kirchhausen T, Murthy VN. Inhibition of dynamin completely blocks compensatory synaptic vesicle endocytosis. Proc Natl Acad Sci U S A. 2006;103(47):17955–60.

155. Gong C, Zhang J, Zhang L, Wang Y, Ma H, Wu W, et al. Dynamin2 downregulation delays EGFR endocytic trafficking and promotes EGFR signaling and invasion in hepatocellular carcinoma. Am J Cancer Res. 2015;5(2):702–13.

156. Yamada H, Takeda T, Michiue H, Abe T, Takei K. Actin bundling by dynamin 2 and cortactin is implicated in cell migration by stabilizing filopodia in human non-small cell lung carcinoma cells. Int J Oncol. 2016;49(3):877–86.

157. Feng H, Liu K, Guo P, Zhang P, Cheng T, McNiven M, et al. Dynamin 2 Mediates PDGFRα-SHP-2-Promoted Glioblastoma Growth and Invasion. Oncogene. 2012;31(21):2691–702.

158. Razidlo GL, Wang Y, Chen J, Krueger EW, Billadeau DD, McNiven MA. Dynamin 2 Potentiates Invasive Migration of Pancreatic Tumor Cells through Stabilization of the Rac1 GEF Vav1. Dev Cell. 2013;24(6):573–85.

159. Preta G, Cronin JG, Sheldon IM. Dynasore - not just a dynamin inhibitor. Cell Commun Signal CCS. 2015 Apr 10;13.

160. Kruth HS. Receptor-independent fluid-phase pinocytosis mechanisms for induction of foam cell formation with native LDL particles. Curr Opin Lipidol. 2011;22(5):386–93.

161. McCluskey A, Daniel JA, Hadzic G, Chau N, Clayton EL, Mariana A, et al. Building a better dynasore: the dyngo compounds potently inhibit dynamin and endocytosis. Traffic Cph Den. 2013;14(12):1272–89.

162. Edmondson R, Broglie JJ, Adcock AF, Yang L. Three-Dimensional Cell Culture Systems and Their Applications in Drug Discovery and Cell-Based Biosensors. Assay Drug Dev Technol. 2014;12(4):207–18.

163. Vinci M, Gowan S, Boxall F, Patterson L, Zimmermann M, Court W, et al. Advances in establishment and analysis of three-dimensional tumor spheroid-based functional assays for target validation and drug evaluation. BMC Biol. 2012;10:29.

164. Lefranc F, Brotchi J, Kiss R. Possible Future Issues in the Treatment of Glioblastomas: Special Emphasis on Cell Migration and the Resistance of Migrating Glioblastoma Cells to Apoptosis: Journal of Clinical Oncology. 2005; 23(10).

165. Pedretti M, Verpelli C, Mårlind J, Bertani G, Sala C, Neri D, et al. Combination of temozolomide with immunocytokine F16–IL2 for the treatment of glioblastoma. Br J Cancer. 2010;103(6):827–36.

166. Kramer N, Walzl A, Unger C, Rosner M, Krupitza G, Hengstschläger M, et al. In vitro cell migration and invasion assays. Mutat Res Mutat Res. 2013;752(1):10–24.

167. Jo U, Park KH, Whang YM, Sung JS, Won NH, Park JK, Kim YH. EGFR endocytosis is a novel therapeutic target in lung cancer with wild-type EGFR. 2014; 5(5):1265-1278

168. Waranuki Z, Kosai H, Osanai N, Ogama N, Mochizuki M, Tamai K et al. Synergistic cytotoxicity of afatinib and cetuximab against EGFR T790M involves Rab11-dependent EGFR recycling. 2014;455(3-4):269-76

169. Henriksen L, Grandal MV, Knudsen SLJ, van Deurs B, Grøvdal LM. Internalization Mechanisms of the Epidermal Growth Factor Receptor after Activation with Different Ligands. PLoS ONE. 2013;8(3).

170. Grant BD, Donaldson JG. Pathways and mechanisms of endocytic recycling. Nat Rev Mol Cell Biol. 2009;10(9):597–608.

171. Pinilla-Macua I, Sorkin A. Methods to study endocytic trafficking of the EGF receptor. Methods Cell Biol. 2015;130:347–67.

172. Sorkin A, Duex JE. Quantitative Analysis of Endocytosis and Turnover of Epidermal Growth Factor (EGF) and EGF Receptor. Curr Protoc Cell Biol Editor Board Juan Bonifacino Al. 2010;CHAPTER:Unit-15.14.

173. Veeraraghavan R, Gourdie RG. Stochastic optical reconstruction microscopy-based relative localization analysis (STORM-RLA) for quantitative nanoscale assessment of spatial protein organization. Mol Biol Cell. 2016;27(22):3583–90.

174. Rust MJ, Bates M, Zhuang X. Sub-diffraction-limit imaging by stochastic optical reconstruction microscopy (STORM). Nat Methods. 2006;3(10):793–6.

175. Helms V. Strutures of Protein Complexes and Subcellular Structures. In: Principles of Computational Cell Biology. 2nd ed. New Jersey USA: Wiley-Blackwell; 2007. p. 202,203.

176. Pollok BA, Helm R. Using GFP in FRET-based applications: Trends in Cell Biology. 1999;9(2): 57-60.

177. Wang Y, Pennock S, Chen X, Wang Z. Endosomal Signaling of Epidermal Growth Factor Receptor Stimulates Signal Transduction Pathways Leading to Cell Survival. Mol Cell Biol. 2002;22(20):7279–90.

178. Fogelgren B, Zuo X, Buonato JM, Vasilyev A, Baek J-I, Choi SY, et al. Exocyst Sec10 protects renal tubule cells from injury by EGFR/MAPK activation and effects on endocytosis. Am J Physiol Renal Physiol. 2014;307(12):F1334-1341.

179. Wu P, Wee P, Jiang J, Chen X, Wang Z. Differential Regulation of Transcription Factors by Location-Specific EGF Receptor Signaling via a Spatio-Temporal Interplay of ERK Activation. PLoS ONE. 2012;7(9).

180. Parachoniak CA, Park M. Dynamics of receptor trafficking in tumorigenicity. Trends Cell Biol. 2012;22(5):231–40.

181. Nishimura Y, Yoshioka K, Bereczky B, Itoh K. Evidence for efficient phosphorylation of EGFR and rapid endocytosis of phosphorylated EGFR via the early/late endocytic pathway in a gefitinib-sensitive non-small cell lung cancer cell line. Mol Cancer. 2008;7:42.

182. Jutten B, rouschop K. EGFR signaling and autophagy dependence for growth, survival, and therapy resistance. Cell Cycle. 2014;13(1):42–51.

183. Tang M-C, Wu M-Y, Hwang M-H, Chang Y-T, Huang H-J, Lin AM-Y, et al. Chloroquine enhances gefitinib cytotoxicity in gefitinib-resistant nonsmall cell lung cancer cells. PloS One. 2015;10(3):e0119135.

184. Onodera Y, Nam J-M, Hashimoto A, Norman JC, Shirato H, Hashimoto S, et al. Rab5c promotes AMAP1-PRKD2 complex formation to enhance β1 integrin recycling in EGF-induced cancer invasion. J Cell Biol. 2012;197(7):983–96.

185. Muller PAJ, Caswell PT, Doyle B, Iwanicki MP, Tan EH, Karim S, et al. Mutant p53 drives invasion by promoting integrin recycling. Cell. 2009;139(7):1327–41.

186. Shafaq-Zadah M, Gomes-Santos CS, Bardin S, Maiuri P, Maurin M, Iranzo J, et al. Persistent cell migration and adhesion rely on retrograde transport of β(1) integrin. Nat Cell Biol. 2016;18(1):54–64.

187. Paul NR, Jacquemet G, Caswell PT. Endocytic Trafficking of Integrins in Cell Migration. Curr Biol CB. 2015;25(22):R1092-1105.

188. Dozynkiewicz MA, Jamieson NB, Macpherson I, Grindlay J, van den Berghe PVE, von Thun A, et al. Rab25 and CLIC3 collaborate to promote integrin recycling from late endosomes/lysosomes and drive cancer progression. Dev Cell. 2012 Jan;22(1):131–45.

189. Paul NR, Allen JL, Chapman A, Morlan-Mairal M, Zindy E, Jacquemet G, et al. α5β1 integrin recycling promotes Arp2/3-independent cancer cell invasion via the formin FHOD3. J Cell Biol. 2015;210(6):1013–31.

190. Liu W, Hsu DK, Chen H-Y, Yang R-Y, Carraway KL, Isseroff RR, et al. Galectin-3 regulates intracellular trafficking of EGFR through Alix and promotes keratinocyte migration. J Invest Dermatol. 2012;132(12):2828–37.

191. McClintock JL, Ceresa BP. Transforming growth factor-{alpha} enhances corneal epithelial cell migration by promoting EGFR recycling. Invest Ophthalmol Vis Sci. 2010;51(7):3455–61.

192. van Weert AW, Geuze HJ, Groothuis B, Stoorvogel W. Primaquine interferes with membrane recycling from endosomes to the plasma membrane through a direct interaction with endosomes which does not involve neutralisation of endosomal pH nor osmotic swelling of endosomes. Eur J Cell Biol. 2000;79(6):394–9.

193. Roberts M, Barry S, Woods A, van der Sluijs P, Norman J. PDGF-regulated rab4-dependent recycling of αvβ3 integrin from early endosomes is necessary for cell adhesion and spreading. Curr Biol. 2001;11(18):1392–402.

7. Annex 1- Antibodies list

Technique	Protein Labelled	Antibody Primary	Dilution	Company	Antibody Secondary	Dilution	Company
Western-Blot	Integrin α5	Integrin α5 H104	1/3000	Santa Cruz Biotechonology, Dallas, USA)	Anti-rabbit IgG HRP conjugate W401B	3/5000	Promega, Madison, USA
	EGFR	EGFR D38B1 rabbit 4267P	1/1000	Cell Signaling Techonology, Danvers, USA			
	GADPH	MS X GAPDH	1/5000	Milipore,Temecula, USA	Anti-mouse IgG HRP conjugate W402B		
Immunofluorescence	EGFR	EGF receptor D38B1 XP (R) rabbit mAb	1/50	Cell Signaling Techonology, Danvers, USA	Alexa Fluor 647 Goat Anti-rabbit IgG (H+L)	1/2000	Life technologies, Carlsbad, USA
	LRP1	LRP1 mouse antibody GTX79843	1/1000	Gentex, Michigan, USA	Alexa Fluor 488 Goat Anti-mouse IgG (H+L)		
	EEA 1	Purified mouse anti-EEA1 610457	1/100	BD Transduction Laboratories, San Jose, USA			
	Integrin β1	Anti- β1 TS2/16	1/200	Santa Cruz Biotechonology, Dallas, USA)			
	Integrin α5	Anti- α5 SNAKA-51	1/200	Milipore,Temecula, USA			
STORM	Integrin β1	Anti- β1 TS2/16	1/400	Santa Cruz Biotechonology, Dallas, USA)	Anti-mouse Alexa 555	1/2000	Life technologies, Carlsbad, USA
	EGFR	EGF receptor D1D4T XP (R) rabbit	1/500	Cell Signaling Techonology, Danvers, USA	Anti-rabbit Alexa 647		